TECHNICAL NOTE
AESD - TN-73-05

A SYNOPSIS OF THE AESD WORKSHOP ON ACOUSTIC-PROPAGATION MODELING BY NON-RAY–TRACING TECHNIQUES 22-25 MAY 1973, WASHINGTON, D.C.

NOVEMBER 1973

C. W. SPOFFORD

ACOUSTIC ENVIRONMENTAL
SUPPORT DETACHMENT
OFFICE OF NAVAL RESEARCH
Arlington, Va.

AESD

UNCLASSIFIED

SECURITY CLASSIFICATION OF THIS PAGE *(When Data Entered)*

REPORT DOCUMENTATION PAGE

READ INSTRUCTIONS BEFORE COMPLETING FORM

1. REPORT NUMBER: AESD TN-73-05

2. GOVT ACCESSION NO.:

3. RECIPIENT'S CATALOG NUMBER:

4. TITLE *(and Subtitle)*: A SYNOPSIS OF THE AESD WORKSHOP ON ACOUSTIC-PROPAGATION MODELING BY NON-RAY-TRACING TECHNIQUES, 22-25 MAY 1973, WASHINGTON, D. C.

5. TYPE OF REPORT & PERIOD COVERED: TECHNICAL NOTE

6. PERFORMING ORG. REPORT NUMBER:

7. AUTHOR(s): C. W. SPOFFORD

8. CONTRACT OR GRANT NUMBER(s):

9. PERFORMING ORGANIZATION NAME AND ADDRESS: Acoustic Environmental Support Detachment, Office of Naval Research, Arlington, Virginia 22217

10. PROGRAM ELEMENT, PROJECT, TASK AREA & WORK UNIT NUMBERS:

11. CONTROLLING OFFICE NAME AND ADDRESS: Acoustic Environmental Support Detachment, Office of Naval Research, Arlington, Virginia 22217

12. REPORT DATE: NOVEMBER 1973

13. NUMBER OF PAGES: 103

14. MONITORING AGENCY NAME & ADDRESS *(if different from Controlling Office)*:

15. SECURITY CLASS. *(of this report)*: UNCLASSIFIED

15a. DECLASSIFICATION/DOWNGRADING SCHEDULE:

16. DISTRIBUTION STATEMENT *(of this Report)*:

17. DISTRIBUTION STATEMENT *(of the abstract entered in Block 20, if different from Report)*:

18. SUPPLEMENTARY NOTES:

19. KEY WORDS *(Continue on reverse side if necessary and identify by block number)*:

Acoustic Propagation Modeling
Transmission Loss
Normal Modes

20. ABSTRACT *(Continue on reverse side if necessary and identify by block number)*:

This report summarizes the proceedings of a workshop sponsored by AESD on the subject of modeling acoustic propagation by non-ray-tracing techniques. Participants were required to have exercised their models against one or more test cases provided by AESD. More than 50 predictions were generated by 17 different models. This report contains descriptions of these models, their respective predictions against the test cases, and summaries of working sessions on a number of relevent topics in acoustic modeling.

DD FORM 1 JAN 73 1473 EDITION OF 1 NOV 65 IS OBSOLETE
S/N 0102-014-6601 |

UNCLASSIFIED

SECURITY CLASSIFICATION OF THIS PAGE *(When Data Entered)*

TECHNICAL NOTE
AESD TN No. 73-05

A SYNOPSIS OF THE AESD WORKSHOP ON ACOUSTIC-PROPAGATION MODELING BY NON-RAY-TRACING TECHNIQUES 22-25 MAY 1973, WASHINGTON, D.C.

by

C. W. SPOFFORD

NOVEMBER 1973

ACOUSTIC ENVIRONMENTAL SUPPORT DETACHMENT
OFFICE OF NAVAL RESEARCH
DEPARTMENT OF THE NAVY
WASHINGTON, D. C.

DEPARTMENT OF THE NAVY
OFFICE OF NAVAL RESEARCH
ACOUSTIC ENVIRONMENTAL SUPPORT DETACHMENT
ARLINGTON, VIRGINIA 22217

IN REPLY REFER TO
AESD:PRT:dw
3 January 1974

From: Head, Acoustic Environmental Support Detachment
To: Distribution List

Subj: Workshop on Acoustic-Propagation Modeling by Non-Ray Tracing Techniques

1. The Acoustic Environmental Support Detachment (AESD) was established in July 1972 as an Advanced Development activity to synthesize, evaluate, document, and distribute a family of Navy standard acoustic models. One of the methods utilized by AESD to keep abreast of promising new techniques in the Research and Exploratory Development communities is the sponsorship of workshops to address particular aspects of the acoustic modeling process.

2. This Technical Note provides a synopsis of such a workshop which addressed the prediction of transmission loss by techniques which did not involve ray-tracing. It is being distributed to disseminate to a much broader audience a summary of the ideas presented.

3. The workshop owes its success to the enthusiastic participation of those who attended. Their contribution and cooperation are gratefully acknowledged.

P. R. Tatro

P. R. TATRO

ABSTRACT

This report summarizes the proceedings of a workshop sponsored by AESD on the subject of modeling acoustic propagation by non-ray-tracing techniques. Participants were required to have exercised their models against one or more test cases provided by AESD. More than 50 predictions were generated by 17 different models. This report contains descriptions of these models, their respective predictions against the test cases, and summaries of working sessions on a number of relevent topics in acoustic modeling.

TABLE OF CONTENTS

A SYNOPSIS OF THE AESD WORKSHOP ON ACOUSTIC-PROPAGATION MODELING BY NON-RAY-TRACING TECHNIQUES 22-25 MAY 1973, WASHINGTON, D. C.

INTRODUCTION

From 22 to 25 May 1973 the Acoustic Environmental Support Detachment (AESD) of the Office of Naval Research sponsored a workshop on non-ray-tracing techniques used to model acoustic propagation in the ocean environment. The basic objectives of the workshop were twofold:

1. To bring together those in the R&D community working on non-ray approaches for an informal, though critical review of the current state-of-the-art.
2. To indicate to the R&D community the requirements of the Navy's Advanced Development Program (as implemented by AESD) in this field, thereby illuminating new areas of concentration and research to meet future Navy needs.

In order to maintain a workshop atmosphere and conform to space limitations, attendance was limited to those with working models who were willing to exercise them against one or more test cases provided by AESD. An additional small group of researchers with recognized credentials in the field was invited to participate in an advisory capacity. The workshop was divided into two basic sections: the presentation by each participant of his model (with some discussion of the predictions for each test case) and workshop discussions of a number of topics of current interest relating to model applications.

It is the purpose of this note to report on these proceedings for the benefit of both the participants and those who were unable to attend. This note consists of five basic sections:

1. A brief description of the test cases.
2. A list of attendees (participants and advisors), the models presented, and the results for the test cases against which each model was exercised.
3. A background discussion of solutions to the wave equation to serve as a basis for:
4. A brief description of the approaches contained in each model with emphasis on the differences between models.
5. Summaries of working sessions on:
    a. Rough-Surface Scattering
    b. Volume Attenuation
    c. Range Dependence of the Environment

d. Modeling the Ocean Bottom
e. Modeling Source Characteristics
f. Smoothing Wave Results
g. Signal-Processing Applications

TEST CASES AND PARTICIPANTS

Three basic test cases were provided to determine the various regimes of applicability of each model. In each case the medium is modeled as stratified (no range dependence) with a simple two-fluid condition at the ocean bottom characterized by a ρc or impedance discontinuity.

Figure 1 illustrates Test Case 1: characterization of a typical North Pacific sound speed profile adjusted to include a very deep surface duct. Case 1A is for a source and receiver in the duct at a frequency of 300 Hz where two modes are expected to be trapped. Case 1B corresponds to a deep-water long-range case. The plane-wave intensity reflection coefficient for the bottom as a function of grazing angle is plotted in the lower right. The numerical values for this case are shown in Figure 2.

Test Case 2 is described in Figures 3 and 4 and is characteristic of the double sound-channel structure found in the Northeast Atlantic. Test Case 3 (Figures 5 and 6) is a shallow water case with a relatively high-loss bottom. At 500 Hz several modes are trapped, while at 50 Hz only 1 mode is trapped. The low-frequency case was chosen to test the versatility of the models, and, as the subsequent comparisons will show, the differences between model predictions for this case are the largest.

Predictions generated by 16 different models were received for one or more of the test cases. Figure 7 lists the models, the participants or principal investigators responsible for the models, and the cases for which results were received. The models were divided into four basic categories and were presented in the order shown. The parentheses around the APL and CU cases indicate that normalization difficulties made comparisons impossible and they have not been included in this synopsis. The NUSC-3 result for test case 3B was off scale and also has been omitted. H. Kutschale of Lamont-Dougherty did not receive an invitation in time to prepare the test cases; F. DiNapoli made the model presentation for W. Kanabis, who was unable to attend.

The distinction between long range "normal mode" and "other approaches" is somewhat arbitrary and this characterization of a model was made by AESD prior to the workshop. The NUSC-1 and NUSC-2 models are approximate and extend normal-mode models respectively. Figure 8 lists all attendees and their organizational affiliations.

The results submitted for each model against each test case are presented in Figures 9 through 64. As a reference (but by no means a standard) predictions using the new Navy Interim Standard Transmission Loss Model (FACT) have been included. FACT is basically a ray model which includes higher order wave corrections for diffraction and surface-image interference. It does not include the full interference of the wave field; hence predictions of transmission loss are usually smoother than normal-mode results.

Predictions For Test Case 1A (Figures 9-20)

The predictions for Test Case 1A are probably the most consistent set of all those submitted. Two predictions from AESD have been provided. The first, "ASRAP", corresponds to the surface-duct module in FACT developed by Clay and Tatro and originally implemented in RP70. It is basically an energy-conserving model intended to yield averaged or smoothed ducted levels. The second prediction, "FACT", was generated by inhibiting the standard Clay/Tatro model, tracing rays in the surface duct, and performing the standard FACT processing of these rays. When compared with the normal-mode results quite good agreement is obtained, and the modal interference pattern (only 2 modes are present) is seen to correspond to the small convergence zones of rays in the duct. It should be noted, however, that for the case selected the two modes are well trapped with very little leakage to a range of 16nm. Had there been more leakage, FACT (which cannot include leakage) would have predicted too high an intensity.

Two predictions using the NUSC-3 model were provided, one allowing for only ducted paths and another allowing for the bottom-reflected paths present for the full sound-speed profile. The second has been included in these predictions since it illustrates the deterioration in the smooth modal interference pattern expected when bottom-reflected energy is also present.

Predictions For Test Case 1B (Figures 21-32)

The primary differences between the various predictions for this case resulted from different treatments of the ocean bottom. This question was clearly resolved by Bartberger of NADC who provided three sets of predictions:

1. Modes corresponding to refracted and RSR paths only (with very deep nulls between the convergence zones).
2. These modes plus those corresponding to rays reflecting at less than the critical angle (quite similar to NUC-1, BTL-1, and NOL).
3. These modes plus the contributions from modes corresponding to rays striking the bottom at greater then critical (NADC, NUSC-1, NUSC-2, NUSC-3, etc.) In the convergence zones all models are in good agreement except perhaps the ARL model which may have undersampled the transmission-loss curve.

Predictions For Test Case 2 (Figures 33-43)

The same level of agreement is present for this case as for case 1B with differences due essentially to the same bottom-related questions. The agreement between FACT and the mode models is somewhat surprising since it might be expected that transmission to a receiver so near the bottom of the upper duct for this type of sound-speed profile would be inadequately modeled by ray theory.

Predictions For Test Case 3A (Figures 44-54)

In this case several modes are present and, with the exception of the ARL model (which may have a normalization error), all predictions are in good agreement. The BTL-1 model tends to show slightly higher losses at longer ranges than the mode models, and the source of this discrepency is not resolved.

Predictions For Test Case 3B (Figures 55-64)

The parameters in this test case were intentionally selected to correspond to a duct at a frequency just below cut-off. Unfortunately, the hand calculation which led to the parameters used a WKB approximation to determine the cut-off and the consensus was that probably one, very leaky mode was present. The mode predictions reflect this critical regime and may be divided into approximately three categories:

1. Very low loss at range (NUSC-2, NUSC-4)
2. Moderate loss at range (NADC, NRL-1, NOL, NRL-2)
3. High loss at range (ARL, NUSC-1, BTL-1).

The FACT predictions may shed some light on these differences. At short range the FACT predictions oscillate rapidly between high-loss bottom-bounce regions and low-loss RBR regions. Since total phases are not computed, the RBR rays propagate successfully and eventually their convergence zones overlap so that the FACT prediction resembles a category 1 prediction. At short ranges where the zones are very narrow FACT resembles the type 2 category.

The large differences between models for this test case are an indication of one of the unresolved areas in modeling. It was also noted that the introduction of a very slight amount of absorption in the bottom would drive the category 2 predictions down to those in category 3. The sensitivity of the predictions to such parameters raises several additional questions for those involved in predictive acoustics.

BACKGROUND FOR ACOUSTIC WAVE MODELS*

It is the purpose of this section to provide the common points of departure for the various classes of models presented at the workshop. The emphasis will be on the differences between these classes with the subsequent section devoted to the differences between specific models within a class.

For a medium with index of refraction

$$n(\underline{r}) = c_0/c(\underline{r}) \tag{1}$$

where c is sound speed and c_0 a reference sound speed, the excess pressure, P, excited by a harmonic point source at location $\underline{r}'$ with angular frequency ω satisfies the inhomogeneous reduced wave equation

$$[\nabla^2 + k^2 n^2(\underline{r})]\, P(\underline{r},\underline{r}') = -\,\delta(\underline{r}-\underline{r}') \tag{2}$$

where the wave number $k = \omega/c_0$ and $\underline{r}$ is the observation point. P must satisfy the radiation condition at infinity and vanish at the ocean surface.

At this point nearly all models assume that the ocean depth and sound velocity profile are independent of range. Then (2) can be expressed in cylindrical coordination as

$$\left[\frac{1}{\rho}\,\frac{\partial}{\partial\rho}\,\rho\,\frac{\partial}{\partial\rho} + \frac{\partial^2}{\partial z^2} + k^2 n^2(z)\right] P(\underline{r},\underline{r}') = -\,\frac{1}{2\pi\rho}\,\delta(\rho)\delta(z-z'). \tag{3}$$

The solution of this boundary value problem can be represented in many forms, each having different properties. Four representations are described here which form the basis for most of the models presented. The first is a contour-integral representation in the plane of the separation constant. Labianca has shown that the other three (Fourier-Bessel integral, the residue series, and the normal-mode solution) are derivable from the λ-plane representation.

The λ-Plane Representation

The λ-plane representation is a contour-integral representation which is applicable to any separable, cylindrical-coordinate, boundary-value problem with symmetry about the z-axis. For the case of equation (3), the solution takes the following form:

---

* The following discussion has been extracted from "Normal modes, virtual modes and alternative representations in the theory of surface-ducted sound propagation" by F.M. Labianca, JASA 53 (1973), 1137-1147.

$$P(\underline{r},\underline{r}') = -\frac{k^2}{2\pi i}\int_{C_\lambda} G_1(\rho;1-\lambda)G_2(z,z';\lambda)d\lambda \ . \tag{4}$$

Here, $G_1(\rho;1-\lambda)$ and $G_2(z,z';\lambda)$ are the one-dimensional Green's functions for the ρ and z coordinates, respectively. They satisfy the differential equations

$$\left[\frac{1}{\rho}\frac{d}{d\rho}\,\rho\,\frac{d}{d\rho} + k^2(1-\lambda)\right] G_1(\rho;1-\lambda) = -\frac{1}{2\pi\rho}\,\delta(\rho) \ , \tag{5a}$$

and (letting $q(z) = 1-n^2(z)$)

$$\left[\frac{d^2}{dz^2} + k^2(\lambda-q(z))\right] G_2(z,z';\lambda) = -\,\delta(z-z') \ , \tag{5b}$$

defined, respectively, on the domains $0 \le \rho \le \rho_1$ and $z_1 \le z \le z_2$. It is seen from Eq. 5a that $G_1(\rho;1-\lambda)$ is required to satisfy the delta-function source condition at $\rho = 0$, which is one of the endpoints of its domain. In addition, it is required to satisfy a linear, homogeneous boundary condition at the other endpoint ρ_1. On the other hand, $G_2(z,z';\lambda)$ satisfies the source condition at a point z' within the endpoints of its domain and is required to satisfy linear, homogeneous boundary conditions at the endpoints z_1 and z_2.

The contour C_λ, over which the integral in Eq. 4 is to be evaluated, encloses the λ-plane singularities of G_2 in a positive sense (counterclockwise) or the singularities of G_1 in a negative sense (clockwise). G_1 is given by

$$G_1(\rho;1-\lambda) = \frac{i}{4}\,H_0^{(1)}\left(k\sqrt{1-\lambda}\,\rho\right), \tag{6}$$

$H_0^{(1)}$ being the Hankel function of the zeroth order and first kind. In order to insure that the radiation condition is satisfied for all complex values of λ, the function $\sqrt{1-\lambda}$ is made single-valued by cutting the λ-plane from $-\infty$ to 1 and requiring $\sqrt{1-\lambda} > 0$ on the entire top Riemann sheet. The contour C_λ is then taken to encircle this cut in a negative sense.

The function $G_2(z,z';\lambda)$ is the characteristic Green's function of the depth geometry, and it is required to vanish at the endpoint $z_1 = 0$ and to satisfy the radiation condition at the endpoint $z_2 = \infty$. Note also that $G_2(z,z';\lambda)$ and $dG_2(z,z';\lambda)/dz$ must be continuous for all z. The

solutions for the eigenvalues, λ, and G_2 basically differentiate the types of models within each class.

The Fourier-Bessel Representation

The Fourier-Bessel representation is obtained from the λ-plane representation by a change of variables and a contour deformation to yield

$$P(\underline{r},\underline{r}') = \frac{1}{2\pi}\int_0^\infty \zeta J_0(\zeta\rho)G_2(z,z';1-\zeta^2/k^2)d\zeta \ . \tag{7}$$

The Residue-Series Representation

The contribution to the integral from the poles within a deformed contour gives the solution

$$P(\underline{r},\underline{r}') = \sum_{j=1}^{\infty} \left\{\frac{i}{4} H_0^{(1)}\left(k\sqrt{1-\lambda_j}\,\rho\right)\right\} U(z,\lambda_j)U(z',\lambda_j) \tag{8}$$

where the U's play the role of eigenfunctions and the λ_j must be found in the complex λ plane. The contour deformation which yields this result is valid only for

$$\rho > \sqrt{3}(z+z'); \tag{9}$$

hence the U_j's are not eigenfunctions (in the sense that they do not form a complete set) and the summation diverges for $\rho < \sqrt{3}(z+z')$.

The Normal Mode Representation

A different contour deformation leads to the normal mode representation

$$P(\underline{r},\underline{r}') = \int_{-\infty}^{\infty} \left\{\frac{i}{4} H_0^{(1)}\ (k\sqrt{1-\lambda}\,\rho)\right\}\hat{\phi}(z,\lambda)\hat{\phi}(z',\lambda)d\lambda, \tag{10}$$

where $\hat{\phi}$ are related to the true eigenfunctions ϕ.

If at some depth the ocean bottom is considered to be isovelocity with a sound speed greater than the minimum sound speed in the water then some of the λ_j are real valued and the integral in Eq. 10 becomes a summation over these discrete modes plus an integral over the continuous

spectrum corresponding to the remaining set of complex λ_j. In terms of a ray description, the discrete modes correspond to rays which are either refracted in the water column or strike the bottom at less than the critical angle. The continuous spectrum (and complex λ_j) corresponds to partially reflected rays striking the bottom at greater than critical plus diffraction fields such as "head waves".

Classification of Models

With this background and from the presentations of the participants we have attempted to classify each of the wave models:

1. λ-plane representation - ARL
2. Fourier-Bessel representation - NUSC-3
3. Residue series - NUC-1, ARL, NADC (special purpose models), CU, NRL-2, NUC-2, LDGO
4. Normal mode - NRL-1, NADC (general ocean model), APL, NOL, NUSC-4, NUSC-1, NUSC-2, NRL-3, BTL-2

As can be seen the initial classification of models in Figure 7 did not distinguish between normal modes and residues, and the NUSC-1 and NUSC-2 models were put in the "Other Approaches" category since they were rather different from the other mode programs.

The BTL-1 model of Tappert and Hardin does not fall into any of the above categories since it departs from all other models by approximating the wave equation and numerically solving the resulting equation without resort to separation of variables or normal modes. This approach will be discussed in detail in the section devoted to it.

PRESENTATION OF MODELS

This section summarizes the presentations of each of the models emphasizing the differences between them. Any inaccuracies in these descriptions are regretted and readers are advised to contact the principal investigators for detailed descriptions of their models.

NUC-1 - Naval Undersea Center - D. Gordon and M. Pedersen

This is a residue model in which the sound speed profile (range-independent) is segmented into an arbitrary number of layers within which $n^2(z)$ varies linearly. This leads to a modified equation for the residues λ, and pseudo-eigenfunctions U of the form

$$\frac{d^2U}{dz^2} + \left(k^2-\lambda^2 - a_i(z-z_i)\right)U = 0 \qquad (11)$$

where z_i is the layer depth and a_i depends on the sound-speed and dn^2/dz in the layer. The technique assumes an implicit transformation such that this depth-dependent equation is a standard form. Either, for a given c(z), the independent variables are transformed such that the resultant equation is of a standard form or, given the equation with the independent variable being z, the speed of sound c(z) is transformed. The deepest layer is a semi-infinite space with a negative sound-speed gradient. At the bottom, a radiation condition is imposed such that only outgoing waves are retained.

In order to determine which mode is in fact being calculated a transformation is employed which essentially corresponds to the Airy function behavior of the depth functions in each layer. This allows a check not only on which mode is being calculated but also that all modes have been found. The model is not particularly sensitive to the choice of layer depths or the number of layers. A complex sound speed may be specified in each layer to simulate volume absorption, though generally this is done only for the bottom.

The time and cost required for the test cases ib a UNIVAC 1108 were as follows:

Cases 1A, 1B: 36 sec. CPU ($6)
Case 2: (120 modes) 1 min. 56 sec. ($19)
Case 2 Contours of loss in range and depth: 3 min, 43 sec. ($36).

The program is written in double precision - with 4,000 program and 1,700 library-subroutine steps. There is a 50K core storage limit which implies 350 modes, 8 layers and 50 receiver depths.

NRL-1 - Naval Research Laboratory - J. Cybulski

This is the oldest model and is the basis for a number of normal-mode models presented by the other Navy laboratories. The model assumes a range-independent environment in which the sound speed varies arbitrarily with depth and is constant in the bottom. Finite-difference techniques are employed using a numerical integration of the depth-dependent solutions. An initial guess for the eigenvalue is obtained by assuming the speed of sound in water is constant. The integration proceeds from the ocean bottom to the surface and if the boundary condition P(0) = 0 is not satisfied the eigenvalue is altered slightly and the process repeated. For each choice of eigenvalue, the zero crossings are counted assuring that no modes are missed. As with most models the solution employs the asymptotic form of the Hankel function valid at distances many wavelengths from the source.

For Case 1B, 43 modes were required taking 6 minutes on a CDC 3800; for Case 2, 50 modes; for Case 3A, 6 modes; and for Case 3B one mode. The core storage for the program is 73K octal. All the eigenvalues are real. (If complex eigenvalues are generated they are discarded.) For example, only one real eigenvalue was found for Case 3B, corresponding to one trapped mode.

NADC - Naval Air Development Center - C. Bartberger

Several NADC models have been developed and can be applied under a variety of conditions. Restricted models treat "oceans" with no bottom, and 1, 2 or 3 layers which are special cases of the NUC Residue model. The square of the index of refraction varies linearly in each layer yielding Airy functions for the eigenfunctions. The bottom, when multi-layered, allows for either volume attenuation or a bottom loss specified as a function of the grazing angle for the ray-equivalent of the mode.

A complete ocean model has also been developed which allows for 50 layers in the sound-speed profile. The original input profile is then effectively approximated by homogeneous layers in a finite-difference algorithm similar to that in NRL-1. Initial guesses for the eigenvalues are obtained using the WKB approximation and the solution is obtainedbby integrating in depth from the bottom to the surface, counting zero crossings and iterating. While the models are fully automated they sometimes have difficulty finding the eigenvalues. Bartberger feels that the arbitrary profile model is as flexible as the present ray models. He suggests that an obvious improvement is to have a variable layer thickness. Furthermore, he believes that there should be at least two models: a surface-duct, bottomless model and a full-ocean model incorporating bottom characteristics.

ARL - Applied Research Laboratory - R. Deavenport and J. Beard

The ARL model uses the λ-plane representation for a specialized case where the inverse square of the velocity field is characterized by a five parameter function, the Epstein profile:

$$\frac{1}{C^2} = A \operatorname{sech}^2 \frac{z-z_o}{H} + B \tanh \frac{z-z_o}{H} + D \qquad (12)$$

This is extendable to seven parameters and the coefficients may be determined to reasonably model refracted energy in deep-ocean sound channels. Surface or bottom-reflected paths cannot be modeled. The depth-dependent Green's function $G_2(z,z';d)$ is given by hypergeometric functions and the eigenvalue spectrum is composed of discrete values and a continuous set. No approximations are employed in arriving at the solution, however, it has been found to be very sensitive to small changes in the velocity

profile. The program is very rapid and was presented as a possible control program to test approximate techniques. The solutions, however, only include those modes with phase velocities close to the sound speed at the source.

There was substantial discussion regarding the ARL output and its relation to the NUC output at short ranges for Case 1B since the "bottomless" ARL model showed higher levels between 10 and 20 miles than the NUC model with bottom-reflected paths. In the course of the discussion it was noted that, in bottom-bounce areas with high loss, important contributions to the field come from only a few modes which are always in phase; the remaining modes tend to destructively interfere with each other and the resulting low level may have been missed in the ARL model by limiting the modes considered.

APL - Applied Physics Laboratory - N. Nicholas

The APL model is also a sound-channel model, (no surface or bottom) in which the sound-speed profile is parabolic in depth:

$$\frac{c_0}{c(z)} = (1 - \alpha^2 z^2)^{1/2} \tag{13}$$

The depth functions for the resulting normal modes are Hermite Polynomials and are finite in number for this type of profile. This model has been used primarily to investigate the periodic focusing regions predicted for parabolic profiles in axis-to-axis geometries. Slightly differing velocity profiles may be accomodated using perturbation techniques analogous to those of quantum mechanics. The corresponding potential function is of the form

$$V(z) = k^2\alpha^2 z^2 + V^1(z) \tag{14}$$

where

$$V^1(z) << k^2\alpha^2 z^2 \tag{15}$$

and $V^1(z)$ is a fourth order polynomial. Strong axial focusing disappears with the introduction of the perturbation potential. Modifications to include boundaries have been explored and give rise to infinite series in addition to the Hermite Polynomials. The radius of convergence of these series of solutions is quite reasonable when tested with conventional power-series convergence criteria.

NOL - Naval Ordnance Laboratory - I. Blatstein, H. Uberall, A. Newman

The NOL model is an outgrowth of the NRL-1 normal-mode model applicable to deep water, and uses a finite-difference technique to

obtain numerical solutions. The continuous portion of the spectrum is ignored for deep water cases and only modes with phase velocities less than the velocity of the bottom are included. The equivalence of the normal-mode and residue techniques is demonstrated by the excellent agreement with NUC-1 for Case 1B. The following table summarizes running statistics of the NOL model for the four test cases:

Case	Modes	Time (sec)	Cost
1B	43	230	$(25.00)?
2	81	350	$ 40.00
3A	5	19	$ 2.40
3B	1	42	$ 4.70

All numerical solutions are single precision and core storage is 60K octal words on a CDC 6400.

Comparisons were shown of predicted convergence-zone levels using ray theory, normal-mode and modified ray theory as given by Silbiger and Sachs.* Within the insonified region the three approaches are in very good agreement, until, in the immediate vicinity of the caustic, the ray theory intensity becomes infinite. In the shadow zone the normal-mode and modified ray-theory results maintain a high level of agreement.

CU - Catholic University - V. Nomady and H. Uberall

This program was specifically designed to consider the effects of earth curvature on wave solutions for a deep ocean at long ranges. The ocean is characterized by a single layer in which the sound speed is given by an Epstein profile. The field is then expressed in terms of spherical harmonics (Legendre and Jacobi polynomiols). By applying the Watson transformation the CW response is obtained in terms of two contour integrals plus a series of residues where the series dominates at long ranges. Physically the solution may be interpreted as standing waves in the depth coordinate and circumferentially outgoing waves on a spherical boundary. Efforts are under way to obtain the solution for a pulsed source.

NRL-2 - Naval Research Laboratory - R. Fitzgerald

This model is essentially the same as the NUC-1 model; the major differences being associated with the treatment of the ocean bottom. The NUC-1 model allows the sound speed to go to zero for very large z, whereas this model terminates the profile exactly as specified allowing for fully trapped modes. As presently configured the program does not attempt to normalize the source. The results were normalized by AESD by comparing key features in the predictions with similar features in other, normalized, predictions.

---

* JASA, Volume 49, 1971, pp. 824-840

NUSC-4 - Naval Undersea Systems Center - W. Kanabis

This program is a normal-mode model nearly identical to NRL-1 and was designed primarily for shallow-water studies. The only modes which are kept correspond to bottom grazing angles which are less than critical and these modes suffer no loss due to interaction with the bottom. For current applications no normalization is attempted.

NUSC-1 - Naval Undersea Systems Center - G. Leibiger

This model is called "Ray-Mode" since it uses ray concepts to assist in obtaining a wave solution. Expressing the field in a Green's function formulation the zeros of the Wronskian (or poles of the Green's function) are found by phase-integral techniques using rays. From this WKB technique the real and imaginary parts of the eigenvalues are determined. Since the λ-plane integral is dominated by contributions near these poles the integral may be replaced by a summation and the contributions from each term may be interpreted physically in terms of rays cycling through the medium. While the model was presented as it might apply to a surface-duct problem, the technique is generally applicable by an appropriate modification to the Wronskian.

NUSC-2 - Naval Undersea Systems Center - H. Weinberg

This is a normal-mode model capable of treating a fully three-dimensional environment (that is both range and azimuth dependences in the sound-speed and bottom descriptions). By employing a stretching of coordinates in the horizontal plane with a small-parameter expansion the field is described in terms of the normal-modes or depth functions of the geometry which areaallowed to vary slowly with range. (In the present version only adiabatic variations are permitted.) Departures from cylindrical symmetry are accounted for by computations of the azimuthal divergence in the amplitude of each mode as given by a ray-trace in a coordinate system orthogonal to the modes. In practice the modes must be recomputed at each range where the sound-speed profile or the bottom depth changes significantly. Predictions were compared with measurements made in a range-dependent environment showing excellent agreement to very long ranges.

NUSC-3 - Naval Undersea Systems Center - F. DiNapoli

This fast field program (FFP) directly integrates the Fourier-Bessel transform allowing for a segmented (range independent) velocity profile and a fluid bottom. After taking the asymptotic expansion for J_0, the integral was found to be strikingly similar to a Fourier Transform. Thus, the solution appeared to be a discrete Fourier Transform from wave number space to range space where the Green's function was

considered to now be a function of wave number. The difficulty was to obtain a Green's function which permitted rapid computation for many wave numbers. Various techniques have been tried and abandoned including numerical integration and solutions in terms of hypergeometric functions. Known solutions were then investigated and it was found that if the sound velocity were described in terms of exponentials then the Green's function became a linear combination of Bessel functions. In fact, the wave number appears only in the order of the Bessel function and recursion relations were found which made the computation feasible. In practice the input sound-velocity profile is fit with several exponential segments which then form the working profile. The program is three years old and has yielded excellent agreement with NADC's model on several test cases. Running times are comparable to those for the NADC and NOL models and the frequency may range from very low to perhaps 3.5kHz. This is the only model which can routinely accomodate such high frequencies. Such cases are, however, severely limited in range.

LDGO - Lamont-Dougherty Geophysical Observatory - H. Kutschale

This program is primarily concerned with under-ice acoustics and, therefore, allows for a solid surface as well as a solid bottom. The solution consists of a branch-line integral plus residue contributions, and FFP techniques (see NUSC Rept. No. 4103) have been incorporated to evaluate the branch-line integral. A liquid bottom gives rise to one branch-line integral while a solid bottom gives rise to two. The contributions to the field from the branch-line integral are felt to be quite important at low frequencies.

BTL-1 - Bell Telephone Laboratories - F. Tappert and R. Hardin

This model's last point of commonality with all other models presented is the wave equation. The model has three basic components, each of them independent of the other two:

1. The model approximates the elliptic wave equation with a parabolic equation equivalent to a small-angle approximation in ray theory.
2. The resulting equation is then solved by means of the recently developed split-step Fourier algorithm.
3. The resulting levels of intensity as a function of range and depth are then contoured using a new, rapid contouring technique.

Beginning with the wave equation for a cylindrically symmetric geometry and letting

$$P(r,z) = \psi(r,z)\, H_0^{(2)}(kr) \qquad (16)$$

and making the following approximations:

$$kr \gg 1$$

$$\psi_{rr} \ll 2ik\psi_r \tag{17}$$

the parabolic equation

$$i\psi_r + \frac{1}{2k}\psi_{zz} + \frac{k}{2}(n^2(r,z)-1)\psi = 0 \tag{18}$$

is obtained. The application of this parabolic equation to a number of problems is discussed in Electromagnetic Diffraction and Propagation Problems edited by Fock (Peagamon Press, 1965). The approximations which yield the parabolic equation are: first, the usual far-field asymptotic expansion for the Hankel function; and second, the assumption that the waves are predominantly radial - that is the corresponding rays are at relatively shallow angles. This second approximation includes the neglect of any backscatter.

For the original elliptic wave equation the boundary conditions must be prescribed on a closed surface (or as a radiation condition), and the direct solution involves iterative approaches such as relaxation techniques. Parabolic equations may be solved by marching the solution away from a surface on which initial conditions are specified. Hence, if $\psi(r,z)$ is specified for any range r then the split-step Fourier algorithm yields at a small step Δr:

$$\psi(r+\Delta r,z) = e^{i\Delta r\, k\,(n^2-1)/2}\, \mathcal{F}^{-1}\left(e^{-i\Delta r \ell^2/2k}\, \mathcal{F}(\psi(r,z))\right) \tag{19}$$

where $\mathcal{F}$,,is a Fourier transform from z to ℓ and $\mathcal{F}^{-1}$ is the inverse transform from ℓ to z.

Application of this technique to ocean-acoustics problems requires the following steps:

1. Define a basic medium which consists of the original medium reflected across the ocean surface.
2. Insert into this geometry the source (or receiver) of interest and its reflection (or image) phase shifted by 180 degrees. This removes the boundary condition at the ocean surface.
3. Extend the medium (and its reflection) with a highly absorbing layer at a depth greater than the deepest portion of the ocean considered.
4. This double medium may now be considered to be infinitely periodic in depth since no energy from the other pairs of sources can penetrate the absorbing layer to affect the field at points of interest. Hence, the region of interest may be sampled with a grid in z and Fast Fourier Transforms may be used to evaluate Eq. 19 resulting in a rapid integration of ψ.

The graphical contour displays are quite useful in analyzing the field properties and examples were shown for each of the test cases plus two range-dependent problems:

1. Long-range transmission in the North Pacific.
2. The field in a weakening surface duct. Figures 65 and 66 illustrate this case for the surface duct of test case 1A which is then allowed to become isovelocity (the range scale of this second plot is slightly more compressed than on the previous plot).

Tappert outlined the strengths and weaknesses of the model. The obvious strengths in terms of the environment are:

1. A range-dependent sound-speed profile.
2. A variable-depth ocean bottom (which is modeled as refracting rather than as a reflecting surface).
3. Variable volume absorption may be included directly in the index of refraction.

The limitations of the model are:

1. The small angle approximation limiting equivalent rays to $\simeq 20°$.
2. The resulting limitation that energy reflecting from steep up-slopes into steeper angles may be improperly modeled.
3. The high-frequency limit determined by the maximum size FFT which can efficiently be used.
4. Discontinuities requiring careful treatment to avoid numerical problems.
5. The present model was not normalized and there are some problems associated with modeling a point source. AESD normalized the predictions in the same way as the NRL-2 predictions.

The advantages of the numerical technique which arise in the solution of parabolic equations are:

1. The accuracy is good to second order in range which implies large steps in range are possible.
2. Energy is conserved.
3. The numerical technique is unconditionally stable.
4. It is easy to implement.
5. It is computationally efficient.

The disadvantages are:

1. The boundary conditions must be periodic in depth.
2. A uniform grid is required.

A number of questions remain concerning specific applications to ocean-acoustics problems since the program was originally developed for electromagnetic applications. The consensus at the close of the workshop was, however, that this was one of the most exciting innovations in propagation modeling in recent years.

NRL-3 - Naval Research Laboratory - F, Ingenito

This is a normal-mode program similar to the NRL-1 and NOL models except that it is limited to three layers. It calculates only discrete modes and has real eigenvalues and real eigenfunctions. At present it is being expanded to consider bottom and surface absorption.

NUC-2 - Naval Undersea Center - H. Morris and H. Bucker

This is the same basic residue model as NUC-1 but restricted to surface-duct geometries and extended to include rough-surface effects. Lambert's Law is applied to the modes (with the angle of incidence obtained from the ray equivalent) to describe rough-surface scattering. The first-order effects are a reduction in intensity in the duct and an enhancement below the duct. Second order effects are being investigated which include cross-coupling between modes. Comparisons with SUDS data showed impressive agreement in many cases though the surface-duct problem is by no means completely solved. This model is described in detail in JASA, volume 48, 1970, pp. 1187-1194.

BTL-2 - Bell Telephone Laboratories - F. Labianca and E. Harper

This is also a surface duct model using normal modes rather than residues. The basic model is documented in JASA volume 53, 1973, pp. 1137-1147. Because normal modes are used, rather than residues, a basis is available for expanding arbitrary functions. This allows for a novel approach to the incorporation of a rough surface in the surface duct by:

1. Decomposing the surface into its Fourier components (assuming the applicability of the method of superposition, i.e. that the surface may be linearized).
2. Expanding the surface profile for each component in terms of the eigenfunctions or normal modes of the surface duct.
3. Considering realistic surfaces with small displacements and slopes.
4. Using perturbation techniques on the basic mode solution to compute the resulting rough-surface effects.

Questions raised and not fully answered about this technique concern the domains of applicability in terms of the relative size of acoustic wavelength, surface wavelength, surface amplitude, and duct thickness.

WORKING SESSIONS

It was the purpose of the working sessions to focus the discussion on specific applications and to assess the state-of-the-art in these areas. While issues are rarely settled at such sessions (and frequently more heat than light is generated) the needs of the advanced development

community, as expressed by AESD, were conveyed to the participants. It is impossible to present fully the discussions in each working session and in this report we will only attempt to reproduce the basic questions and our resulting assessment of the state-of-the-art.

A. Rough-Surface Scattering

The basic question is: how may a rough ocean surface be incorporated in acoustic wave propagation programs.

The NUC-2 and NUSC-1 models are the only ones which currently consider rough-surface effects. For the coherent field an effective reflection coefficient is used. The incoherent field is scattered in all directions using Lambert's Law. The mode reflection coefficient is inferred from the plane-wave reflection coefficient for an angle of incidence given by the ray equivalent of the mode and is limited to statistically rough surfaces of small amplitude. The parameter required is "significant wave height" which may be related to rms wave amplitude and thence to wind speed.

The BTL rough-surface approach described by Labianca is the only one under consideration which does not require the mixture of ray and mode concepts and hence is on a rigorous theoretical basis. The approach has not yet been implemented and the questions regarding relative lengths remain to be resolved.

A detailed presentation of the mathematical formulation of surface scattering was made by Richard Holford of BTL. He presented an exact analytical solution for plane-wave scattering from a periodic surface. The basic assumption of physical optics is not made and the solution is presented in the form of an integral equation of the second kind which is solved by matrix inversion where convergence is assured. This technique may serve as a useful control for comparisons with approximate techniques and Holford showed a sample case where the method of physical optics clearly breaks down. This approach to scattering is available in several BTL reports.

George Zipfel presented work from a paper he and John Disanto of NRL published on surface scattering (Journal of Math Physics 13, 1972, pp. 1903.) The surface is treated as a multi-variant Gaussian distribution and the results are presented as an ensemble average in terms of correlation functions. A series of diagramatical rules similar to Feynman diagrams enable a straightforward approach to the problem to be implemented.

With the above techniques the modal approaches to incorporation of rough surface in wave programs appeared to be heading in the right direction for the problem of paramount importance - the surface duct. Tappert felt that the parabolic equation technique could be applied to rough surfaces, especially for the surface duct where the angles of incidence are small.

B. Volume Attenuation

The volume attenuation question is primarily one of measurement. While measuring volume attenuation at high frequencies is relatively straightforward, low-frequency measurements require extremely long baselines and have led to several conflicting results. The basic technique is to measure long-range transmission loss at a number of frequencies in an axis-to-axis geometry using explosive charges or "shots". Departures from cylindrical spreading are then ascribed to volume attenuation with least square fits made to the loss after removal of the cylindrical spreading term.

The basic assumption of this technique is that the range dependence of the spreading losses associated with axis-to-axis transmission measured using bandpass filtering of shot signals exhibits a 1/R average behavior. This assumption has been justified by the observation that the rms sum of normal modes (representing a range average of a CW signal level) behaves cylindrically, and by calculations of DiNapoli using the FFP model which indicate that the influence of boundaries on axis-to-axis propagation is felt only at extremely low frequencies.

The questions left unanswered are:

1. What frequency/range dependent effects are introduced by the shots and the filtering?
2. What frequency/range dependent effects are introduced by range-dependent changes in the sound-speed profile?

While geometries for experiments are chosen with great care to avoid the issues raised in question 2, data from the KIWI measurements were shown showing significant range dependence in the "absorption" which appears to be explainable in terms of unanticipated intervening bathymetry.

It has also been pointed out by Labianca that the introduction of a complex index of refraction makes the wave equation non-self-adjoint and appears to radically alter the eigenvalue spectrum. (In the example of a surface duct the spectrum jumps from real-continuous to complex-discrete). Whether this is an important distinction is not resolved but the inclusion of volume absorption by a complex index of refraction may cause unexpected problems.

C. Range Dependences in the Environment

The key question here is how are range dependences in the sound-speed profile and/or bottom profile accomodated. There are four basic approaches to the problem:

1. The parabolic equation technique (BTL-1) which, within its small-angle limitation handles range variations with no additional approximations.

2. The NUSC-2 model which includes only first order mode-coupling (i.e. an adiabatic approximation) but also includes effects due to the lack of cylindrical symmetry.

3. Other adiabatic approaches (NUC-1, NRL-3) where only the rms sum of modes is considered.

4. A non-adiabatic technique where the medium changes discontinuously at specific ranges. At such a range the field (as computed from the modes in the first region) is expanded in terms of the normal modes of the new region (thus giving the mode amplitudes). Fitzgerald of NRL is using this technique neglecting all backscatter from the discontinuity, and DiNapoli is considering FFP techniques where the backscattered field is also included in an iterative way.

Only the parabolic equation contains the full coupling between modes. Additional work at CU is under way to approximate mode coupling. Holford presented an exact solution he had obtained for the field due to a line source (taken to be the z axis) for a biquadratic variation in n^2 with range and depth. The solution is written in terms of an integral of the form

$$\psi \sim \int_{-\infty}^{\infty} g(\xi) e^{ikf(x,y;\xi)} \, d\xi \qquad (20)$$

While this solution does not permit boundaries it does allow for a range dependent sound channel and may prove quite useful as a control case. This result is documented in a BTL report.

D. Modeling the Ocean Bottom

The basic approaches to modeling the ocean bottom are relatively straightforward within the context of each model. Kutschale and DiNapoli have devoted considerable attention to the problem of layering in the bottom and its implications for propagation. Both felt that contributions from the continuous spectrum in modeling the response from the bottom at short ranges could not be neglected.

Some of the normal-mode programs (NADC, NUC-1) allow for the full computation of the mode amplitudes for a layered bottom or the introduction of a "reflection coefficient" as a function of angle of incidence for plane waves at the angle of the ray equivalent for the mode. DiNapoli had made comparisons of FFP with the CONGRATS Ray-Tracing Program where

the FFP was used to determine the plane-wave reflection coefficients for a multi-layered bottom which were then used by CONGRATS for rays reflecting from the ocean-bottom interface. Comparisons of full FFP and CONGRATS runs showed alarmingly large differences in the bottom-bounce regions. This also raised several interesting (and unanswered) questions concerning the reverse problem - that is how to use measured plane wave reflection coefficients (presumably determined with the aid of ray-tracing) in wave models.

E. Modeling Source Characteristics

The two primary questions in modeling sources are:

1. How to model broadband shots (and the shot processor)?
2. How to model source directionality?

The obvious brute-force way to model broadband sources is by running normal-mode programs at a variety of frequencies and convolving the result with the source spectrum. DiNapoli is in the process of extending the FFP to do this in a more elegent (if not more efficient) way.

Source patterns can be modeled with multipole expansions (presently being studies at CU), though this involves reworking the problem for each new environment. No direct weighting of mode amplitudes with the directivity pattern for the ray equivalent has been attempted. The parabolic equation technique might be applied to this problem since in its transform space the independent variable is quite similar to an angle.

F. Smoothing Wave Results

The question was posed as to how one obtains mean transmission loss with normal mode programs. DiNapoli fits the results of the FFP to cyclindrical spreading plus a constant which is determined by regression analysis. This technique fails if there are strong convergence zones. Bartberger has an extremely simple approach which is to use a weighted sliding window. Examples were presented which showed that as the width of the window was increased the rapid oscillations were removed yielding results very similar to the FACT predictions.

G. Signal-Processing Applications

The entire field was not considered - only the question of coherence and wave-front distortion. Simulation work is being done by DiNapoli on the problem of wave-front distortion in the vertical plane. The problems of horizontal coherence across arrays are considerable and at present are being addressed only by ray acoustics. Application of the

NUSC-2 Model to this problem might be fruitful if the necessary environmental information were available.

SUMMARY AND ACKNOWLEDGEMENTS

From the point of view of AESD the workshop was quite successful in assessing the state-of-the-art in non-ray-tracing acoustic propagation models. Subsequent feed-back from participants suggests a consensus view that it was successful from their viewpoint in helping both to avoid duplication of effort and to illuminate potential areas of R&D relevent to the Navy's advanced development needs. 17 models were presented with a total of over 50 predictions. The success of this workshop was the direct result of the enthusiastic support and participation of everyone concerned.

TEST CASE NO. 1

PACIFIC PROFILE

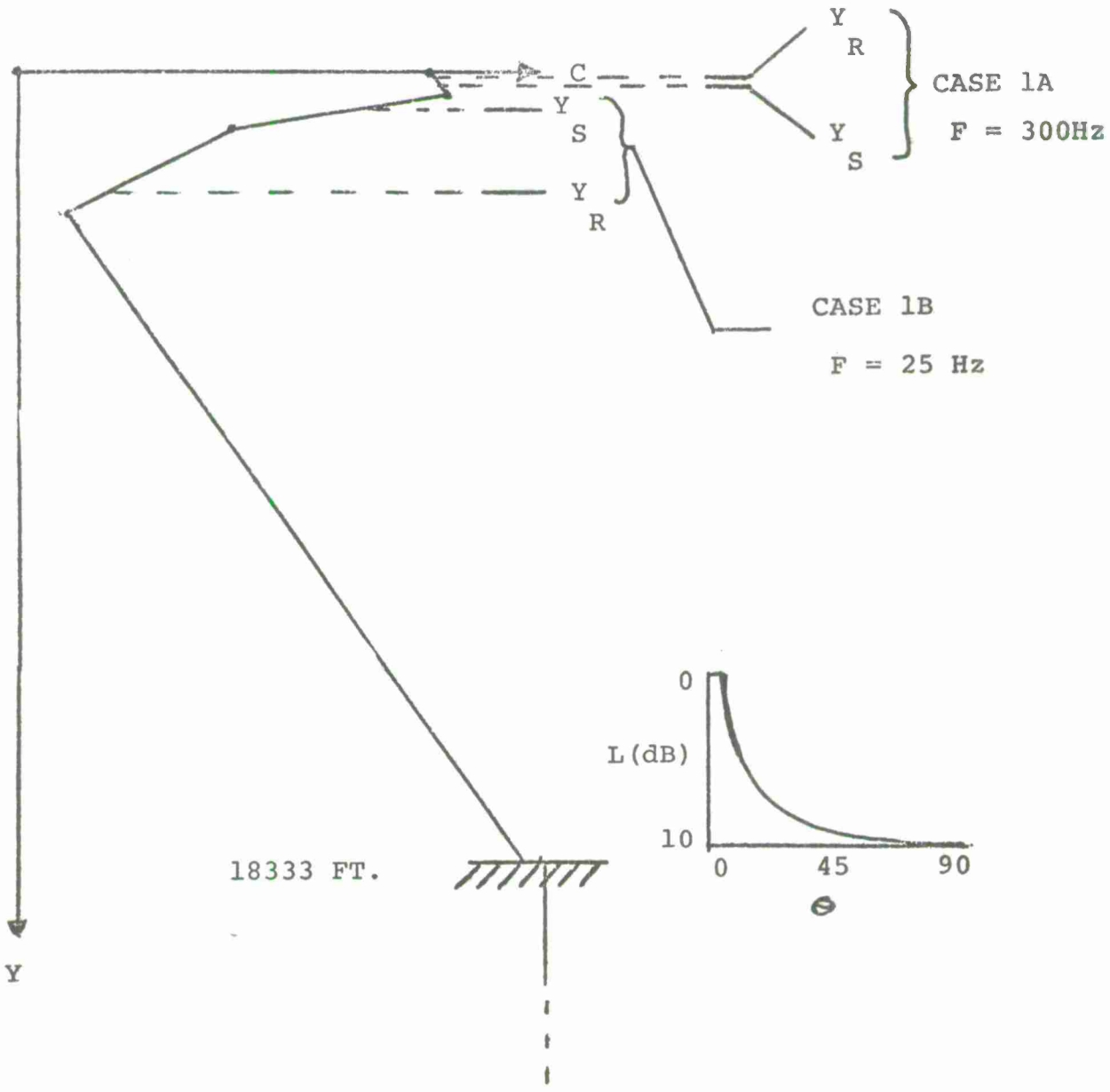

FIGURE 1

TEST CASE NO. 1

Z(F)	C(F/S)	ρ(gm/cc)
0	5041	1.0
500	5050	1.0
1333	4925	1.0
3333	4829	1.0
18333	5084	1.0
18333+	5103.42	1.9176

1a. Short Range - Surface duct (profile below thermocline, and bottom-bounce may be ignored)

YS = 300' YR = 90' f = 300Hz

Range = 0 to 20nm

Scales: 10dB/inch
2nm/inch

1b. Long Range

YS = 833' YR = 2833' f = 25Hz

Range = 0 to 120nm

Scales: 10dB/inch
10nm/inch

FIGURE 2

TEST CASE NO. 2

NORTHEASTERN ATLANTIC PROFILE

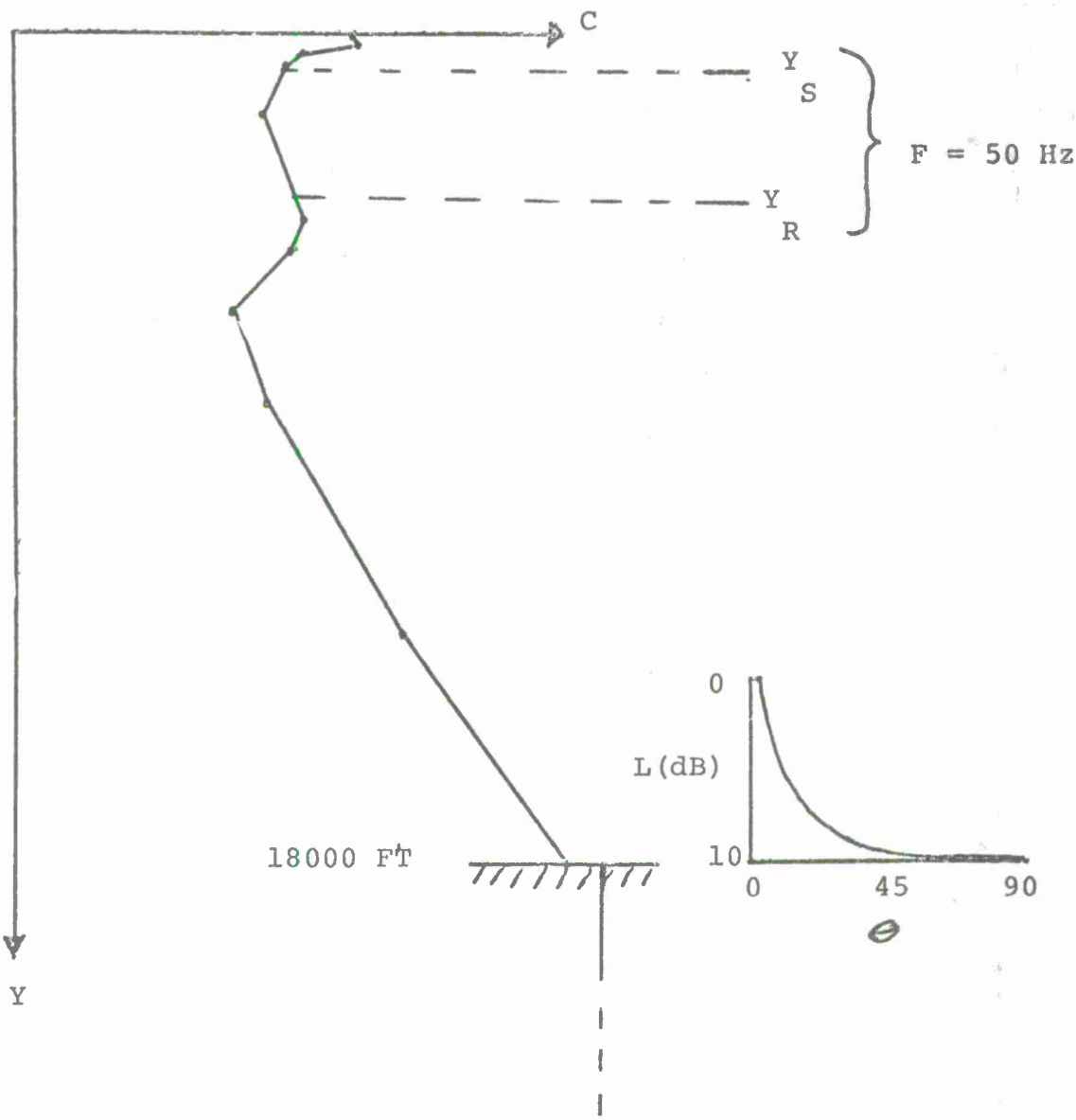

FIGURE 3

TEST CASE NO. 2

Z(F)	C(F/S)	ρ(gm/cc)
0	4984	1.0
200	4988	1.0
300	4958	1.0
600	4945	1.0
1600	4934	1.0
4000	4960	1.0
4600	4950	1.0
6000	4920	1.0
8000	4937	1.0
13000	5012	1.0
18000	5100	1.0
18000+	5119.4	1.9176

YS = 800' YR = 3600' f = 50Hz

Range = 0 to 300nm

Scales: 10dB/inch
25nm/inch

FIGURE 4

TEST CASE NO. 3

SHALLOW WATER

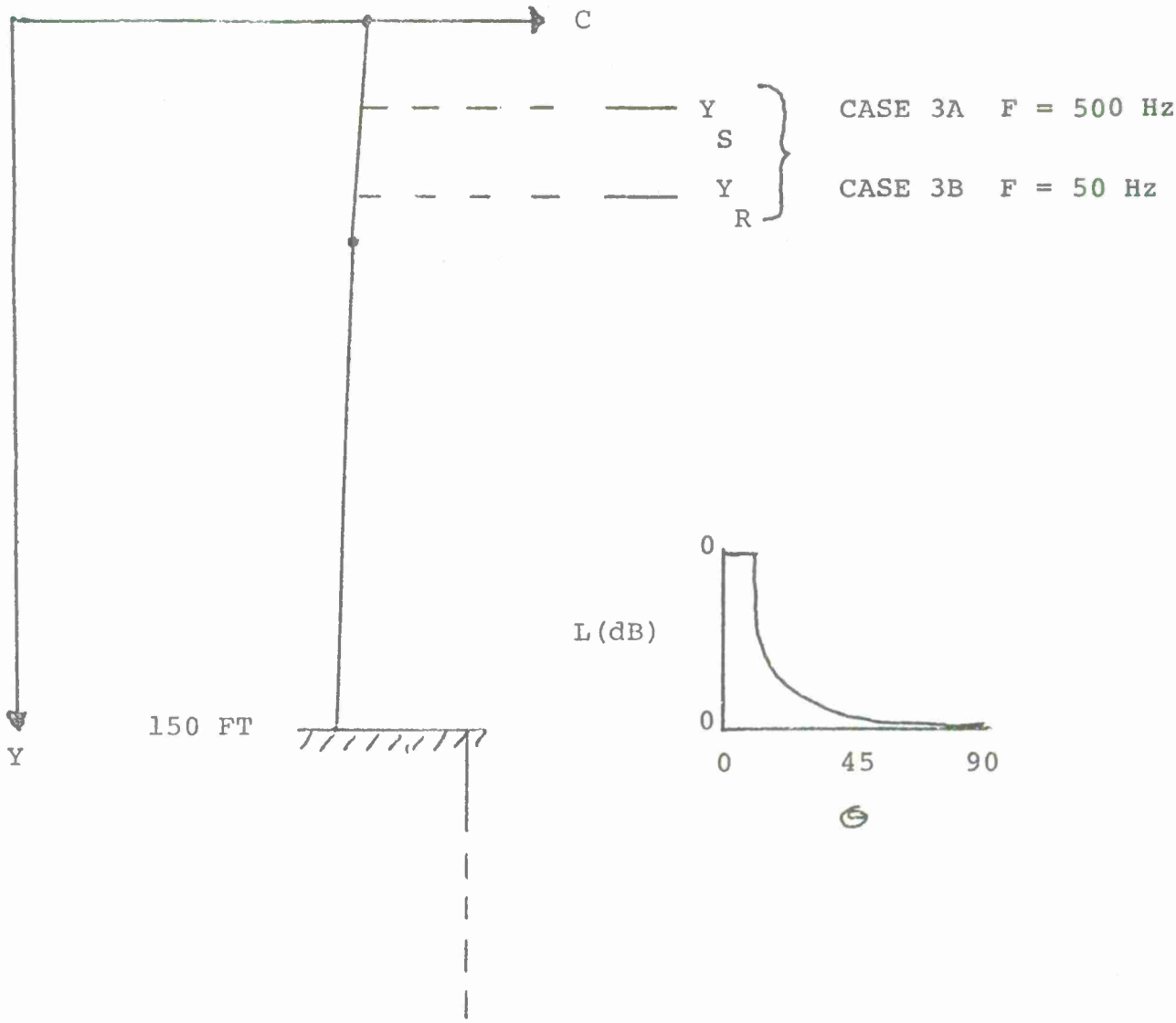

FIGURE 5

TEST CASE NO. 3 - Shallow Water

Z(F)	C(F/S)	ρ(gm/cc)
0	5000	1.0
50	4990	1.0
150	4980	1.0
150+	5056.8	1.4

YS = 20' YR = 40'

Range = 0 to 25nm

3a. f = 500Hz

3b. f = 50Hz

Scales: 10dB/inch
2.5nm/inch

FIGURE 6

MODELS AND PARTICIPANTS

		CASES				
LONG RANGE "NORMAL MODE"		1A	1B	2	3A	3B
NUC-1	GORDON, PEDERSEN	X	X	X		
NRL-1	CYBULSKI		X	X	X	X
NADC	BARTBERGER	X	X	X	X	X
ARL	DEAVENPORT, BEARD	X	X		X	X
APL	NICHOLAS		(X)			
NOL	BLATSTEIN, UBERALL, NEWMAN		X	X	X	X
CU	NOMADY, UBERALL		(X)			
NRL-2	FITZGERALD	X	X	X		
NUSC-4	KANABIS	X	X	X	X	X
LONG RANGE OTHER APPROACHES						
NUSC-1	LEIBIGER	X	X	X	X	X
NUSC-2	WEINBERG		X	X	X	X
NUSC-3	DINAPOLI	X	X	X	X	(X)
LDGO	KUTSCHALE					
BTL-1	TAPPERT, HARDIN	X	X	X	X	X
SHALLOW WATER						
NRL-3	INGENITO				X	X
SURFACE DUCT						
NUC-2	MORRIS, BUCKER	X				
BTL-2	LABIANCA, HARPER	X				

FIGURE 7

ATTENDEES AND ORGANIZATIONAL AFFILIATION

NAME	ORGANIZATION
Mr. D. Gordon	Naval Undersea Center
Mr. M. Pedersen	Naval Undersea Center
Mr. C. Bartberger	Naval Air Development Center
Mr. J. Cybulski	Naval Research Laboratory
Mr. B. Palmer	Naval Research Laboratory
Mr. R. Deavenport	Applied Research Laboratory
Dr. J. Beard	Applied Research Laboratory
Dr. N. Nicholas	Applied Physics Laboratory
Dr. I. Blatstein	Naval Ordnance Laboratory
Dr. H. Uberall	Catholic University
Dr. A. Newman	Naval Research Laboratory
Dr. V. Nomady	Catholic University
Dr. R. Fitzgerald	Naval Research Laboratory
Dr. G. Leibiger	Naval Underwater Systems Center
Dr. H. Weinberg	Naval Underwater Systems Center
Dr. F. DiNapoli	Naval Underwater Systems Center
Dr. F. Tappert	Bell Telephone Laboratories
Dr. F. Labianca	Bell Telephone Laboratories
Dr. R. Holford	Bell Telephone Laboratories
Dr. J. Polak	Bell Telephone Laboratories
Dr. F. Ingenito	Naval Research Laboratory
Ms. H. Morris	Naval Undersea Center
Dr. H. Bucker	Naval Undersea Center
Dr. L. Solomon	Planning Systems Incorporated
Dr. B. Koopman	Arthur D. Little, Inc.
Dr. W. Hardy	University of Hawaii
Dr. P. Smith	Bolt, Beranek and Newman
Dr. D. Stickler	Applied Research Laboratory (Penn State)
Dr. J. Anton	Systems Control, Inc.
Dr. R. Cavanagh	Acoustic Environmental Support Detachment
Dr. R. Buchal	Acoustic Environmental Support Detachment
Mr. H. Brock	Acoustic Environmental Support Detachment
Dr. H. Kutschale	Lamont-Dougherty Geophysical Observatory
Dr. G. Zipfel	Naval Research Laboratory
Mr. C. Spofford	Acoustic Environmental Support Detachment
CDR P. Tatro	Acoustic Environmental Support Detachment

FIGURE 8

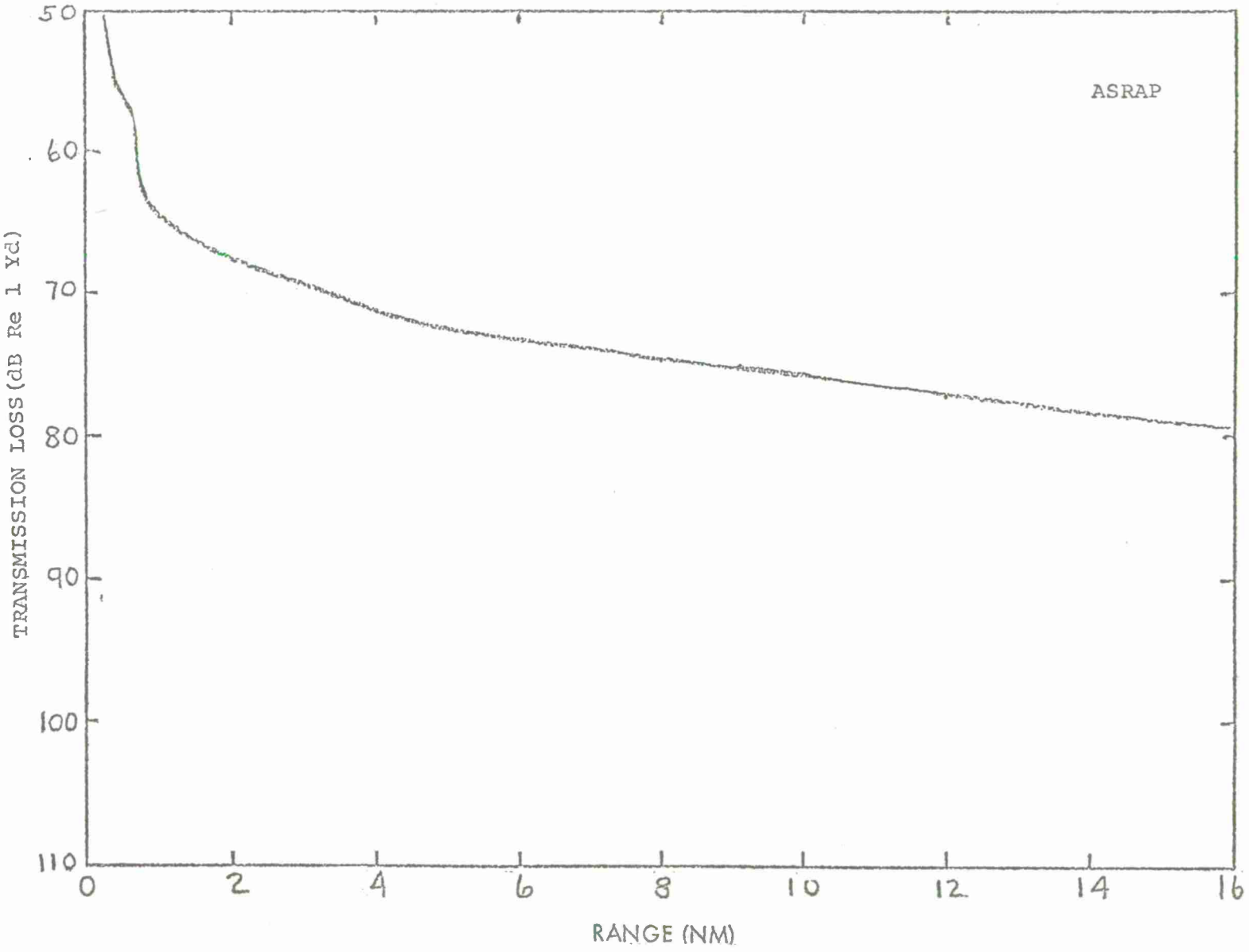

CASE 1a - SURFACE DUCT - Y_S = 300 FT Y_r = 90 FT F = 300 HZ

FIGURE 9

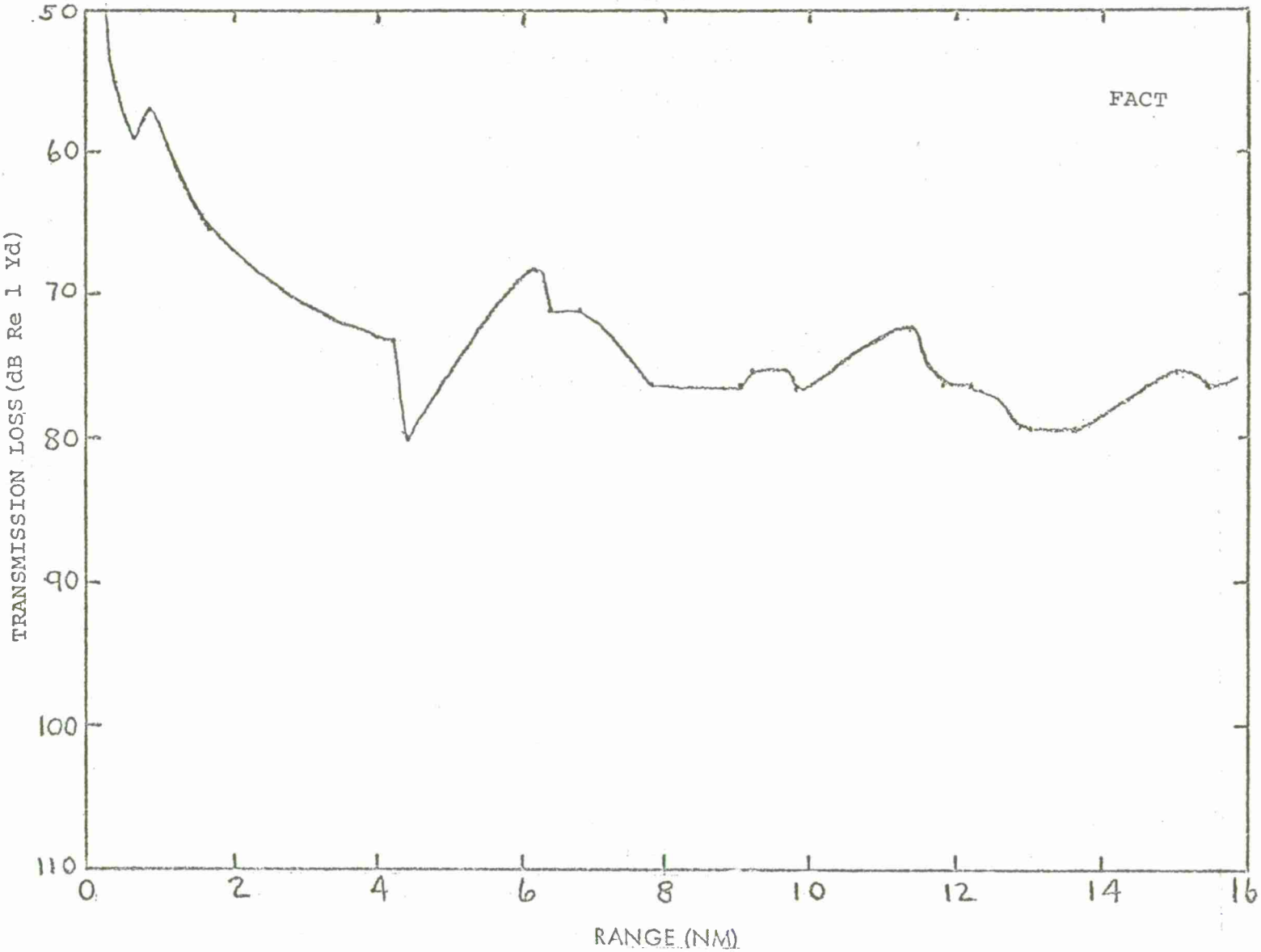

CASE 1a - SURFACE DUCT - Y_S = 300 FT Y_r = 90 FT F = 300 HZ

FIGURE 10

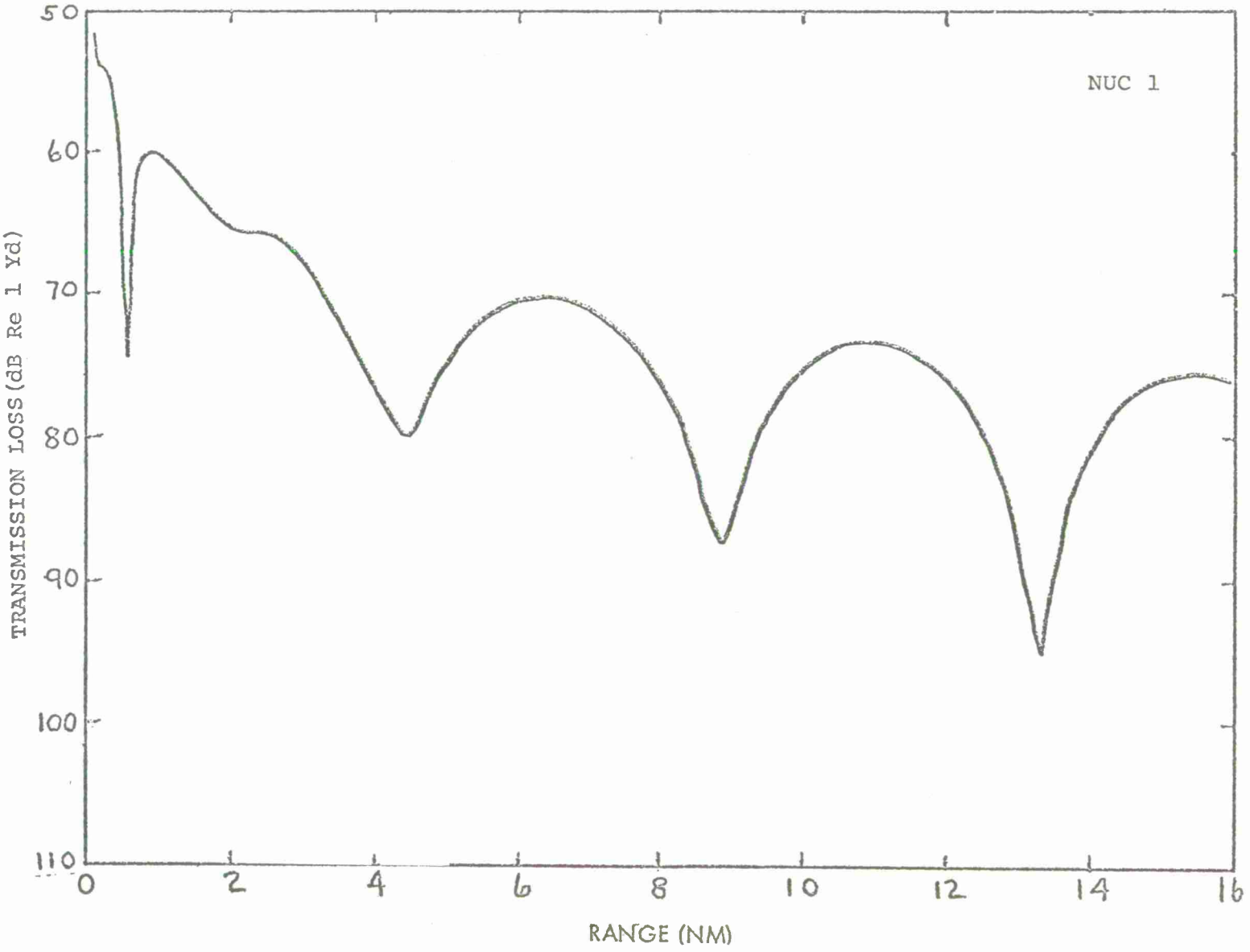

CASE 1a - SURFACE DUCT - Y_S = 300 FT Y_T = 90 FT F = 300 HZ

FIGURE 11

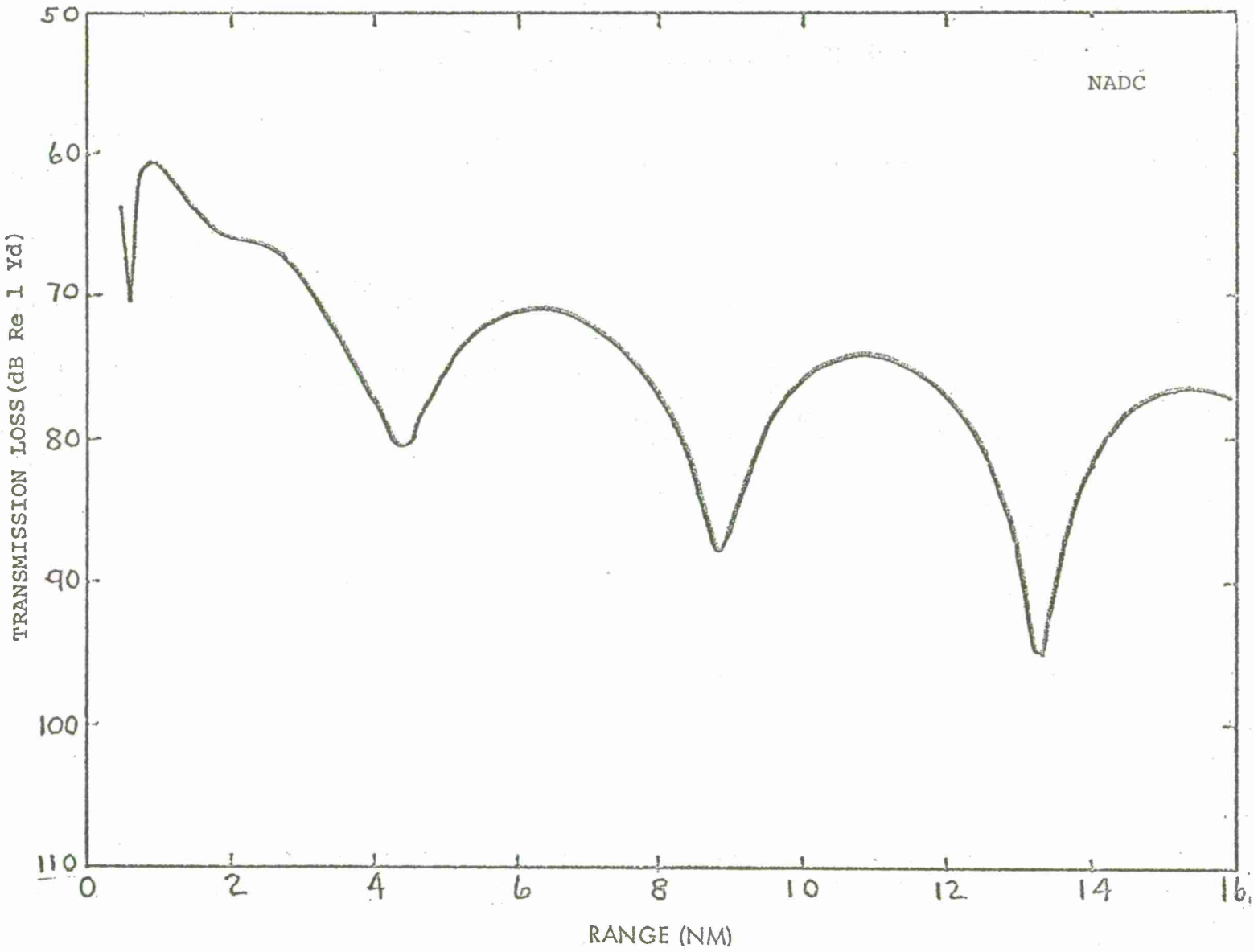

CASE 1a - SURFACE DUCT - Y_S = 300 FT Y_r = 90 FT F = 300 HZ

FIGURE 12

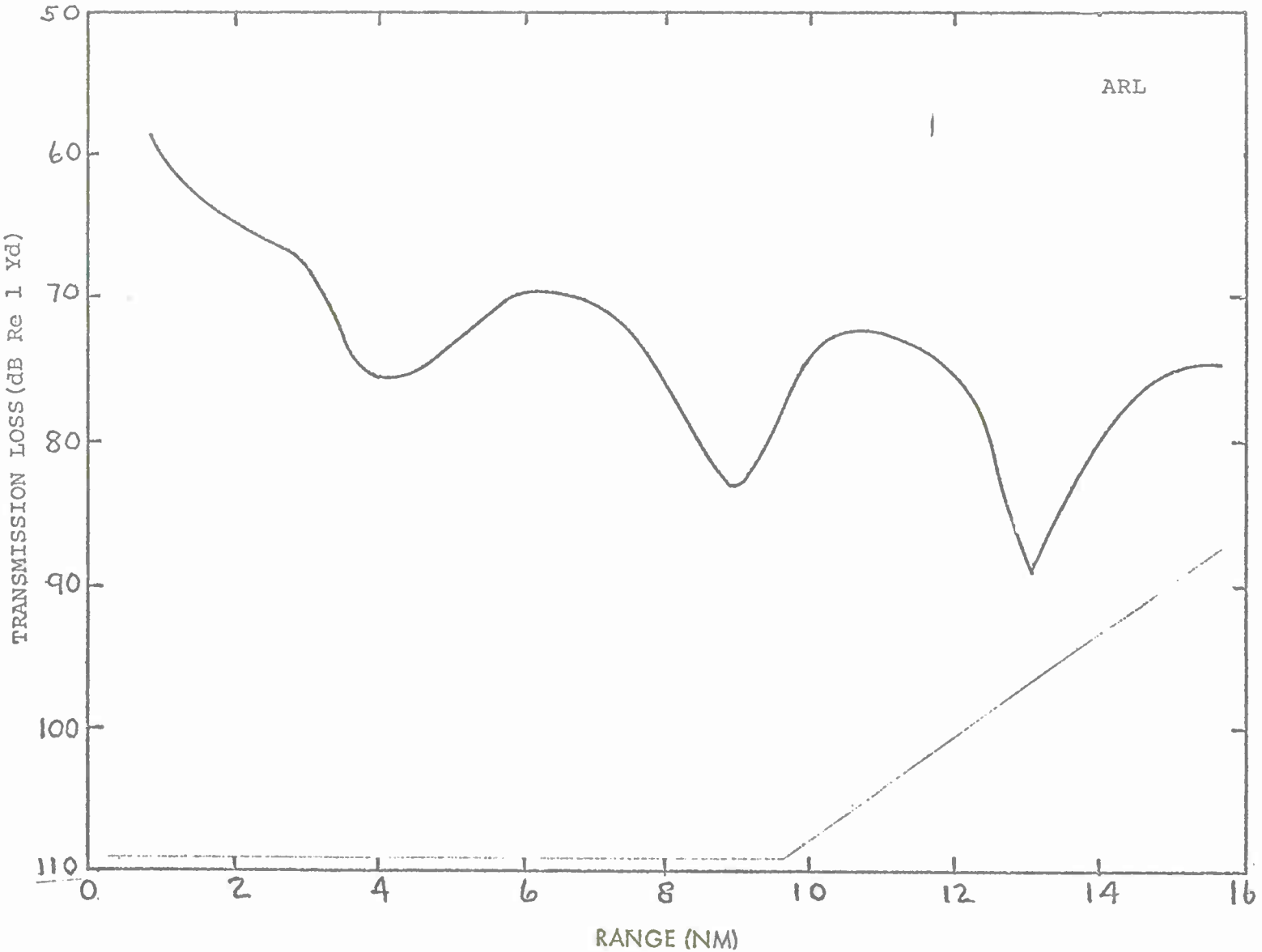

CASE 1a - SURFACE DUCT - Y_s = 300 FT Y_r = 90 FT F = 300 HZ

FIGURE 13

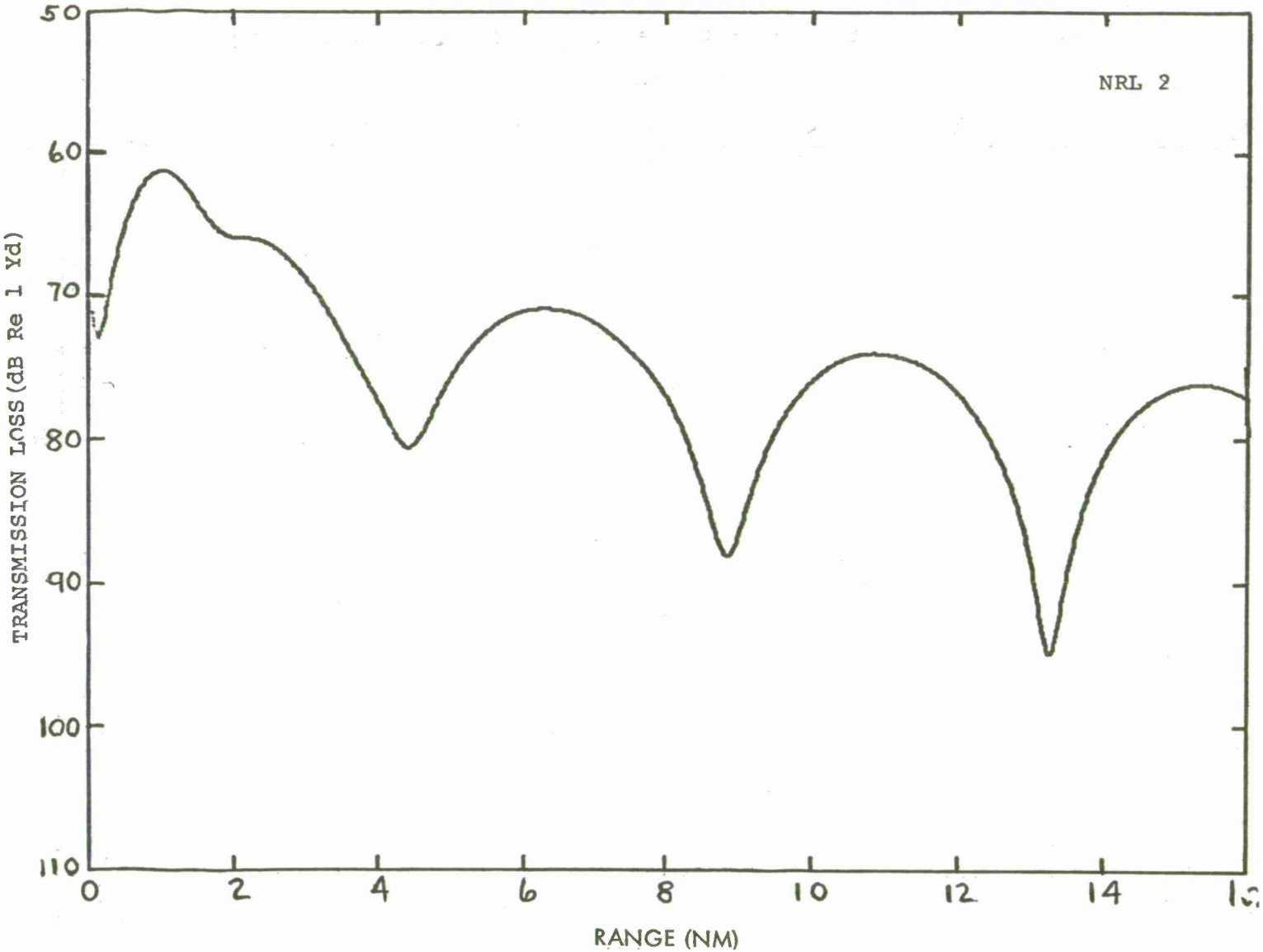

CASE 1a - SURFACE DUCT - Y_S = 300 FT Y_r = 90 FT F = 300 HZ

FIGURE 14

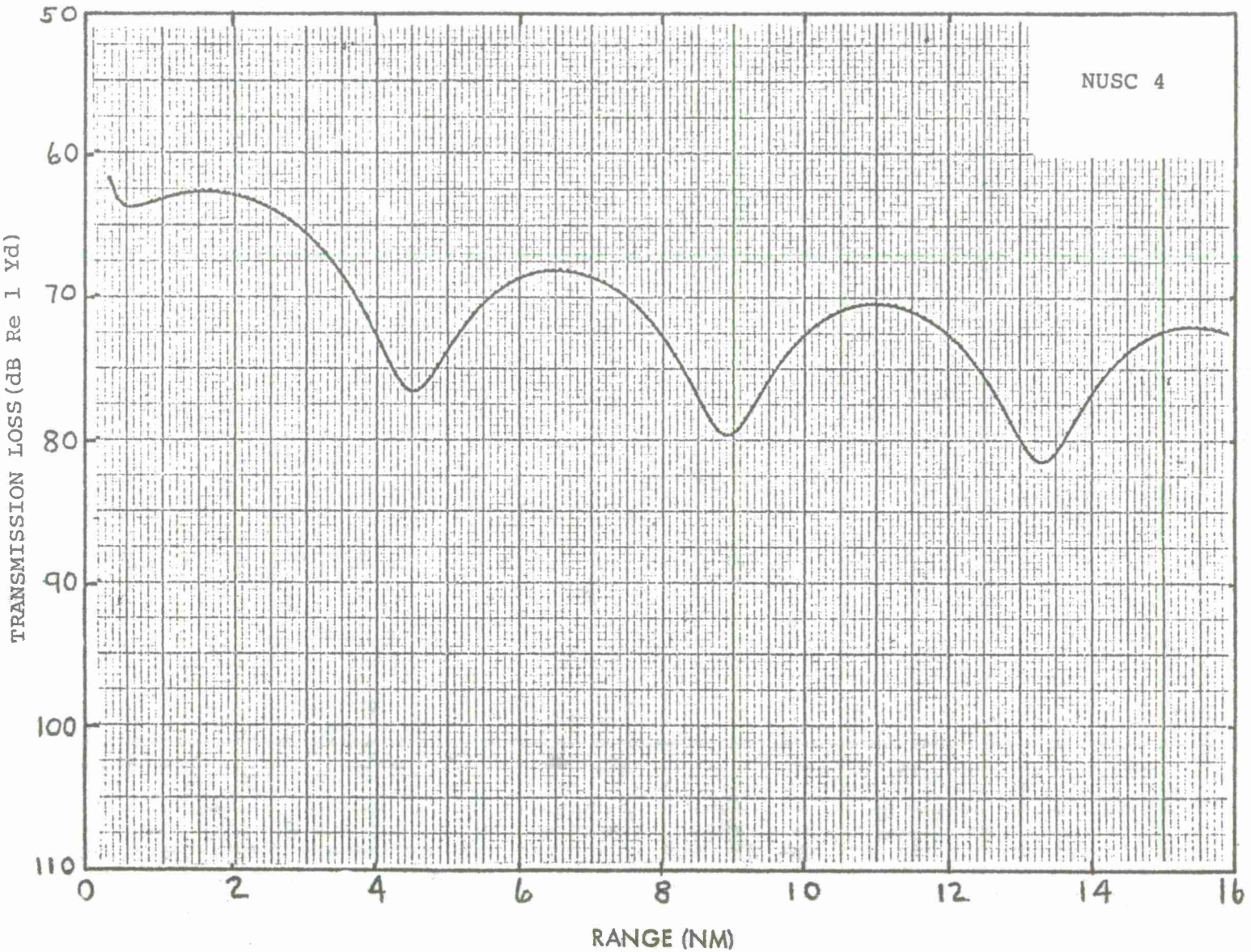

CASE 1a - SURFACE DUCT - Y_S = 300 FT Y_r = 90 FT F = 300 HZ

FIGURE 15

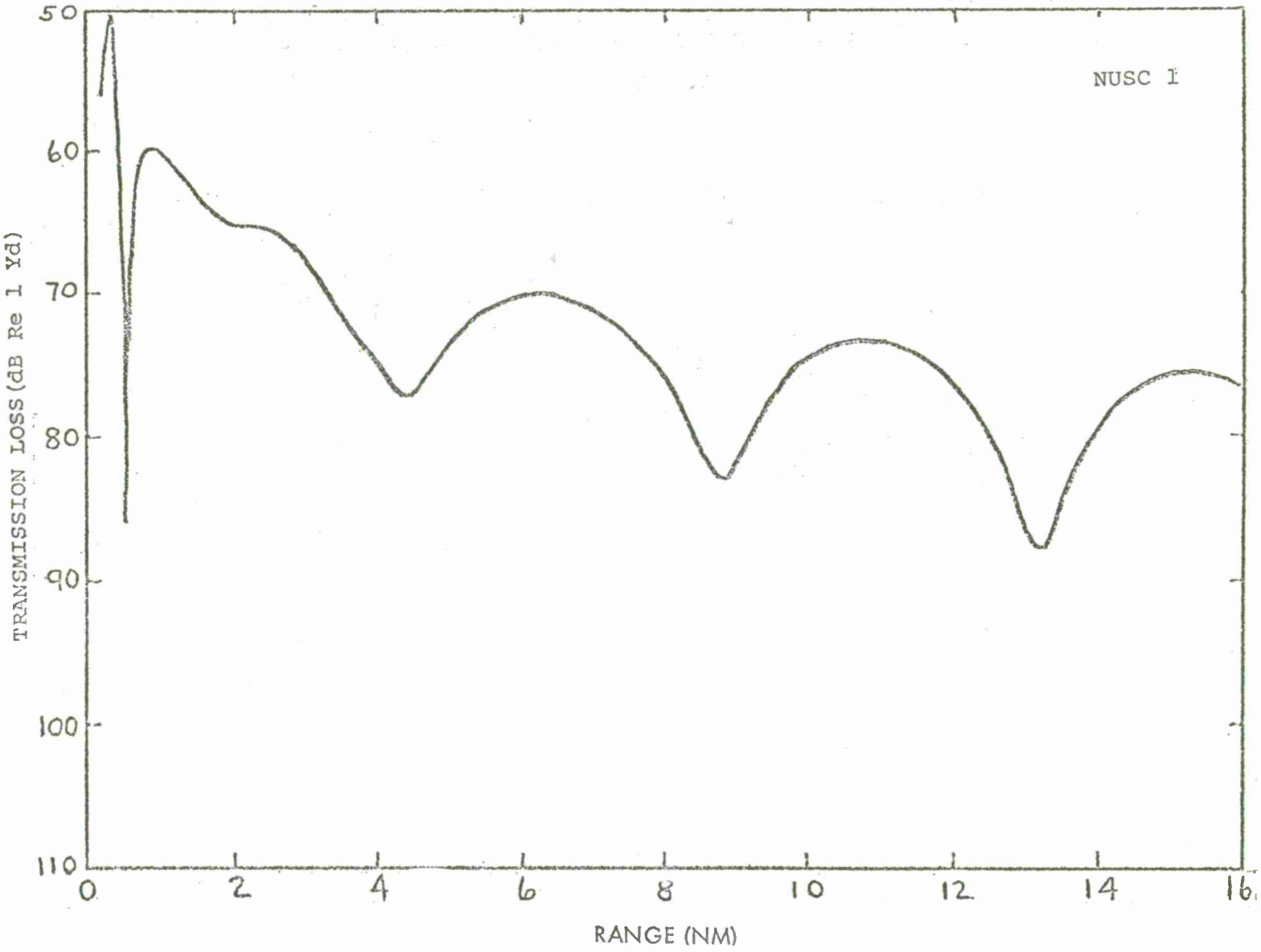

CASE 1a - SURFACE DUCT - Y_S = 300 FT Y_r = 90 FT F = 300 HZ

FIGURE 16

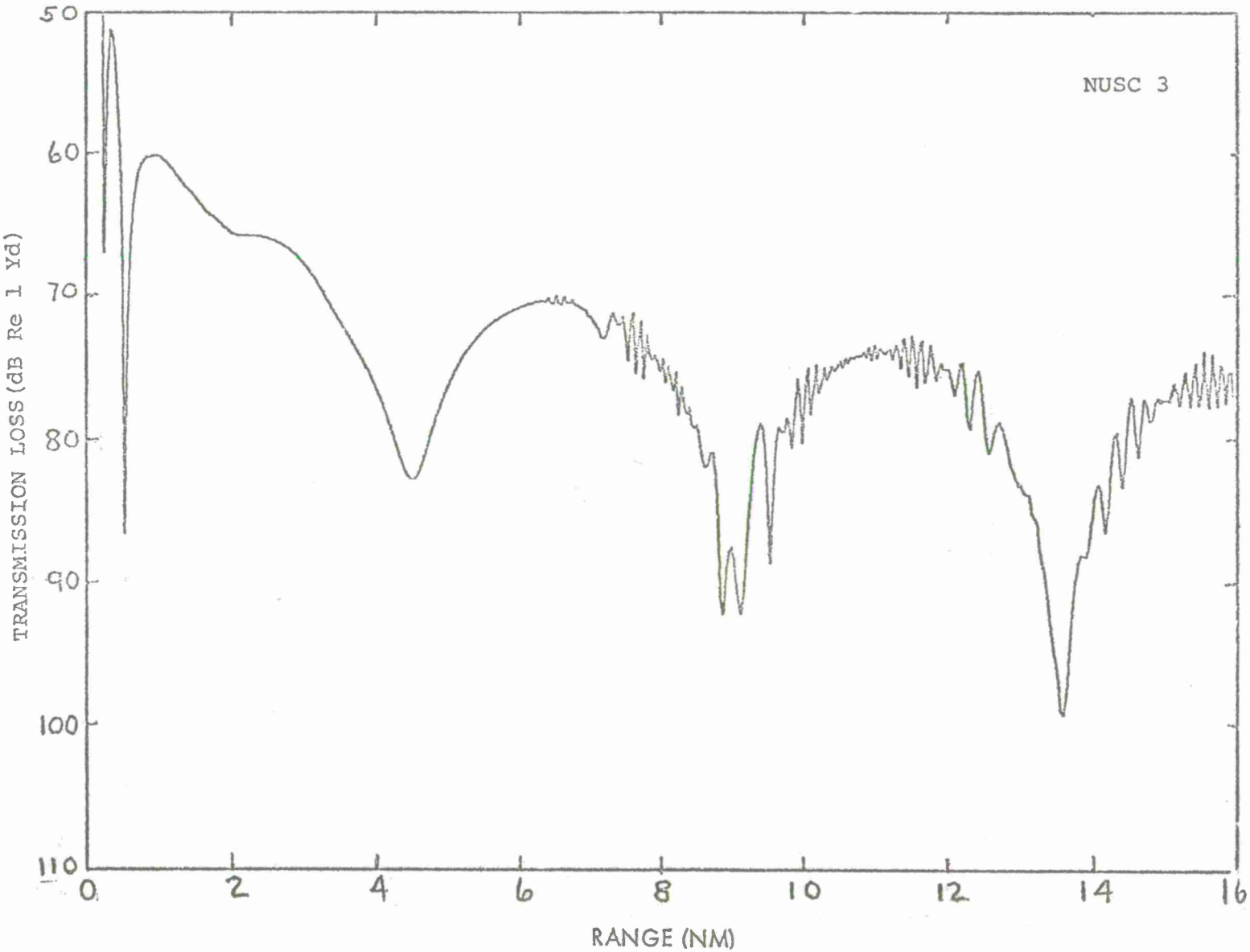

CASE 1a - SURFACE DUCT - Y_S = 300 FT Y_r = 90 FT F = 300 HZ

FIGURE 17

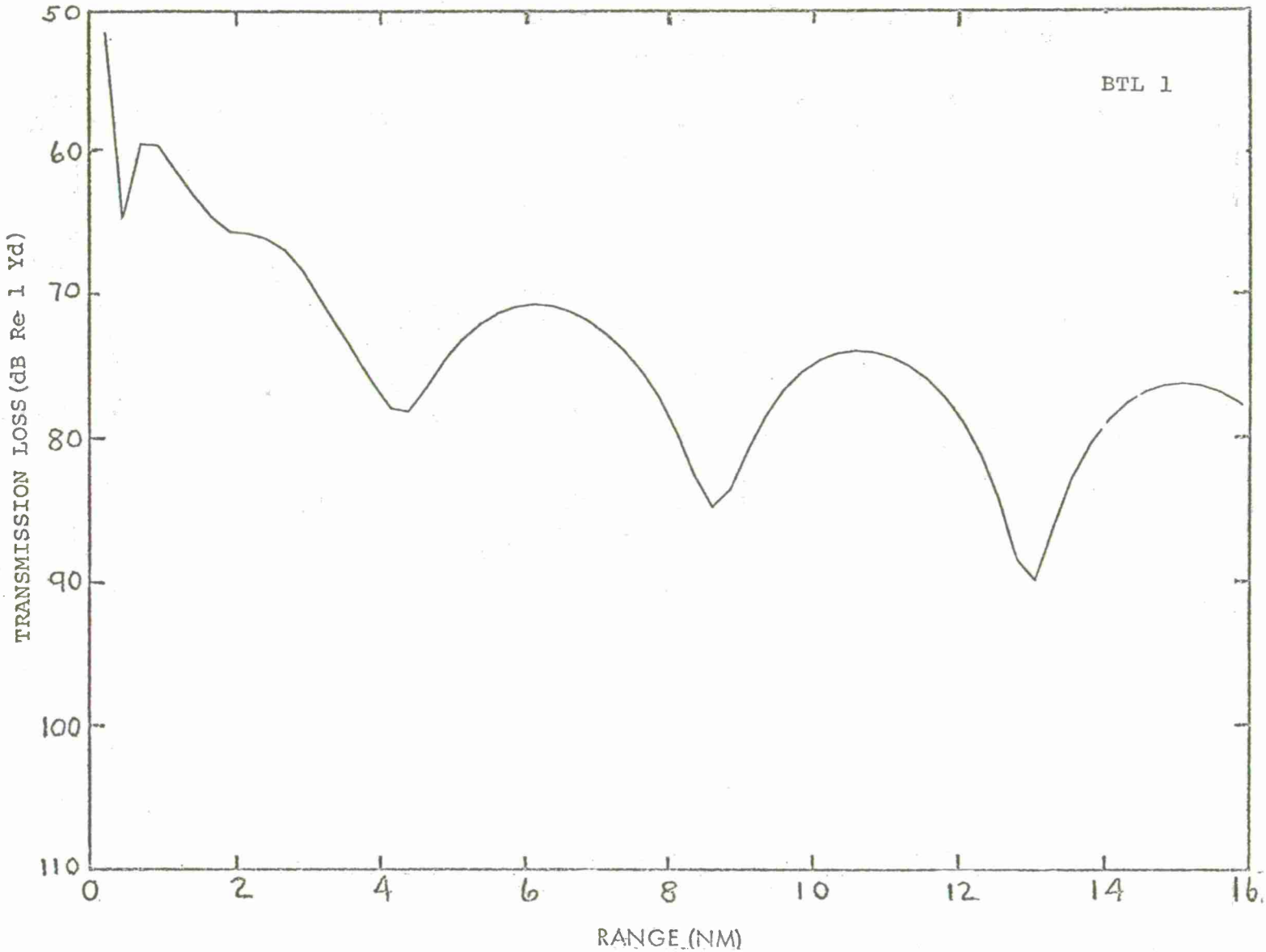

CASE 1a - SURFACE DUCT - Y_S = 300 FT Y_r = 90 FT F = 300 HZ

FIGURE 18

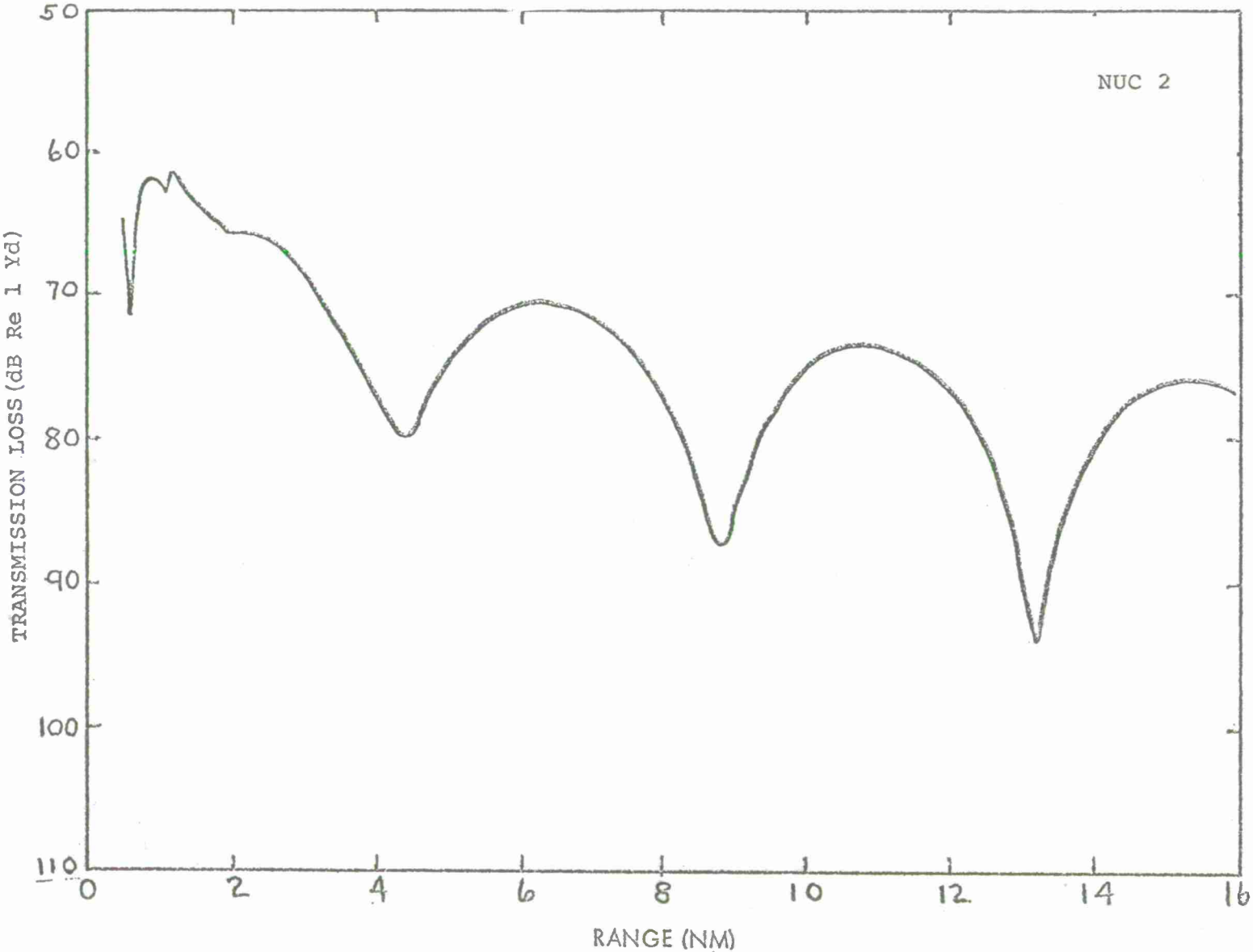

CASE 1a - SURFACE DUCT - Y_S = 300 FT Y_r = 90 FT F = 300 HZ

FIGURE 19

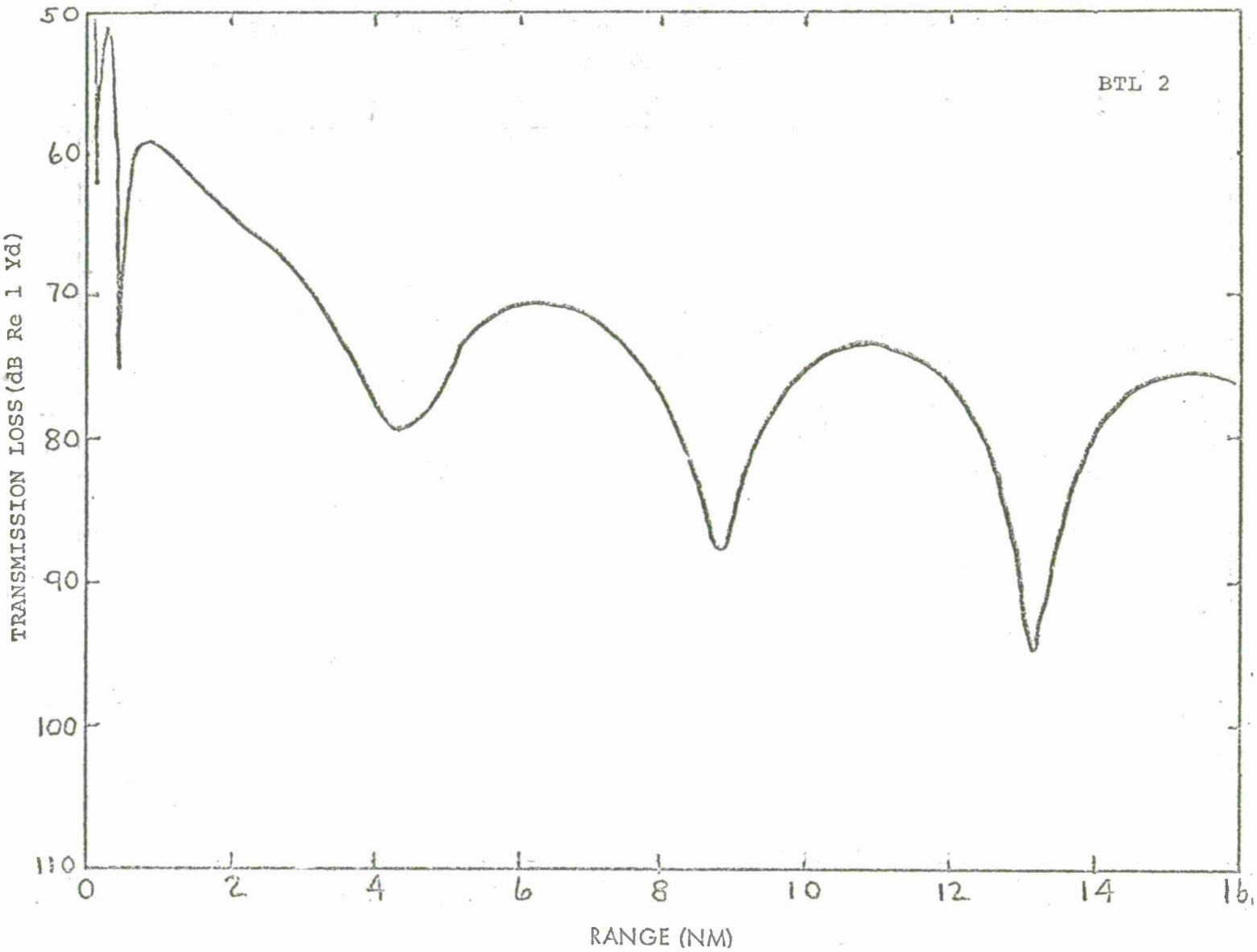

CASE 1a - SURFACE DUCT - Y_S = 300 FT Y_r = 90 FT F = 300 HZ

FIGURE 20

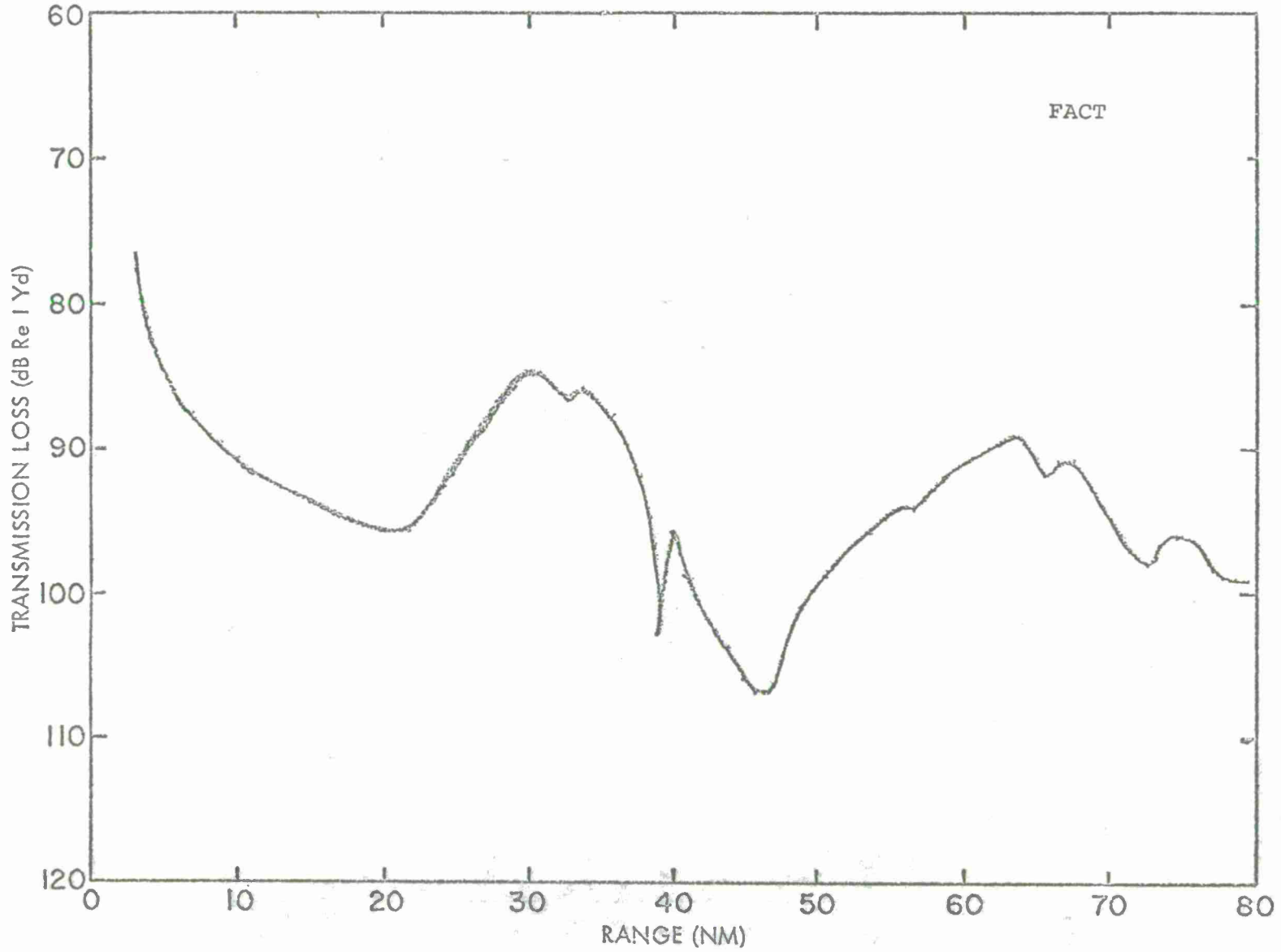

CASE Ib - PACIFIC PROFILE Y_s = 833 FT Y_r = 2833 FT F = 25 HZ

FIGURE 21

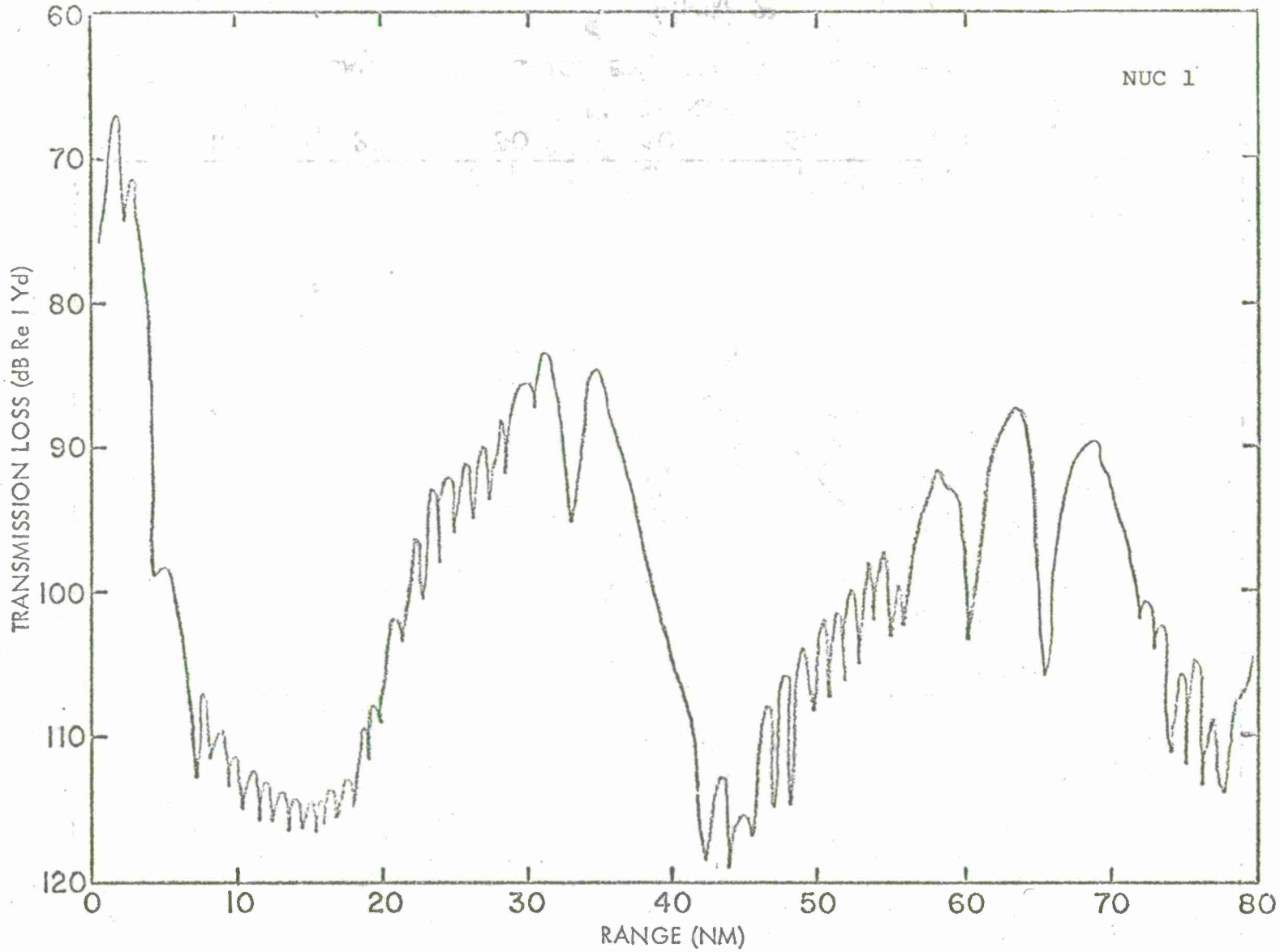

CASE Ib - PACIFIC PROFILE Y_s = 833 FT Y_r = 2833 FT F = 25 HZ

FIGURE .22

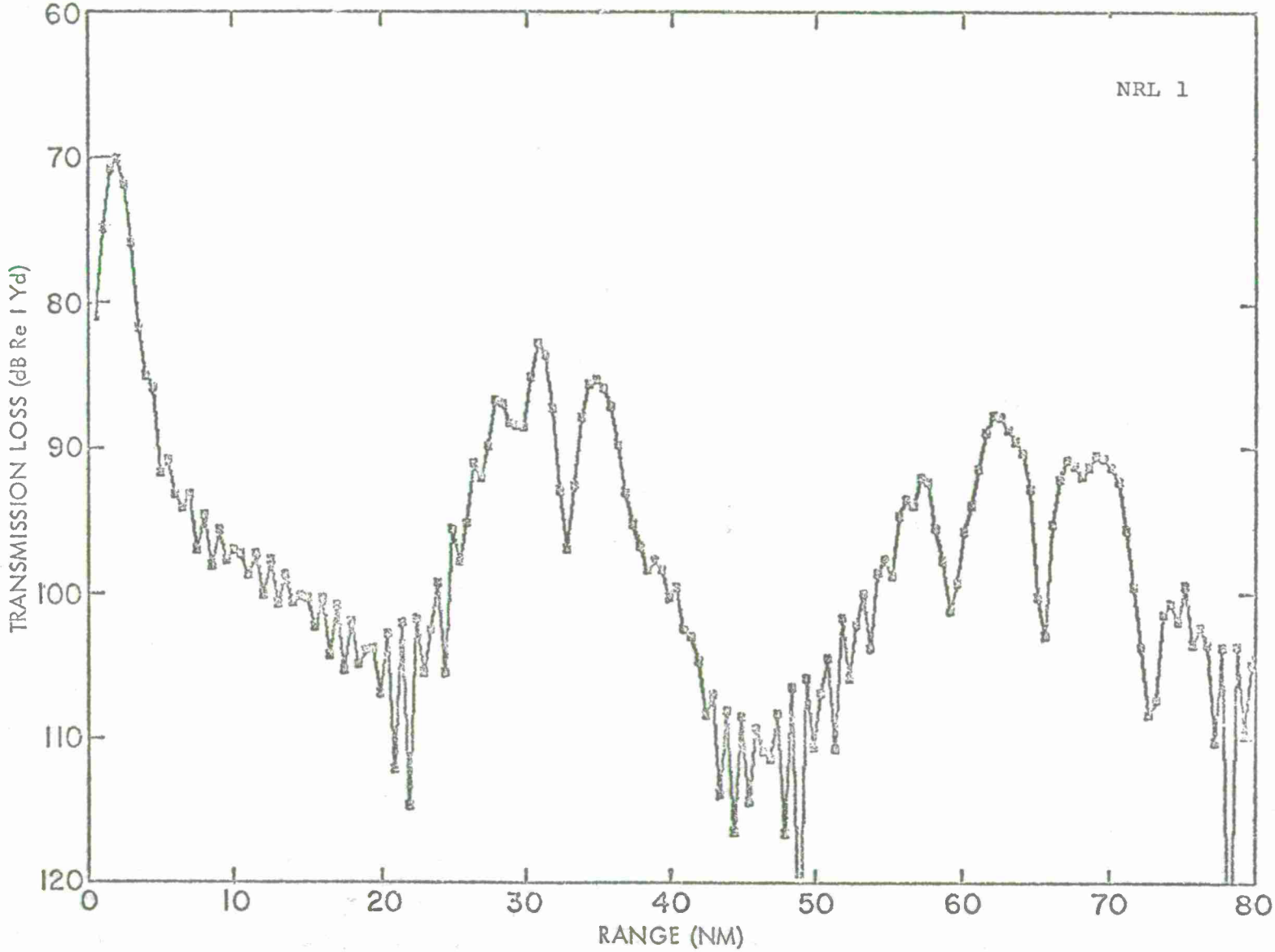

CASE Ib - PACIFIC PROFILE Y_s = 833 FT Y_r = 2833 FT F = 25 HZ

FIGURE 23

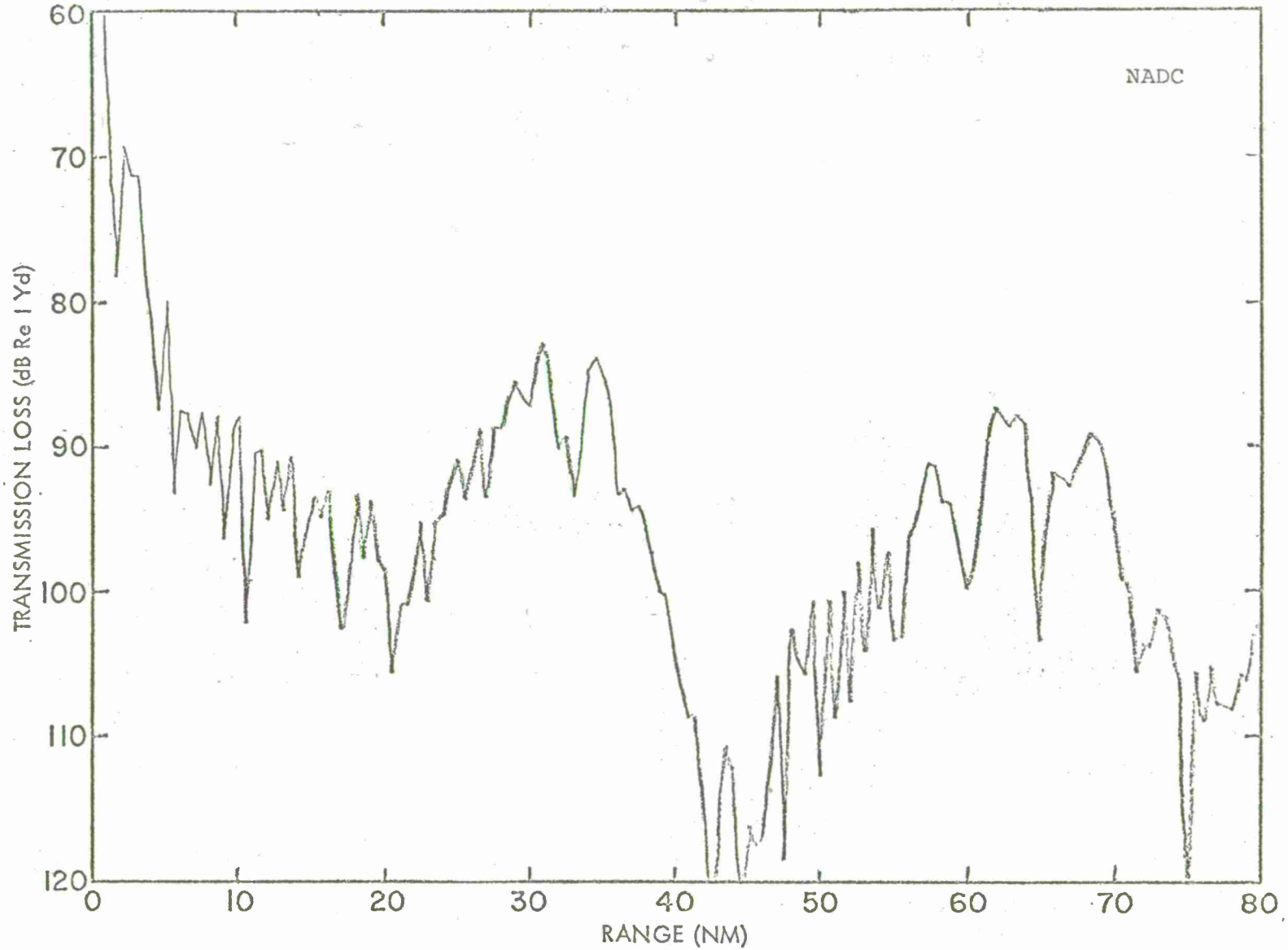

CASE Ib - PACIFIC PROFILE Y_s = 833 FT Y_r = 2833 FT F = 25 HZ

FIGURE 24

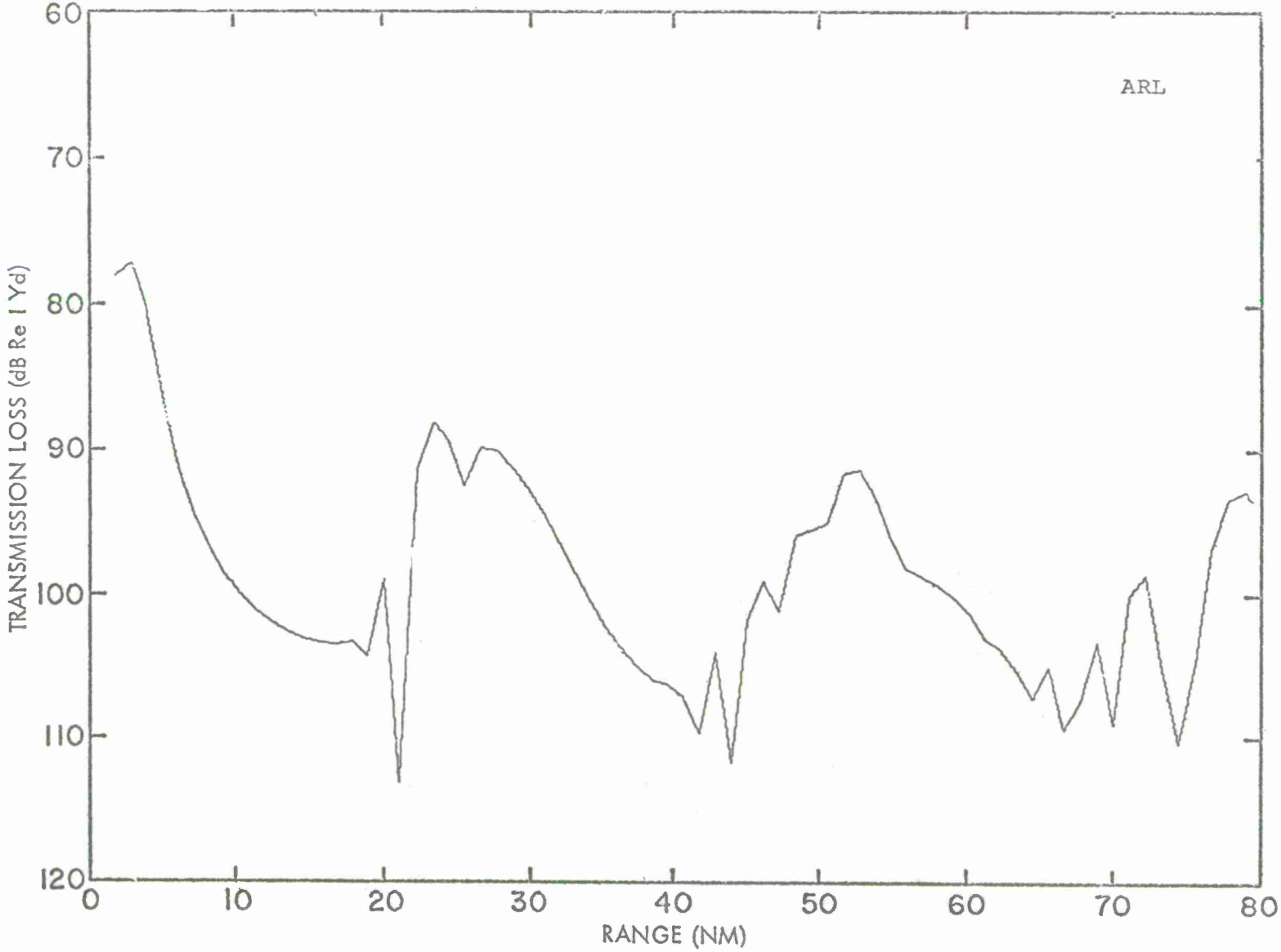

CASE Ib - PACIFIC PROFILE Y_s = 833 FT Y_r = 2833 FT F = 25 HZ

FIGURE 25

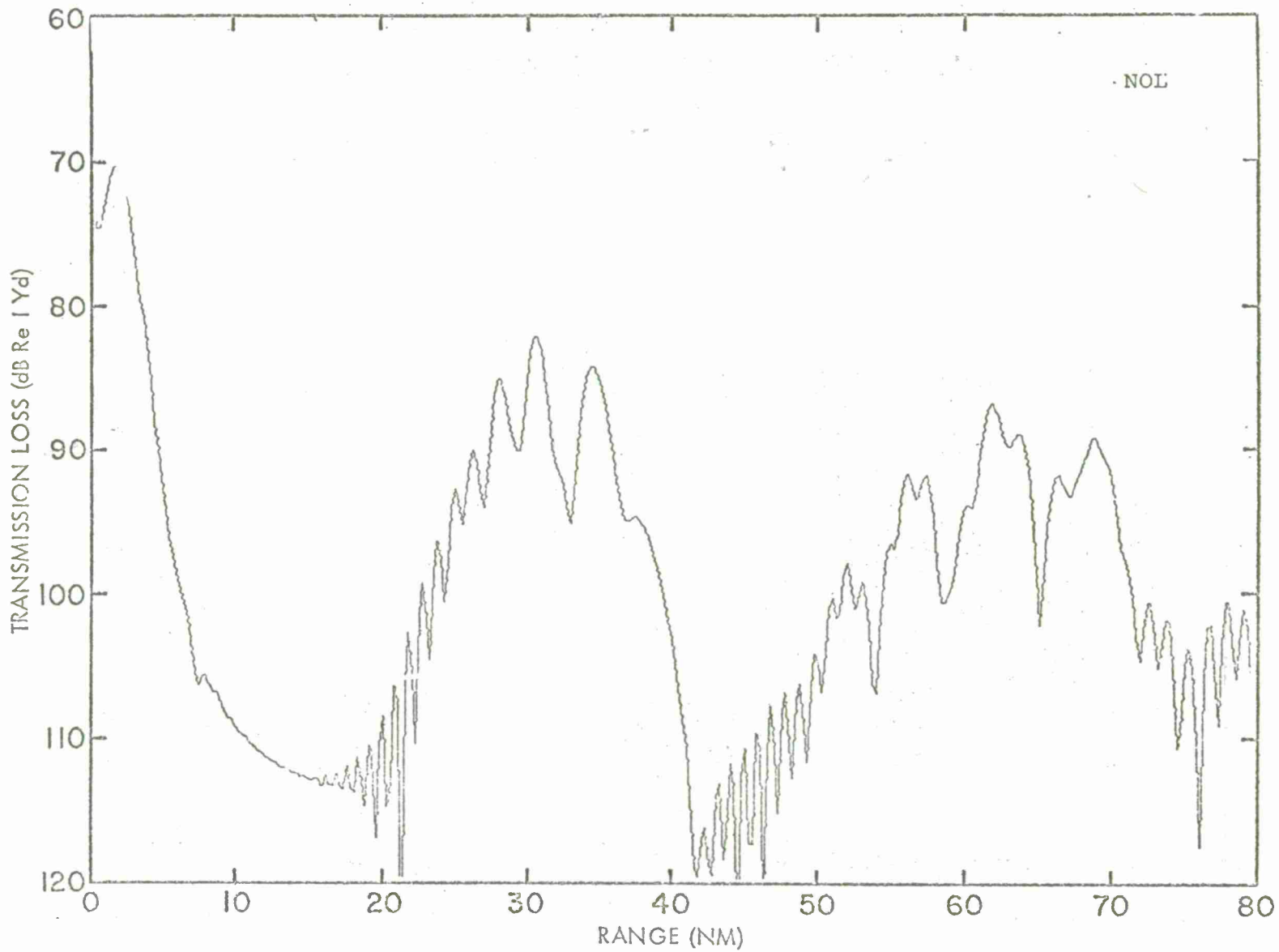

CASE Ib - PACIFIC PROFILE Y_s = 833 FT Y_r = 2833 FT F = 25 HZ

FIGURE 26

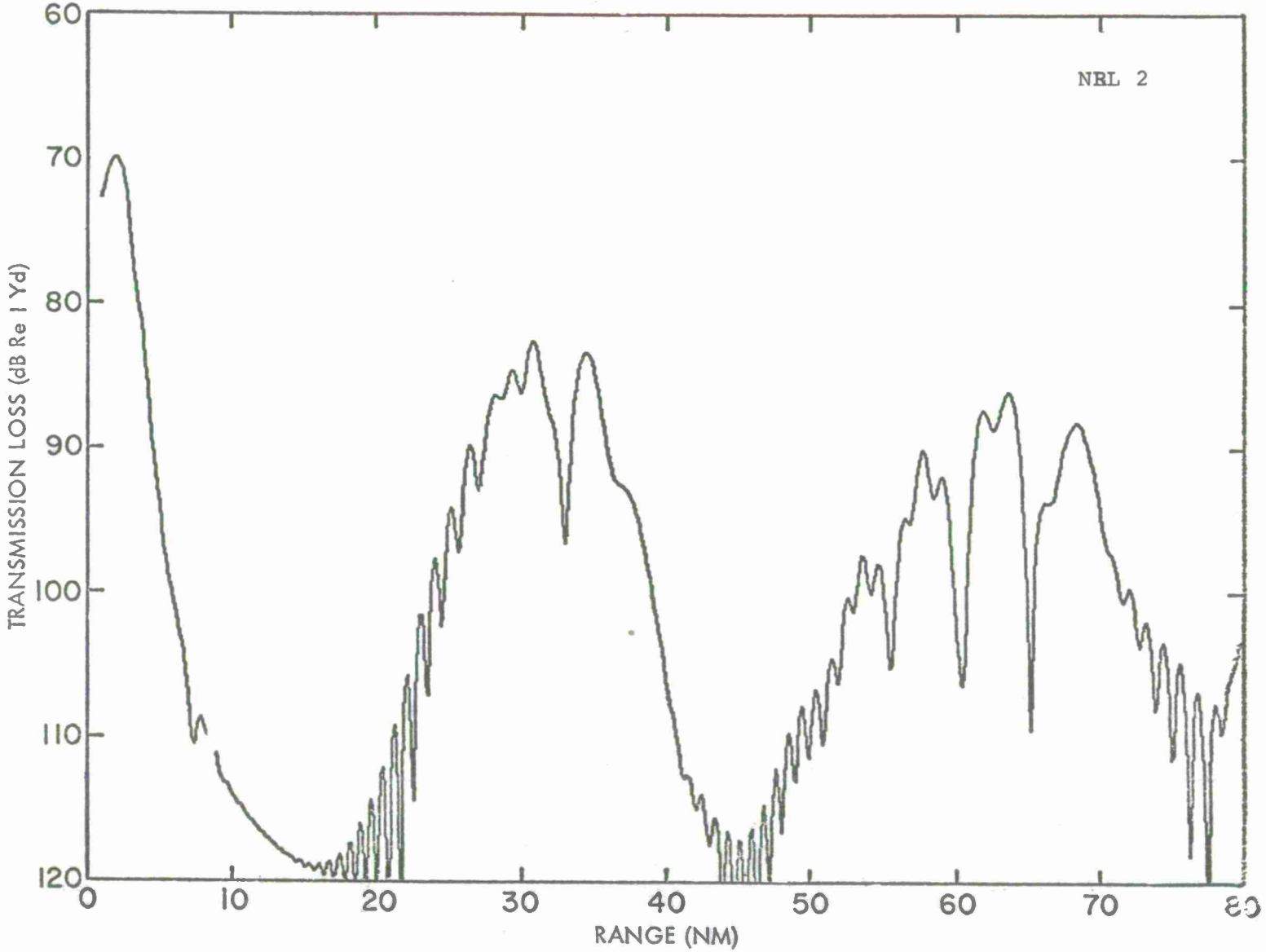

CASE Ib - PACIFIC PROFILE Y_s = 833 FT Y_r = 2833 FT F = 25 HZ

FIGURE 27

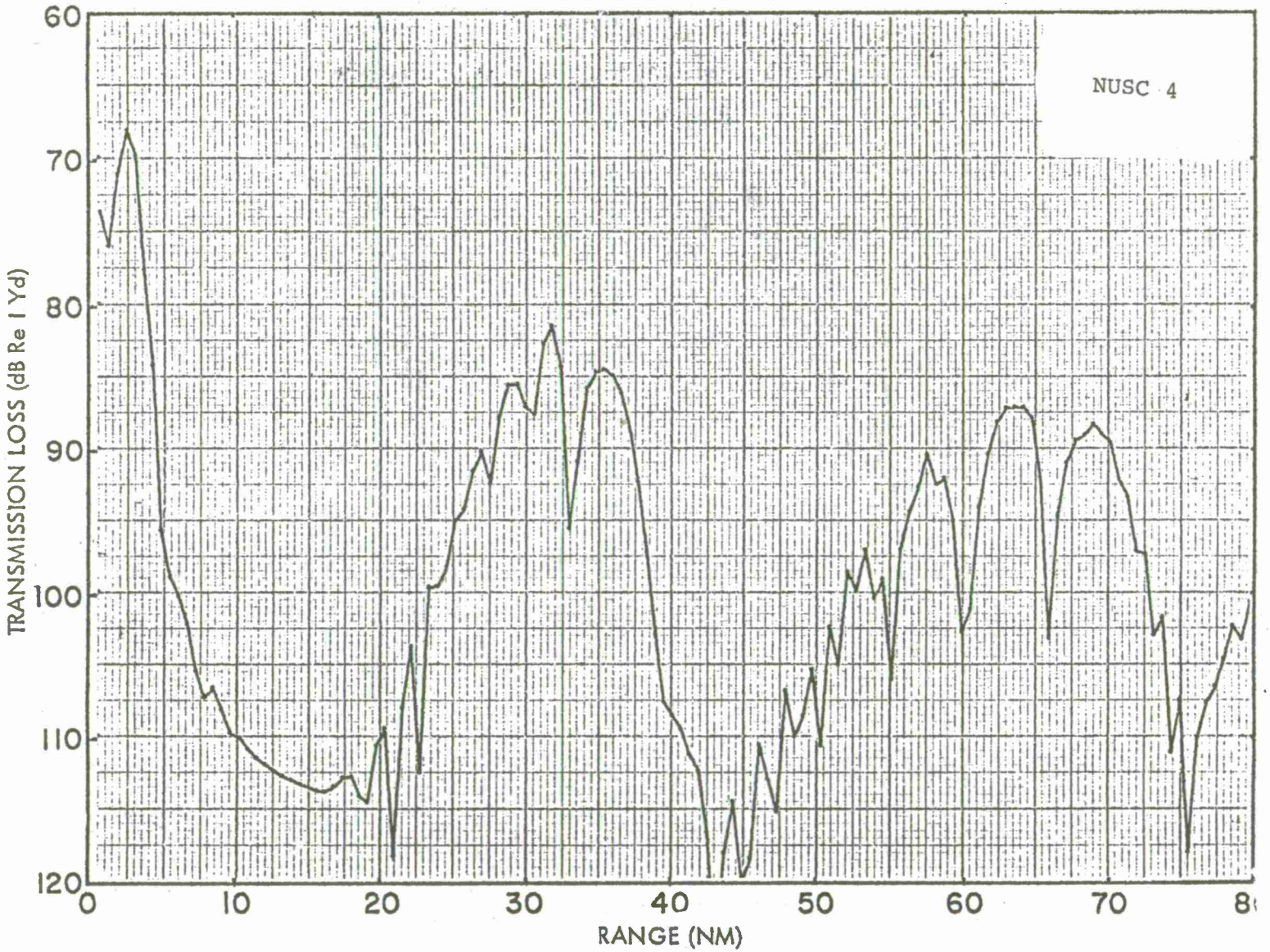

CASE Ib - PACIFIC PROFILE Y_s = 833 FT Y_r = 2833 FT F = 25 HZ

FIGURE 28

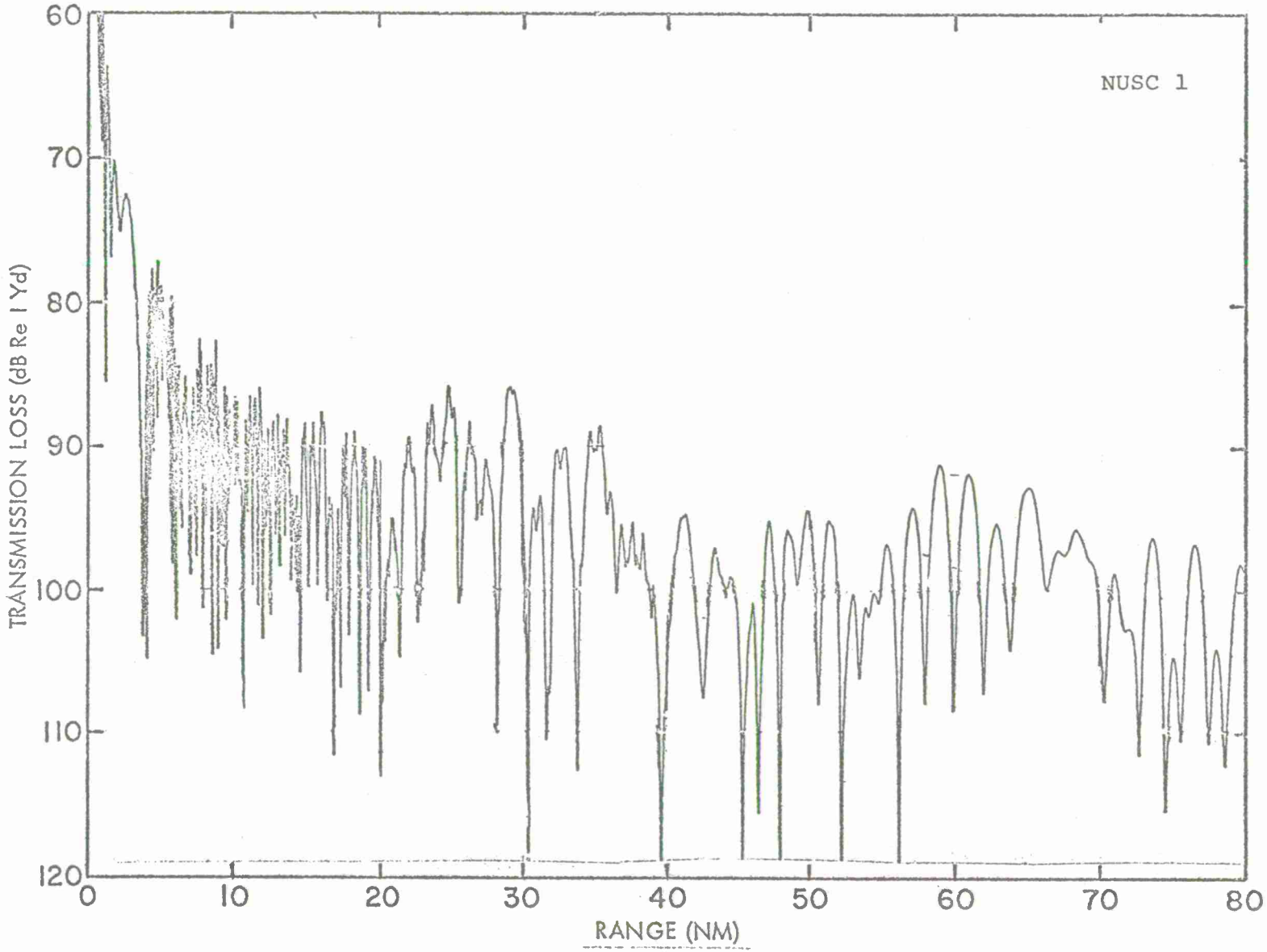

CASE Ib - PACIFIC PROFILE Y_s = 833 FT Y_r = 2833 FT F = 25 HZ

FIGURE 29

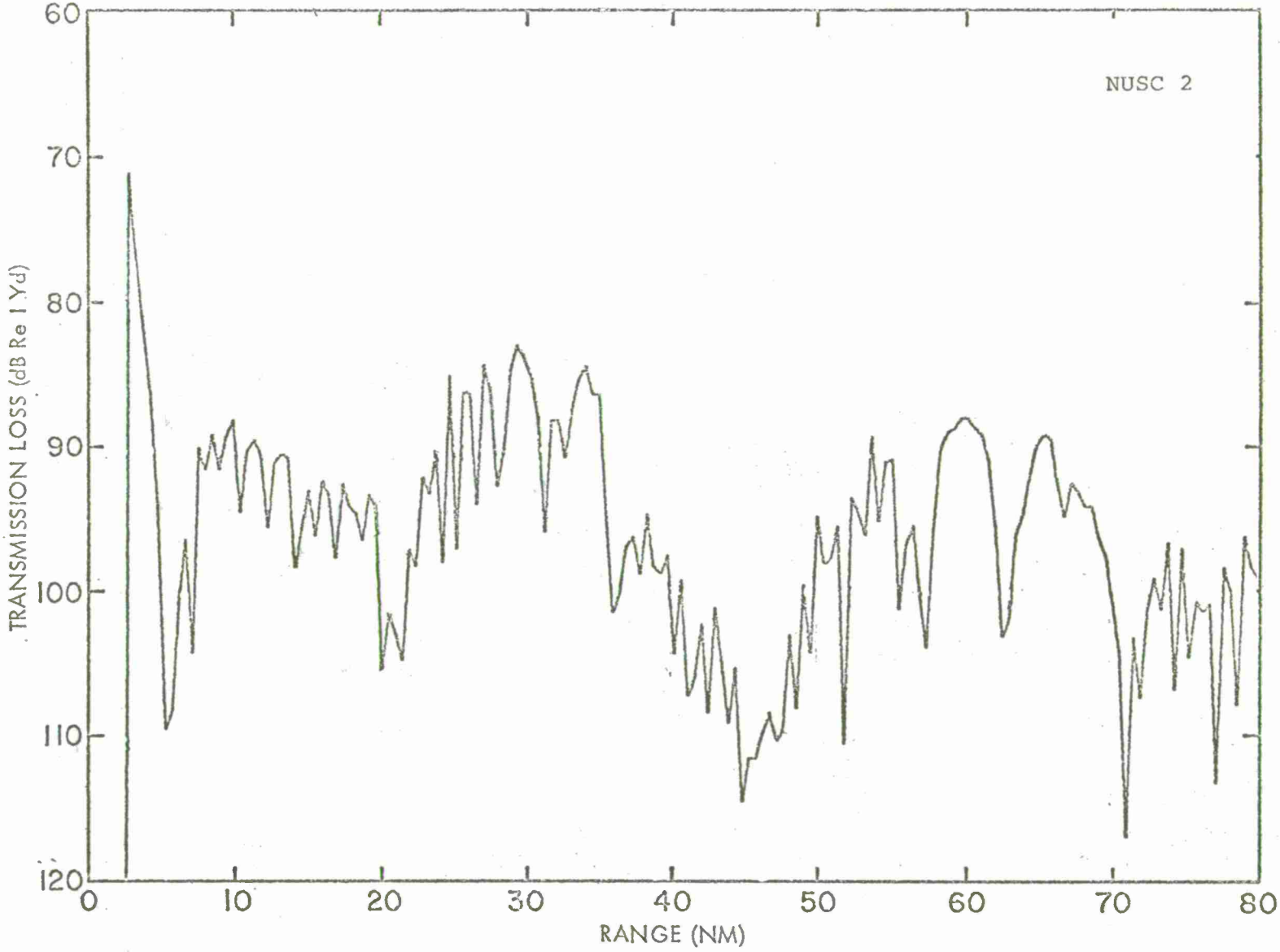

CASE Ib - PACIFIC PROFILE Y_s = 833 FT Y_r = 2833 FT F = 25 HZ

FIGURE 30

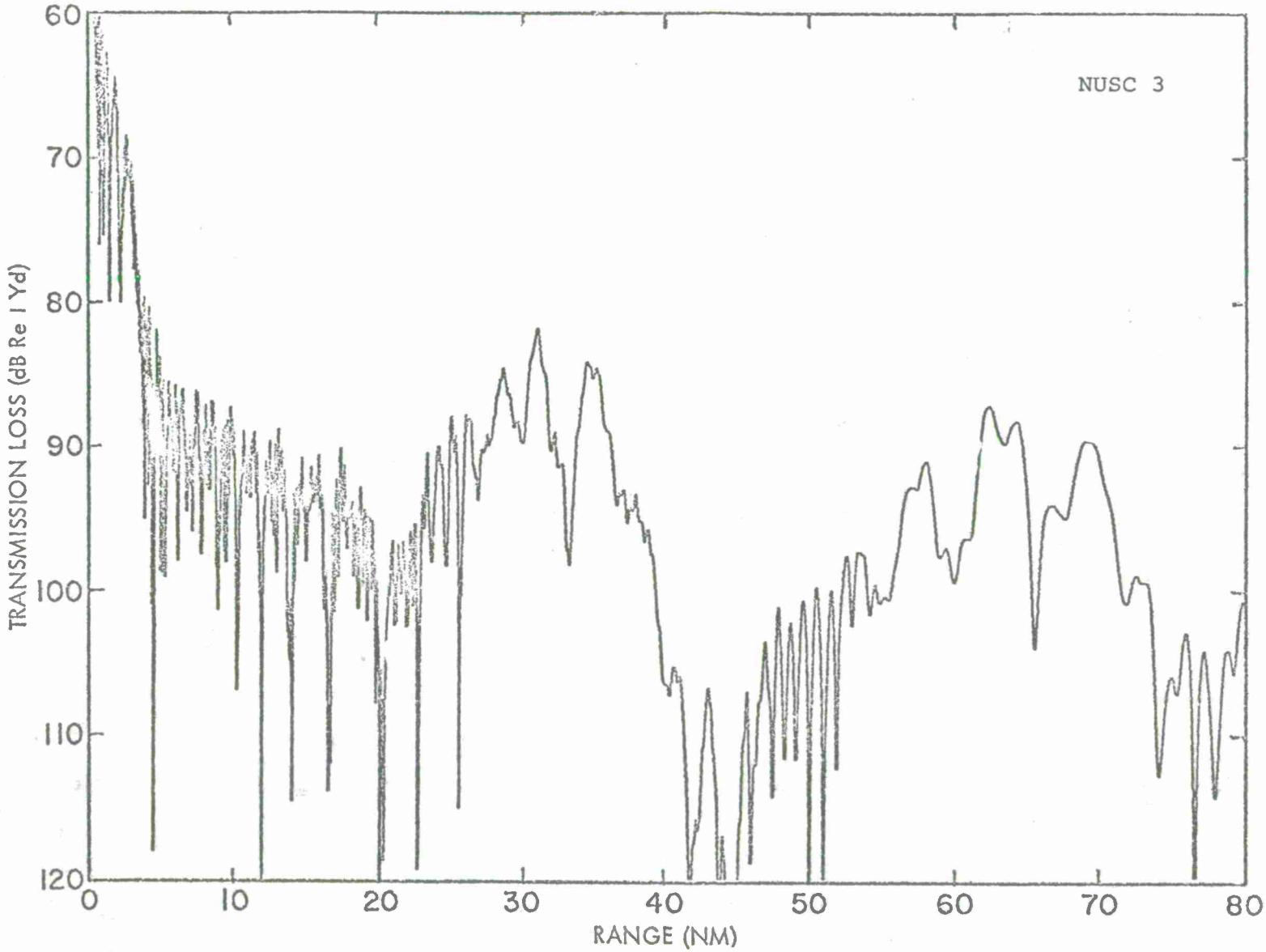

CASE Ib - PACIFIC PROFILE Y_s = 833 FT Y_r = 2833 FT F = 25 HZ

FIGURE 31

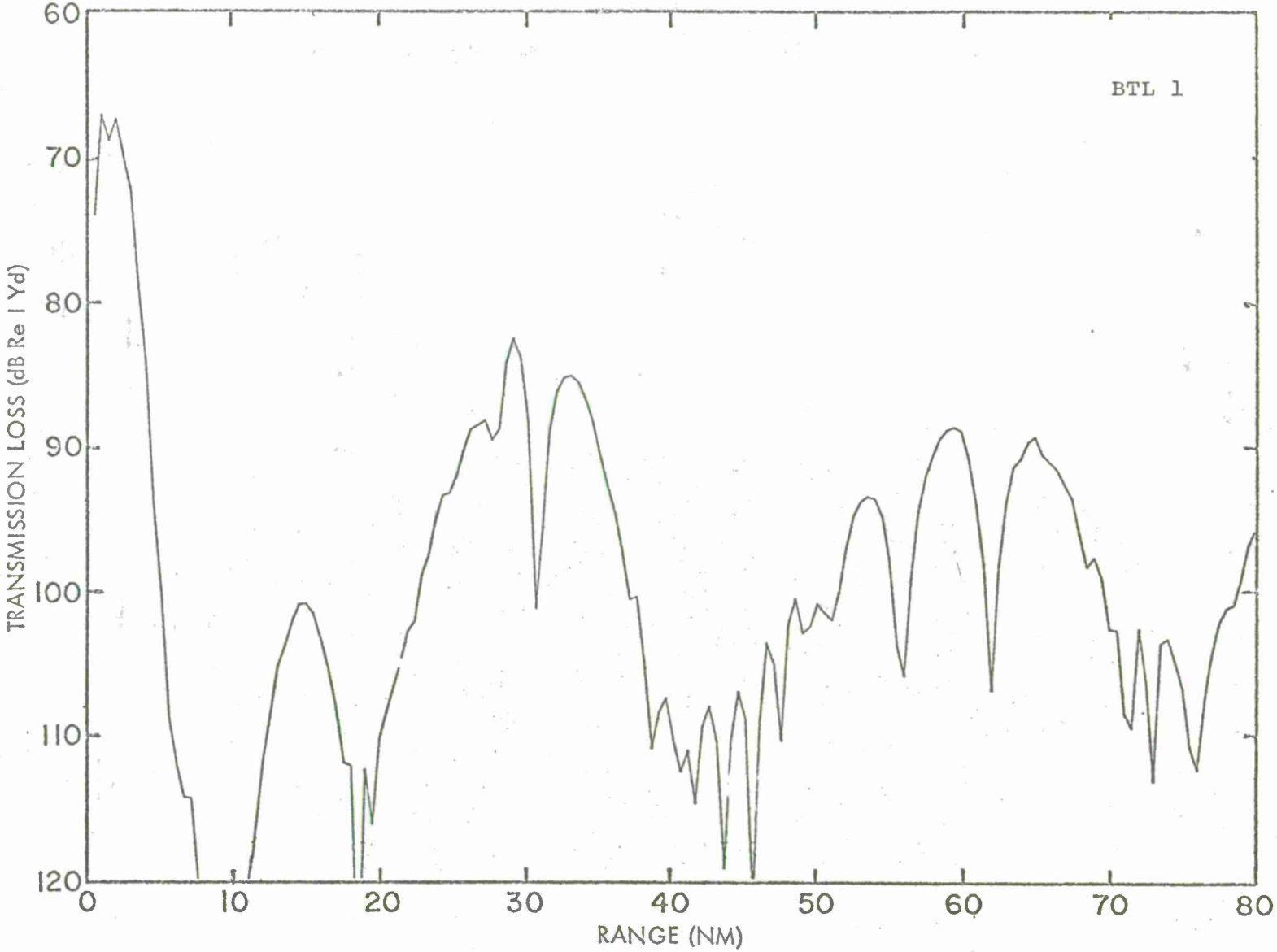

CASE Ib - PACIFIC PROFILE Y_s = 833 FT Y_r = 2833 FT F = 25 HZ

FIGURE 32

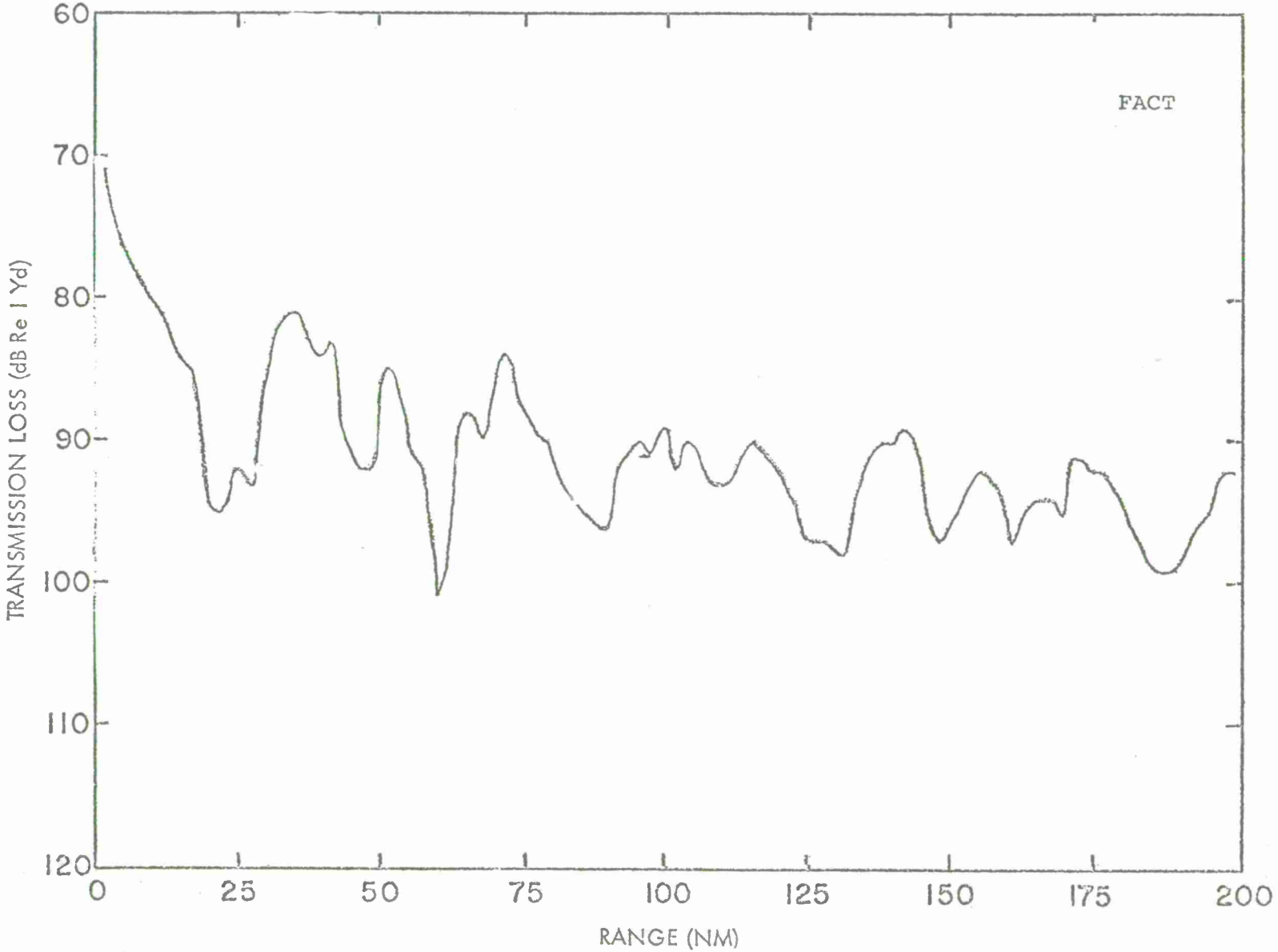

CASE 2 - EASTERN ATLANTIC PROFILE Y_s = 800 FT Y_r = 3600 FT F = 50 HZ

FIGURE 33

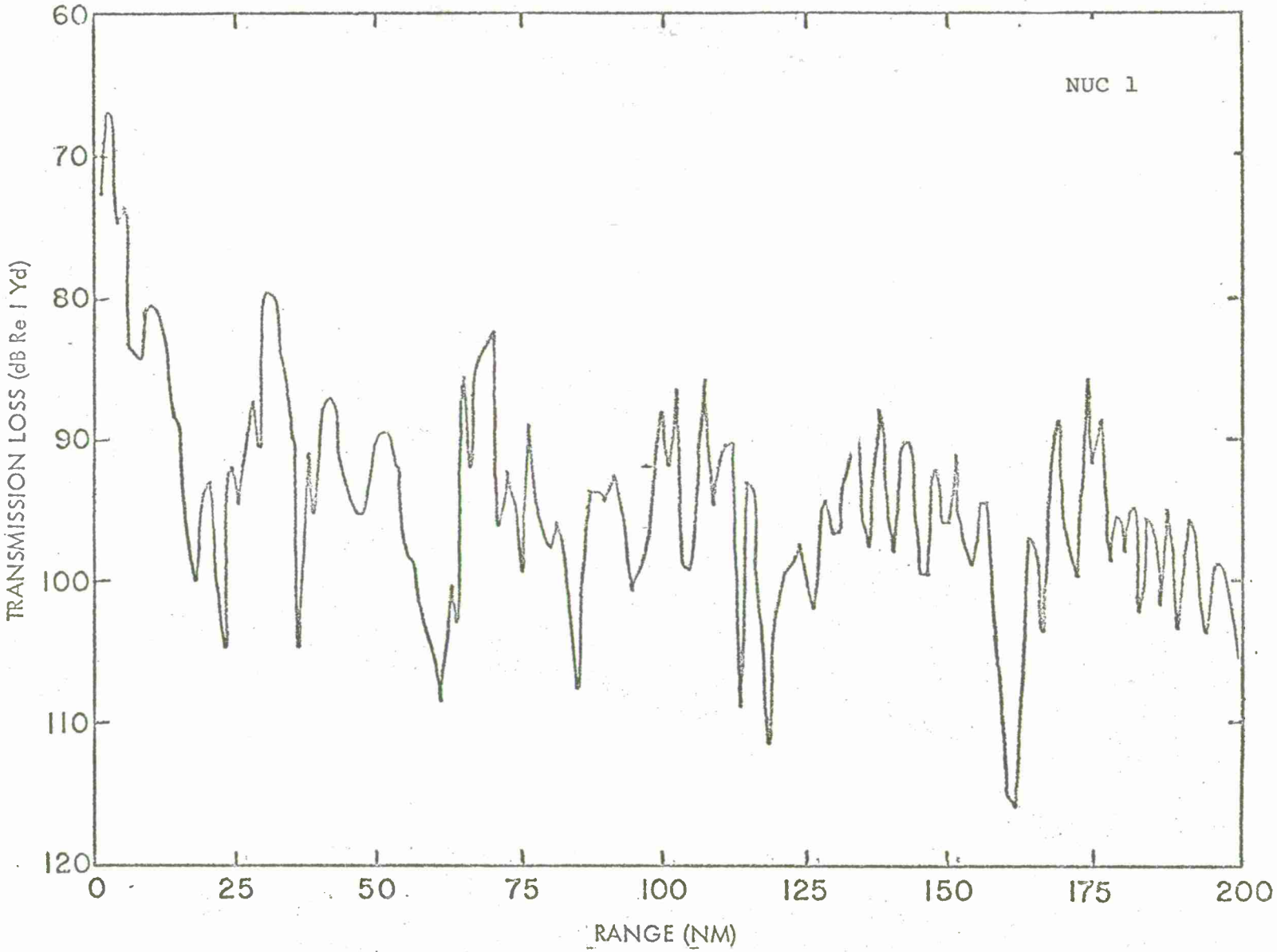

CASE 2 - EASTERN ATLANTIC PROFILE Y_s = 800 FT Y_r = 3600 FT F = 50 HZ

FIGURE 34

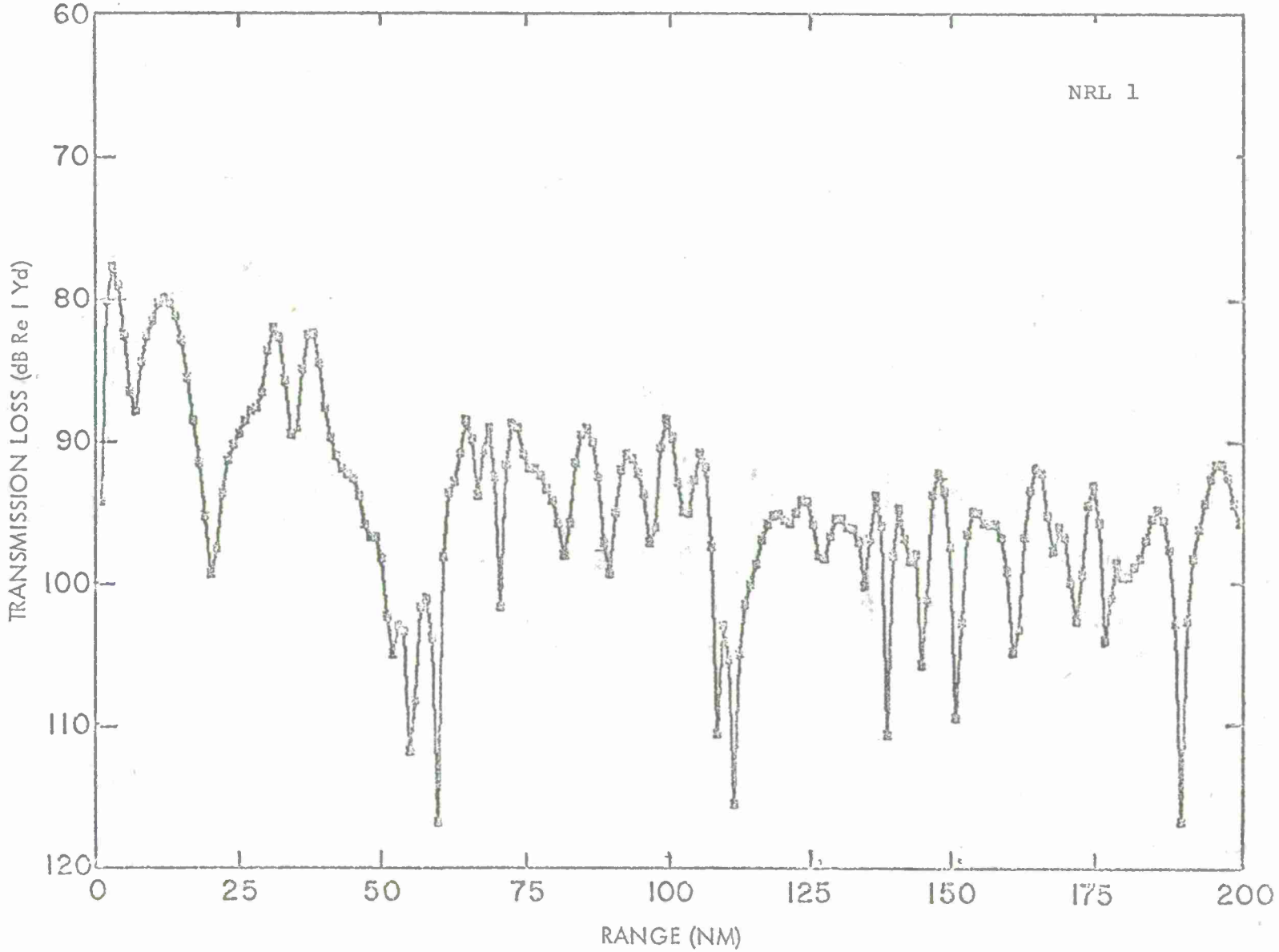

CASE 2 - EASTERN ATLANTIC PROFILE Y_s = 800 FT Y_r = 3600 FT F = 50 HZ

FIGURE 35

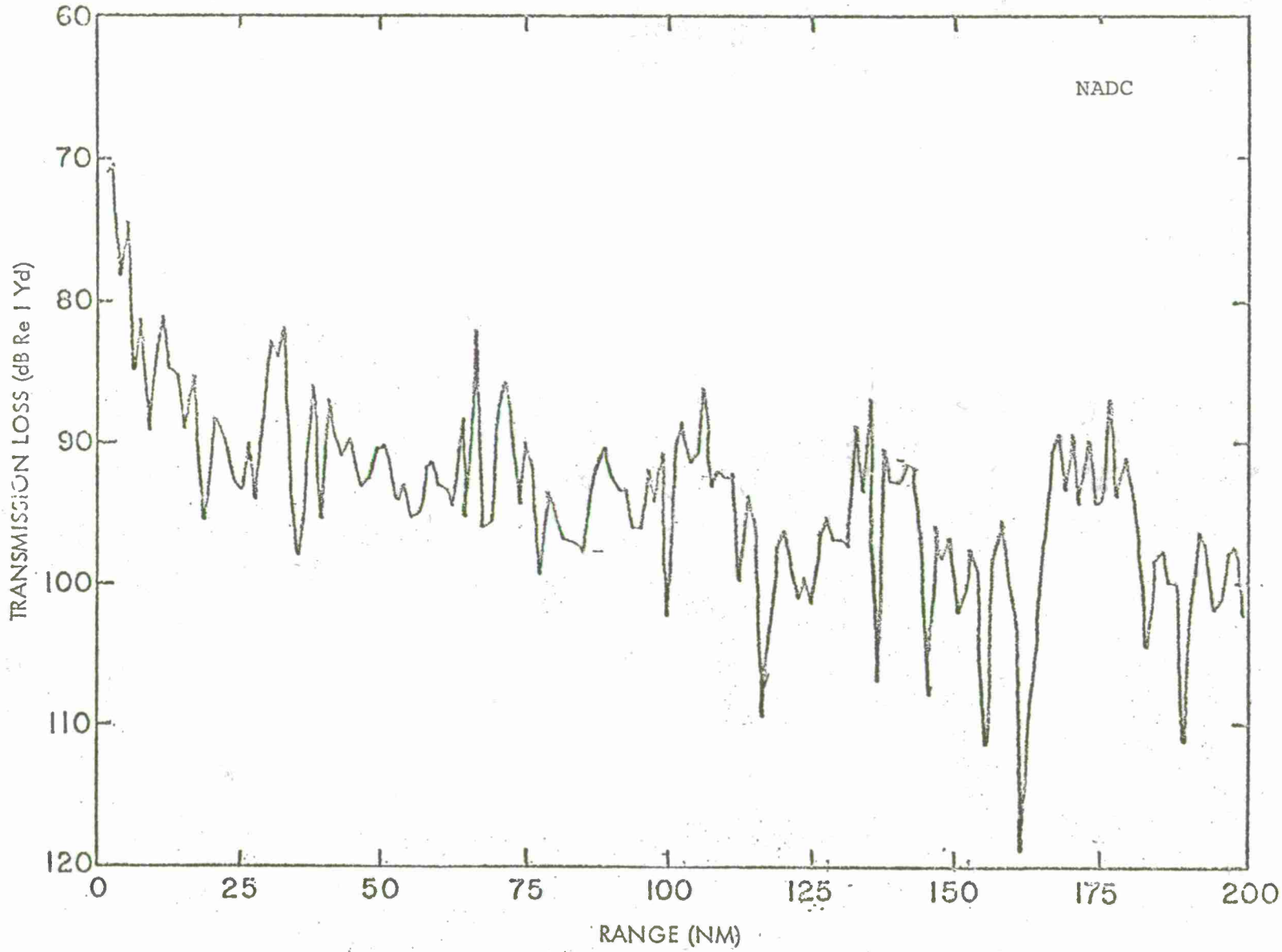

CASE 2 - EASTERN ATLANTIC PROFILE Y_s = 800 FT Y_r = 3600 FT F = 50 HZ

FIGURE 36

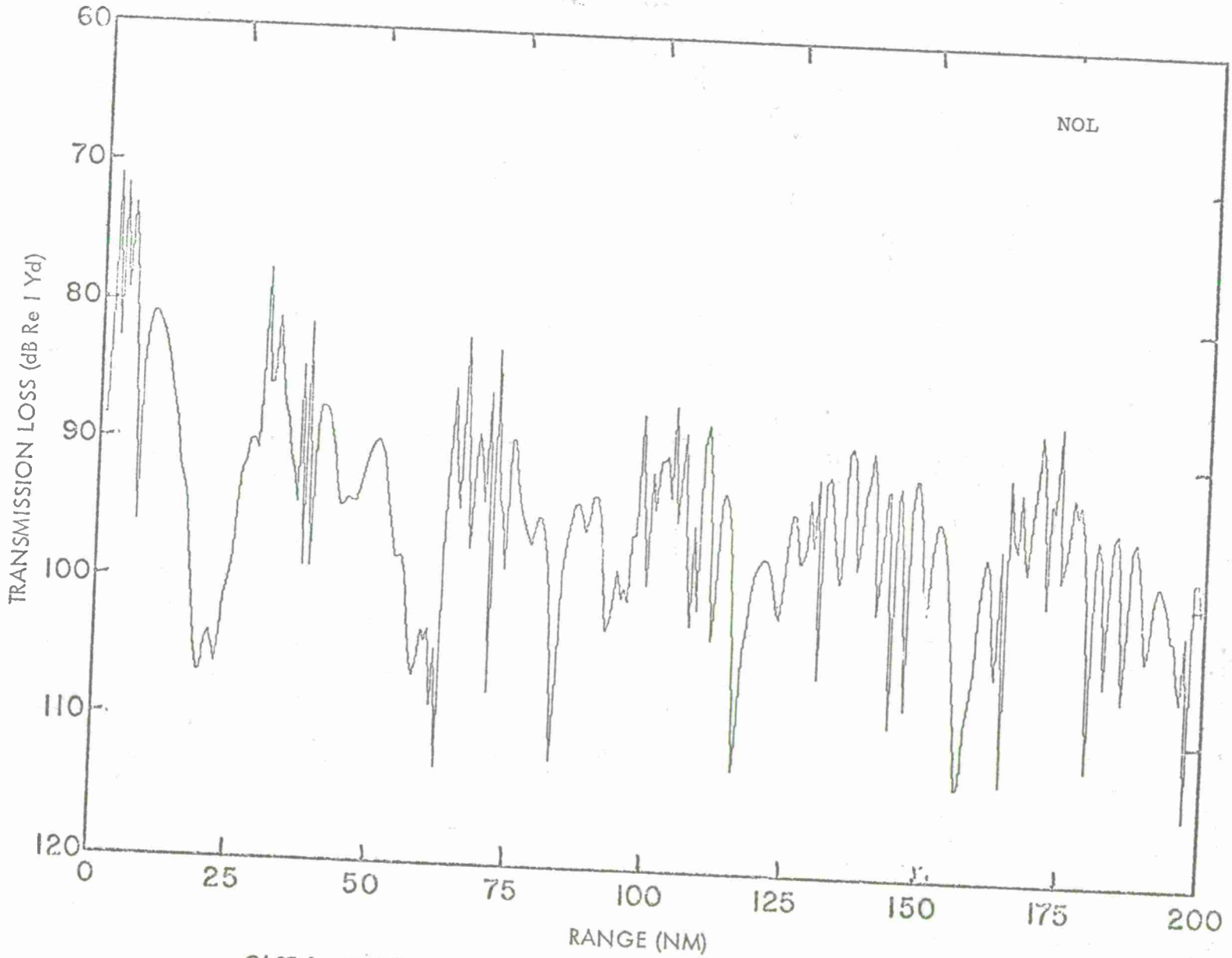

CASE 2 – EASTERN ATLANTIC PROFILE Y_s = 800 FT Y_r = 3600 FT F = 50 HZ

FIGURE 37

FIGURE 38

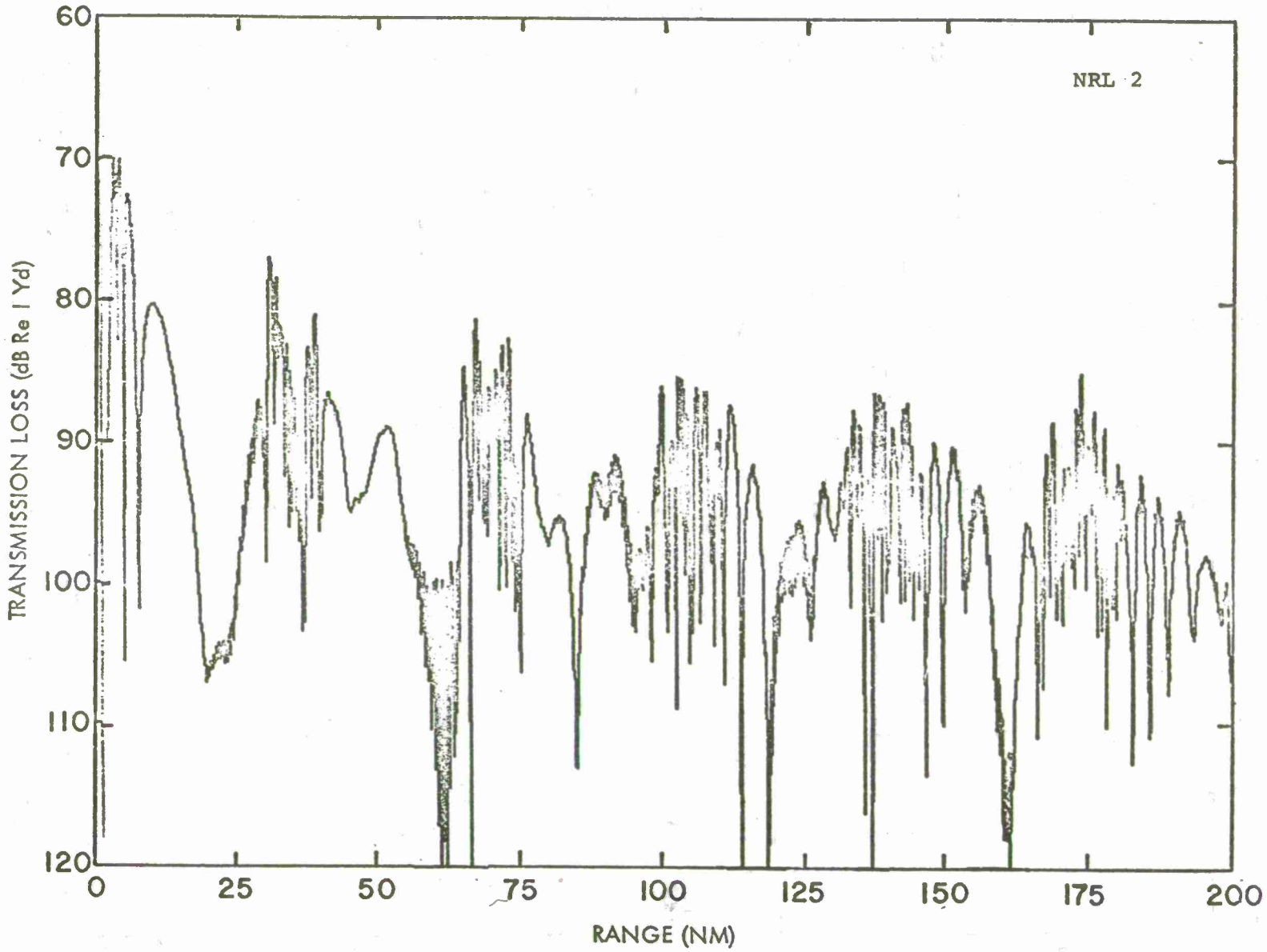

CASE 2 - EASTERN ATLANTIC PROFILE Y_s = 800 FT Y_r = 3600 FT F = 50 HZ

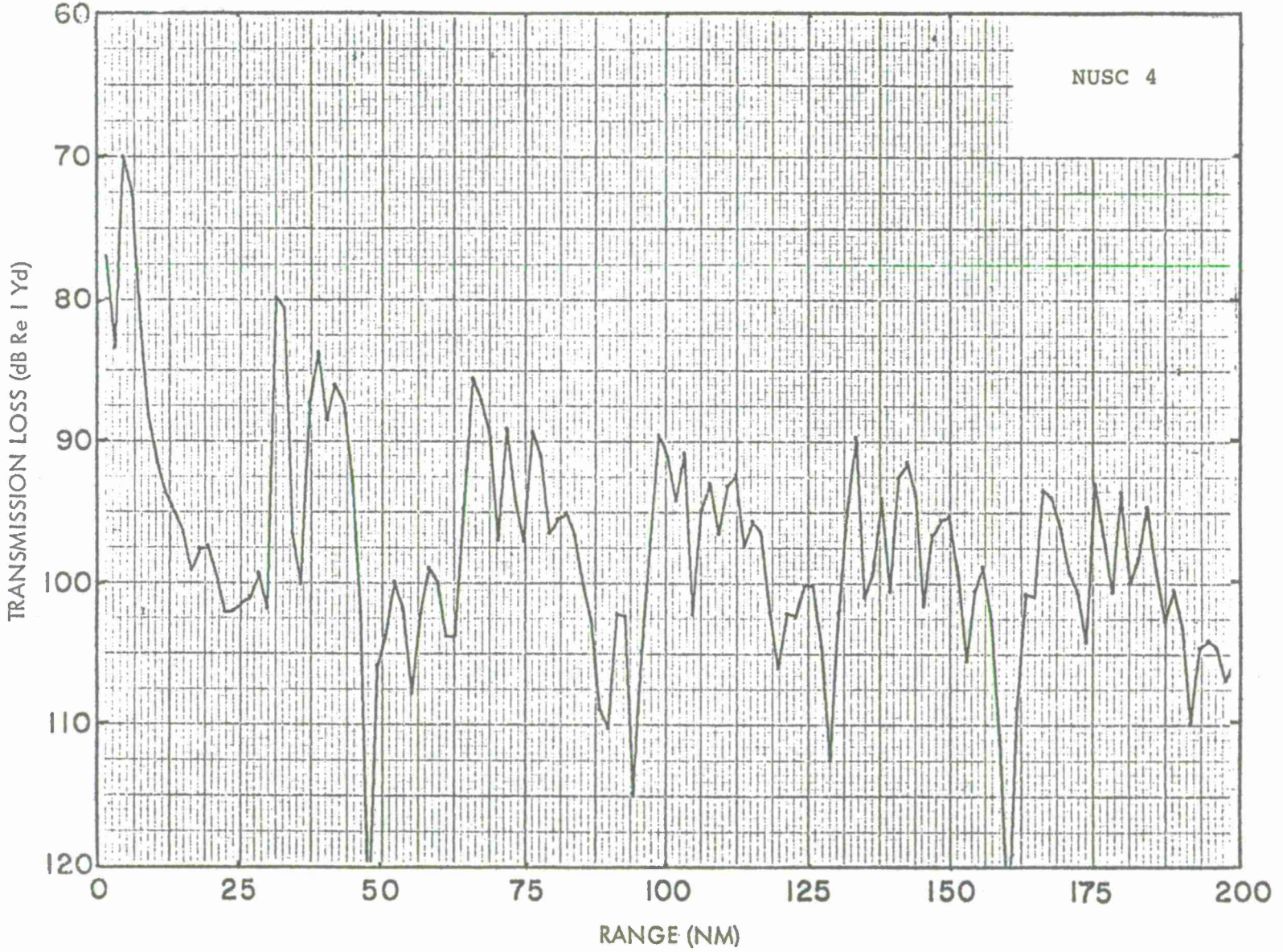

CASE 2 - EASTERN ATLANTIC PROFILE $Y_s = 800$ FT $Y_r = 3600$ FT F = 50 HZ

FIGURE 39

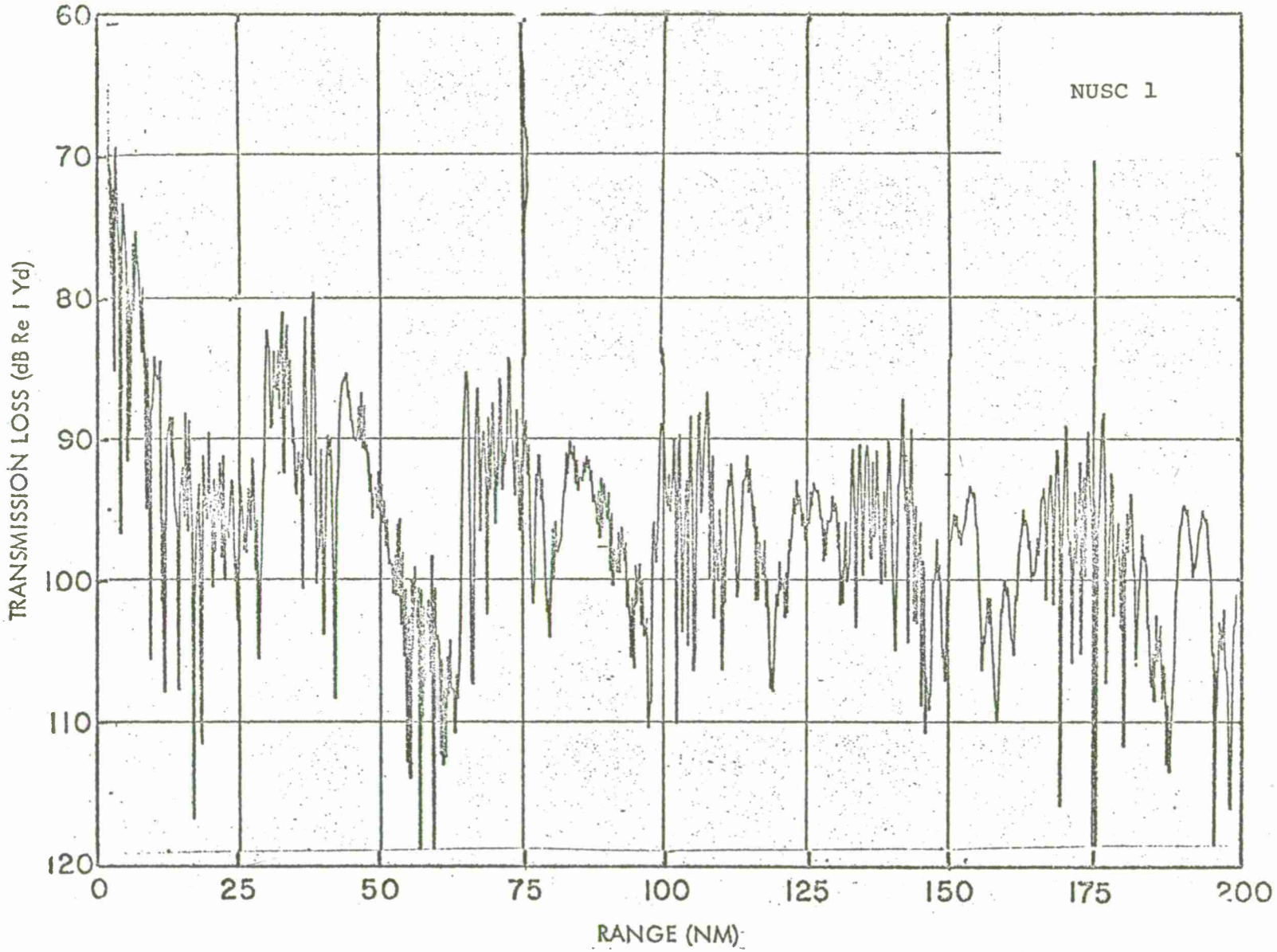

CASE 2 - EASTERN ATLANTIC PROFILE $Y_s = 800$ FT $Y_r = 3600$ FT F = 50 HZ

FIGURE 40

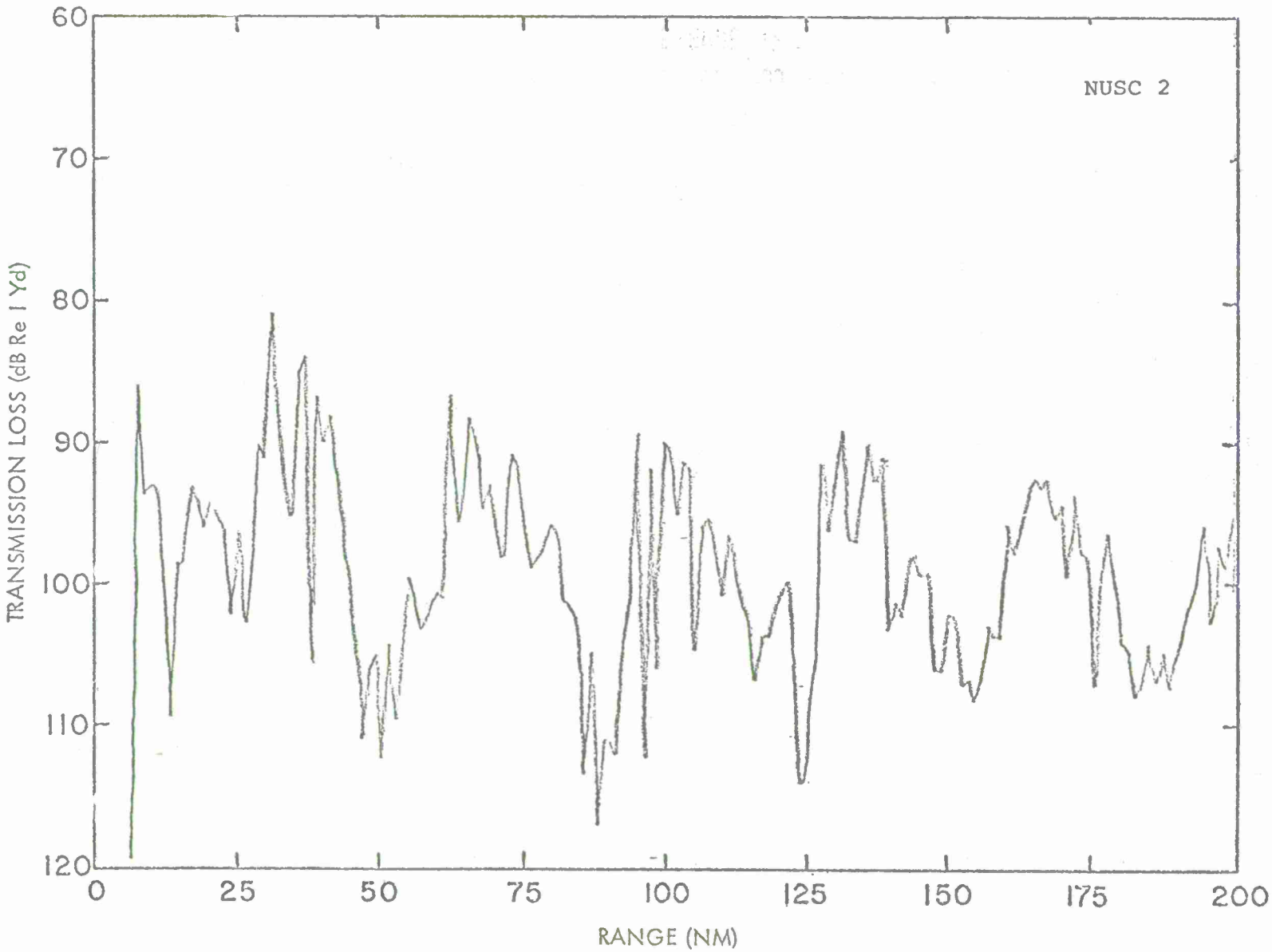

CASE 2 - EASTERN ATLANTIC PROFILE Y_s = 800 FT Y_r = 3600 FT F = 50 HZ

FIGURE 41

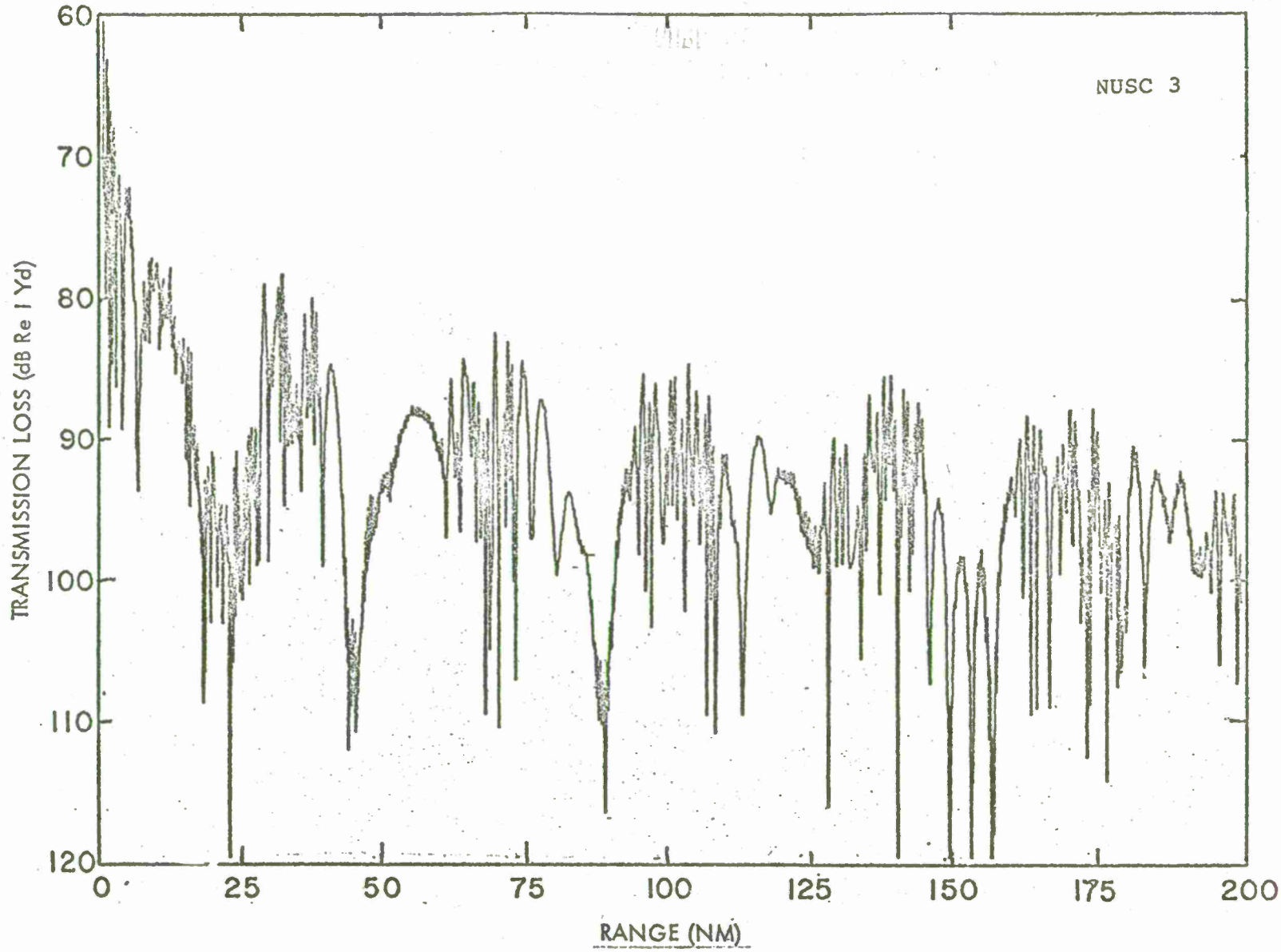

CASE 2 - EASTERN ATLANTIC PROFILE $Y_s = 800$ FT $Y_r = 3600$ FT F = 50 H7

FIGURE 42

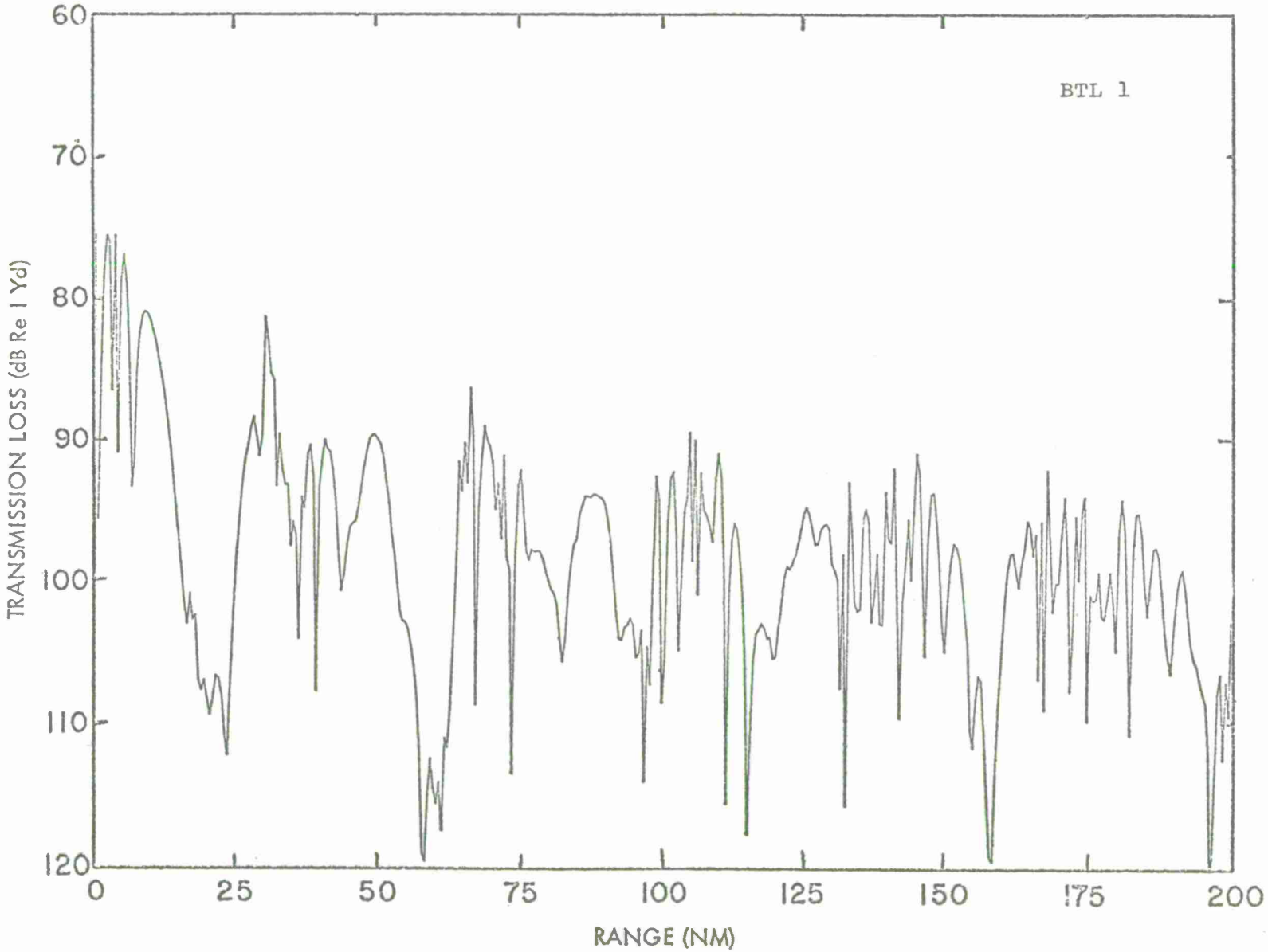

CASE 2 - EASTERN ATLANTIC PROFILE Y_s = 800 FT Y_r = 3600 FT F = 50 HZ

FIGURE 43

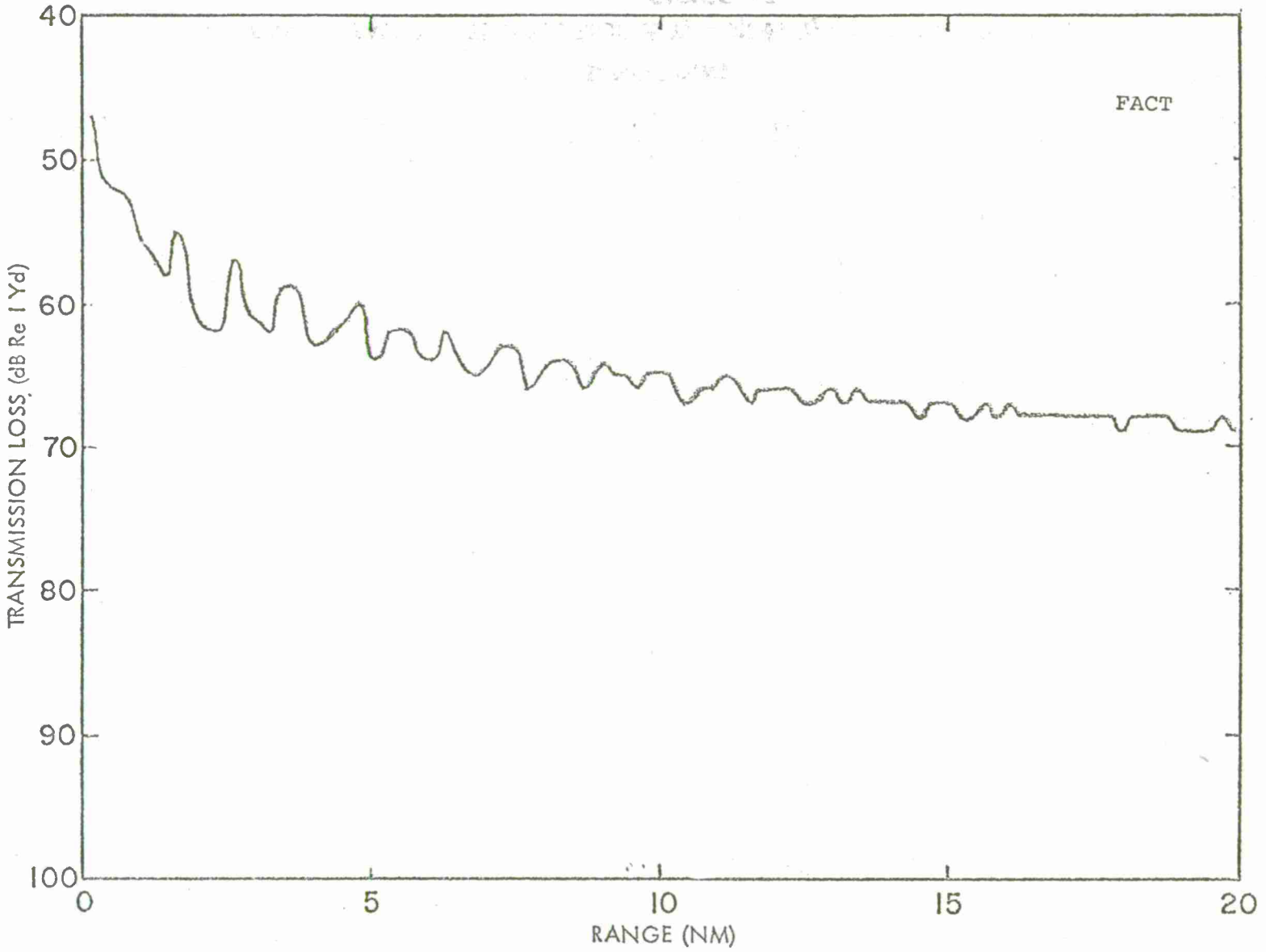

CASE 3a - SHALLOW WATER - Y_s = 20 FT Y_r = 40 FT F = 500 HZ

FIGURE 44

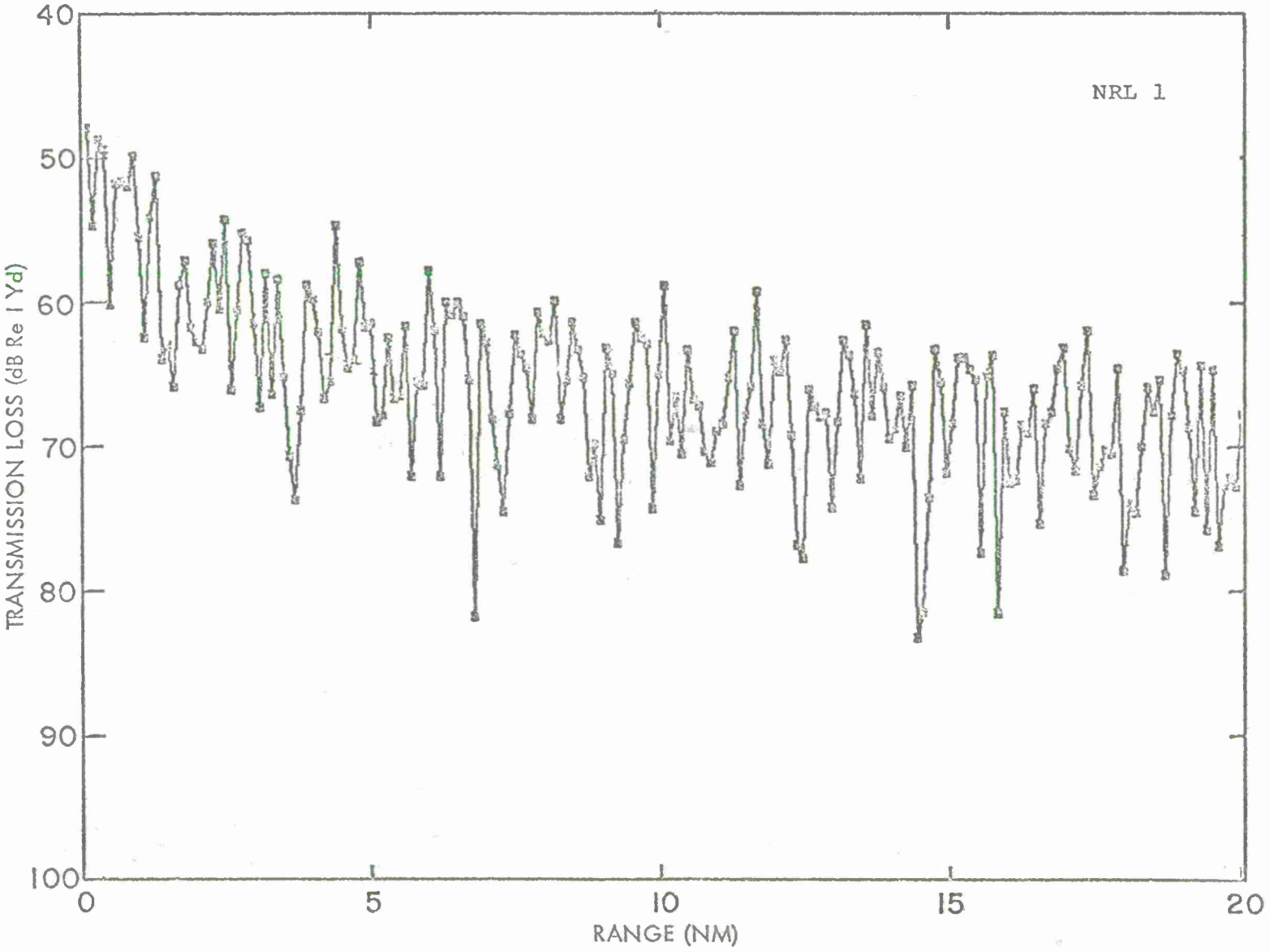

CASE 3a - SHALLOW WATFR - Y_s = 20 FT Y_r = 40 FT F = 500 HZ

FIGURE 45

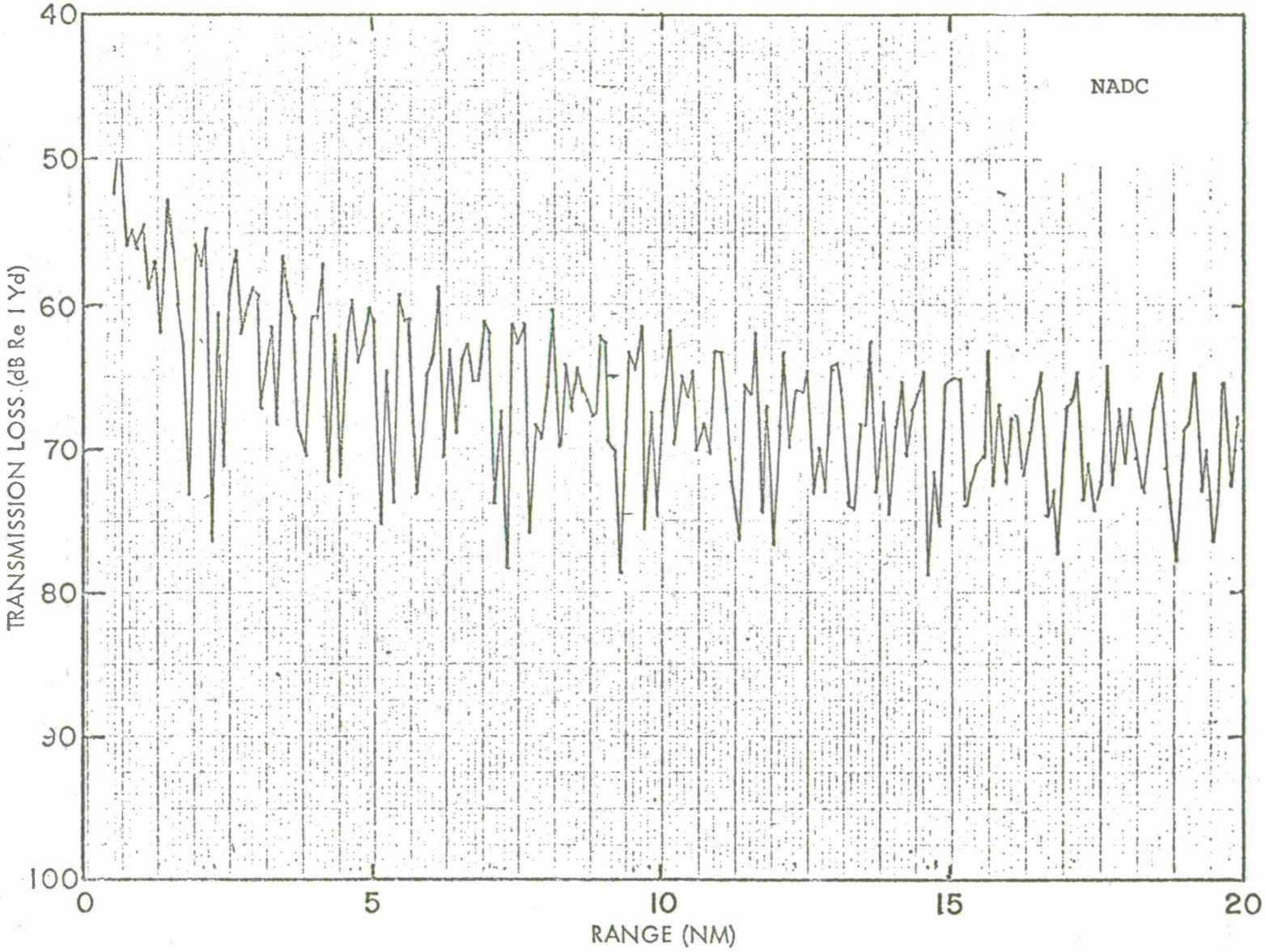

CASE 3a - SHALLOW WATER - Y_s = 20 FT Y_r = 40 FT F = 500 HZ.

FIGURE 46

FIGURE 47

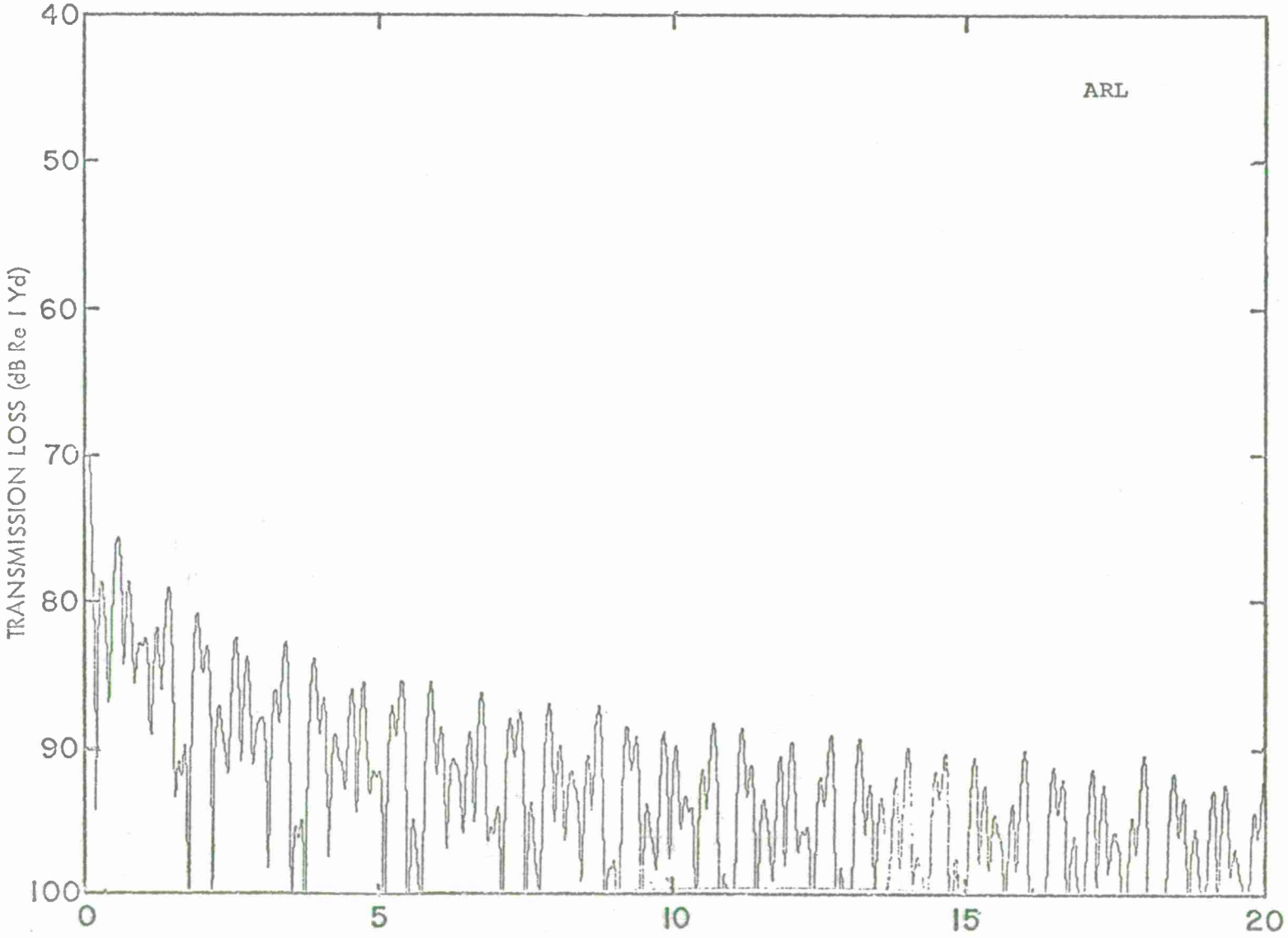

FIGURE 48

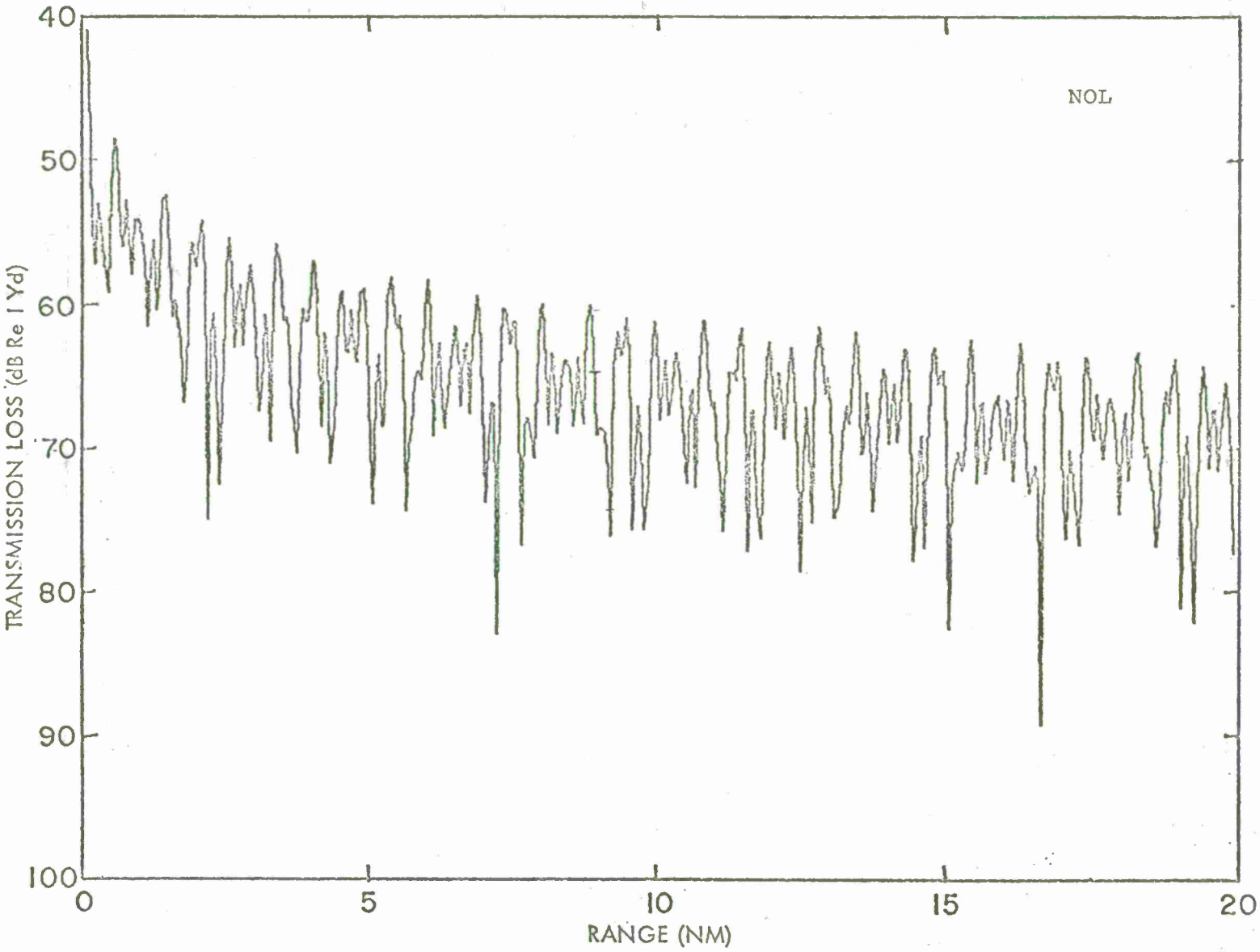

CASE 3a - SHALLOW WATER - Y_s = 20 FT Y_r = 40 FT F = 500 HZ

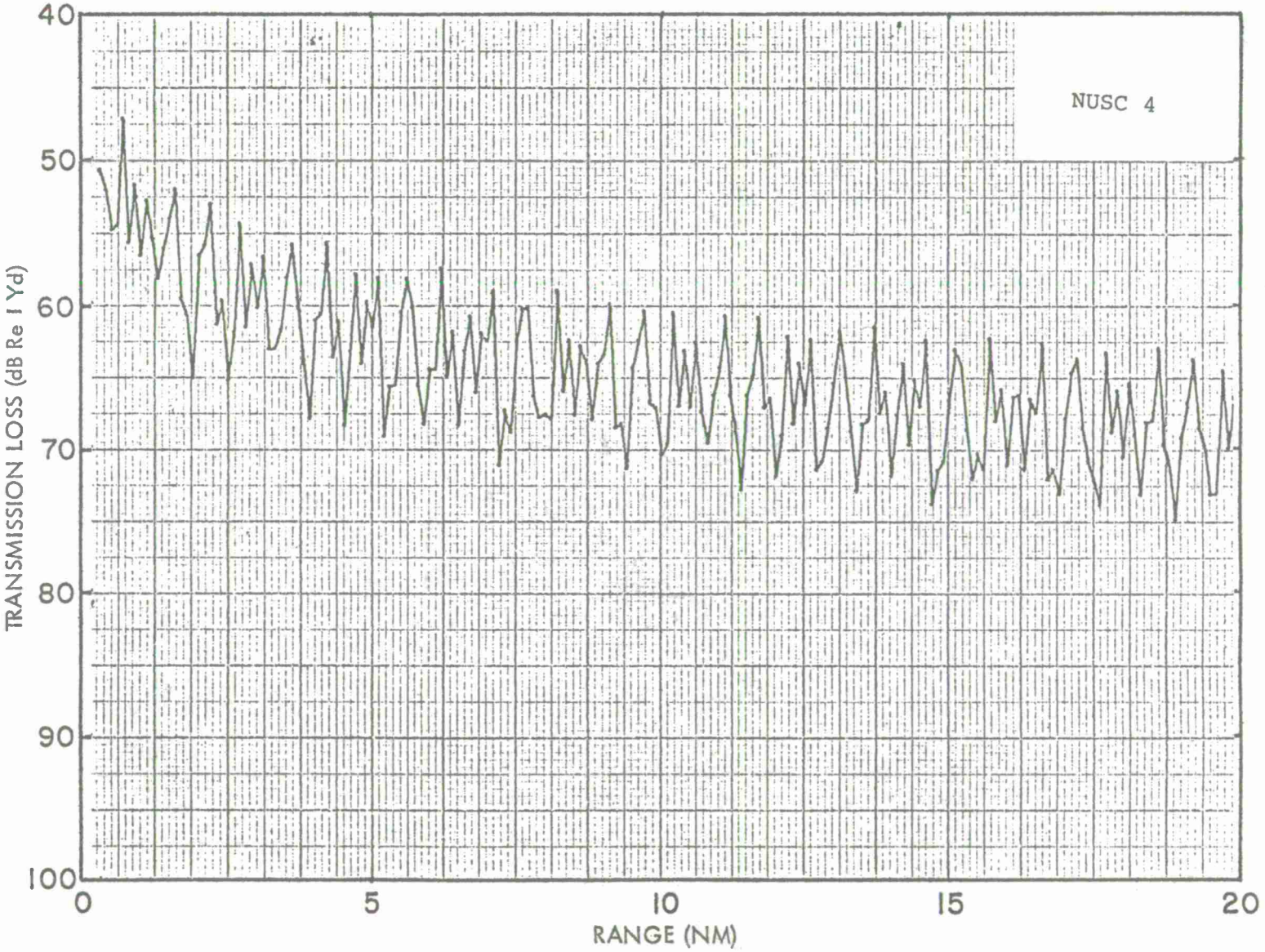

CASE 3a - SHALLOW WATER - $Y_s = 20$ FT $Y_r = 40$ FT F = 500 HZ

FIGURE 49

FIGURE 50

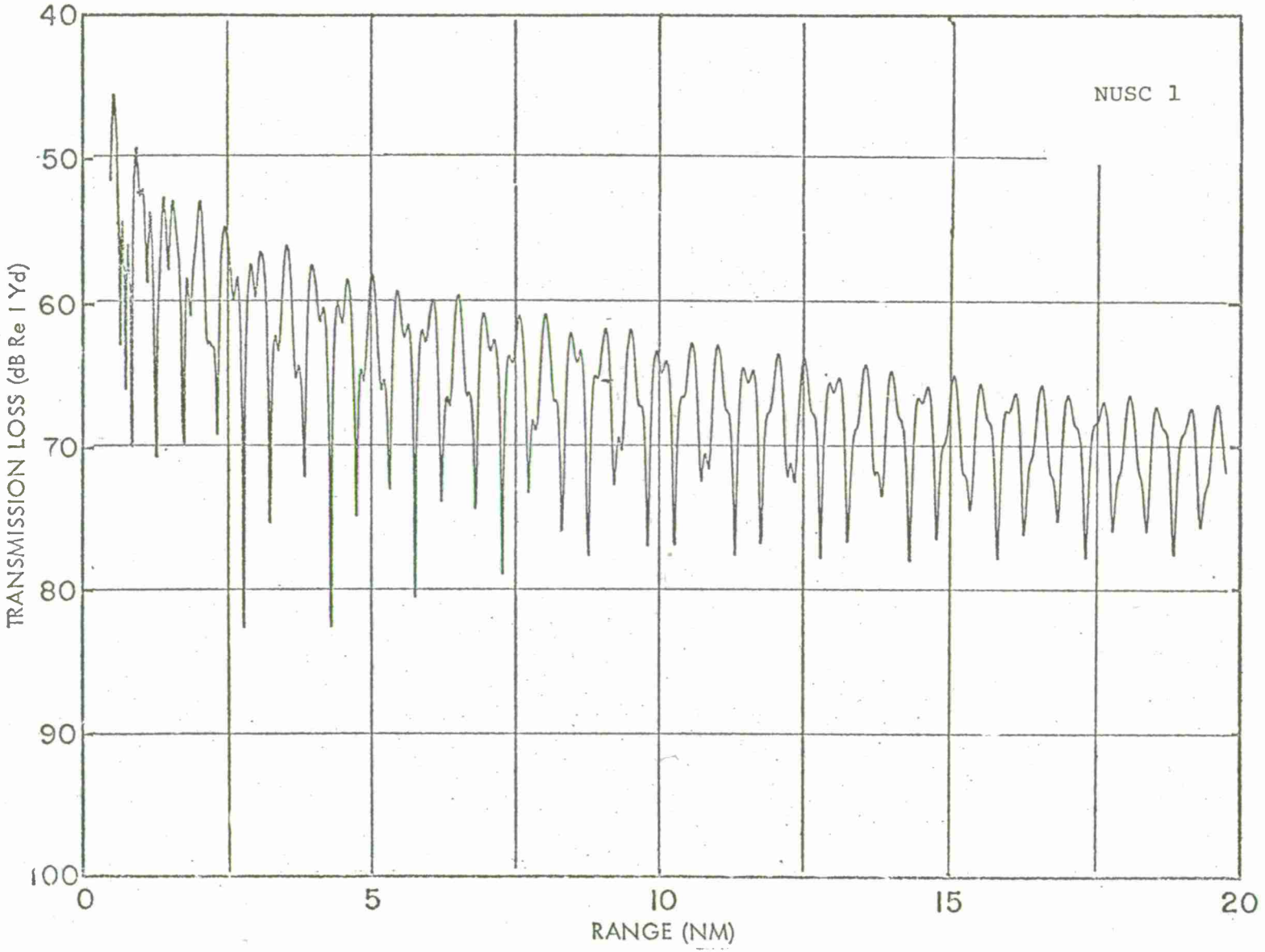

CASE 3a - SHALLOW WATER - Y_s = 20 FT Y_r = 40 FT F = 500 HZ

FIGURE 51

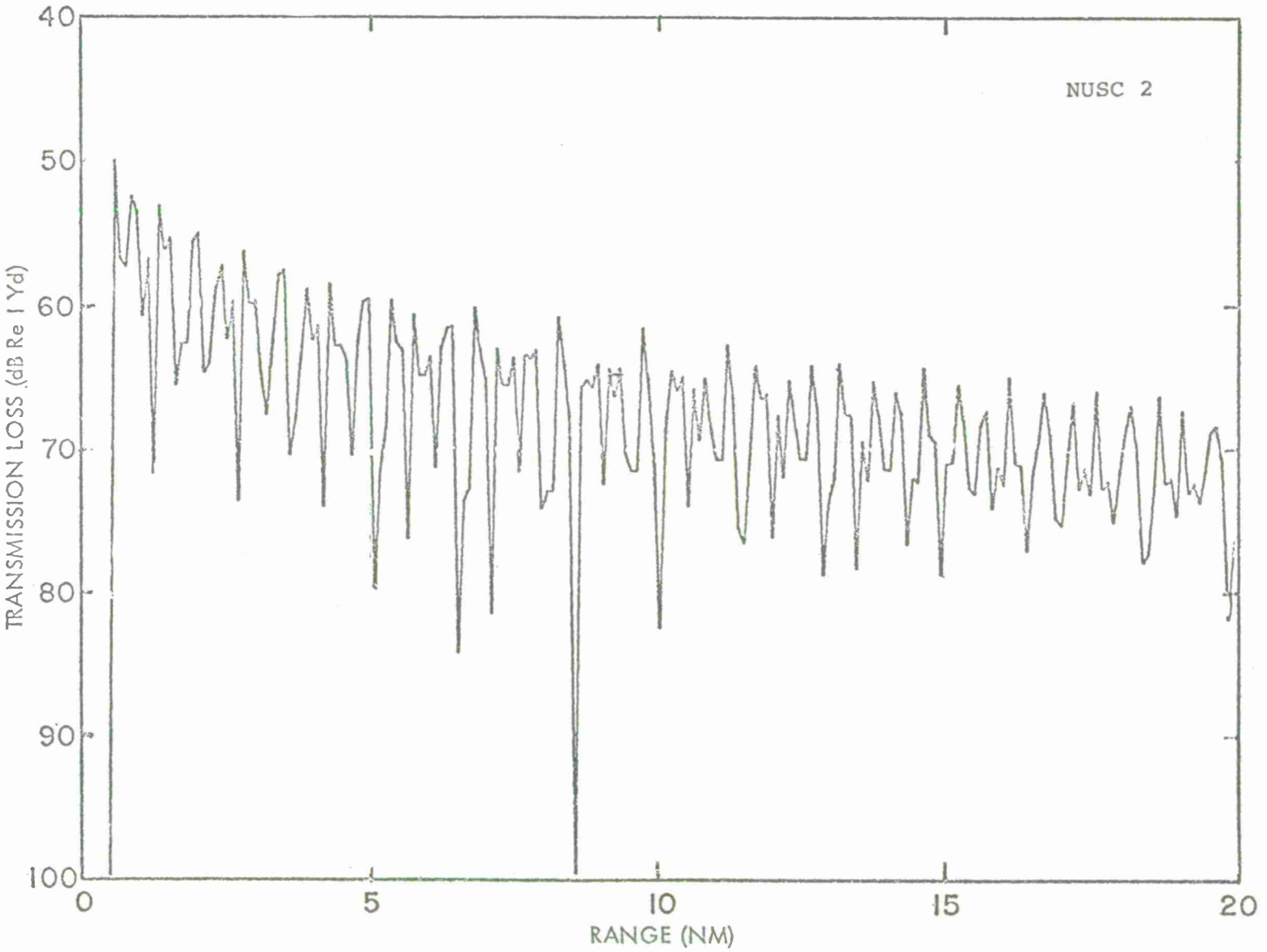

CASE 3a - SHALLOW WATER - Y_s = 20 FT Y_r = 40 FT F = 500 HZ

FIGURE 52

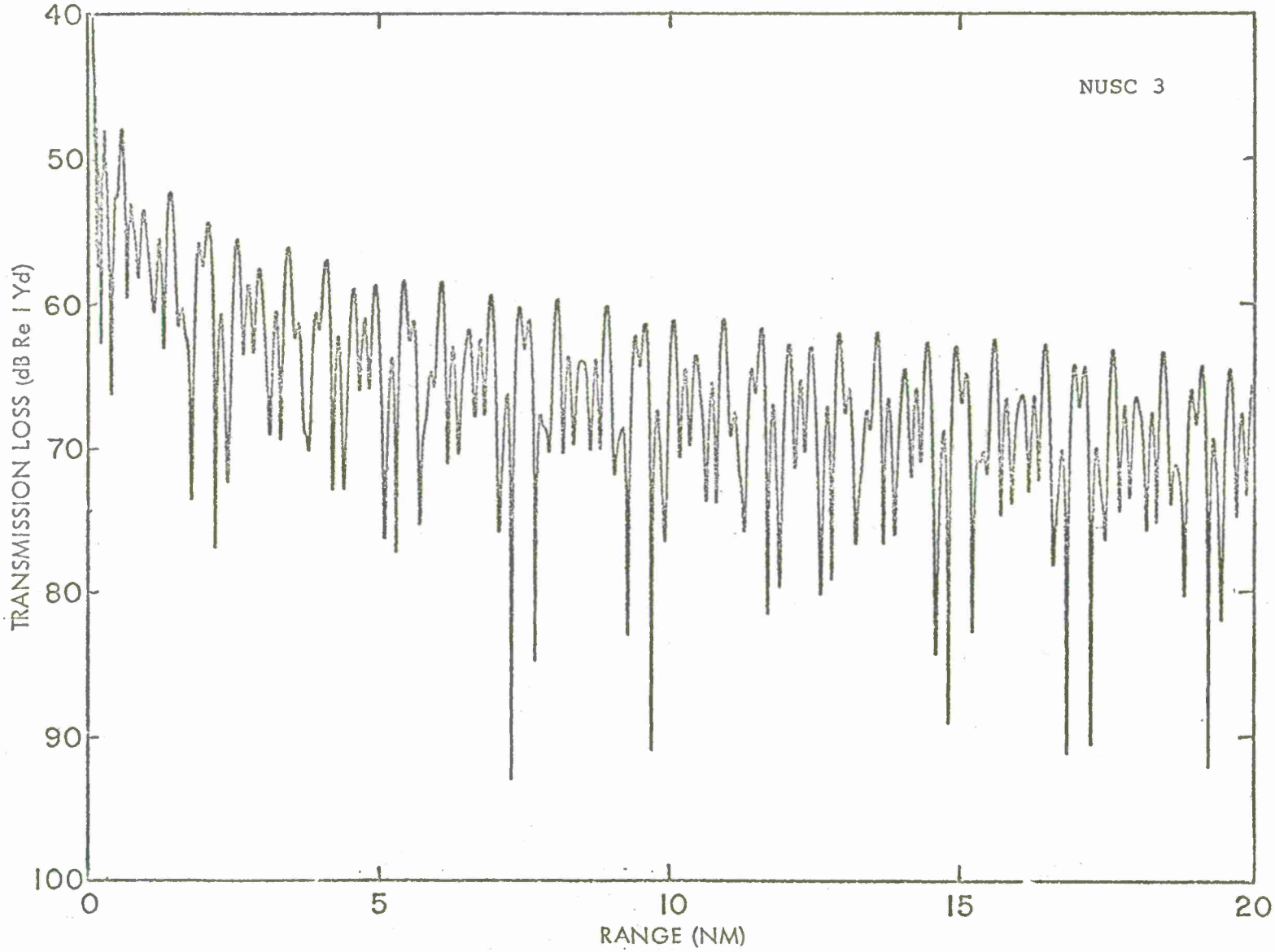

CASE 3a - SHALLOW WATER - Y_s = 20 FT Y_r = 40 FT F = 500 HZ

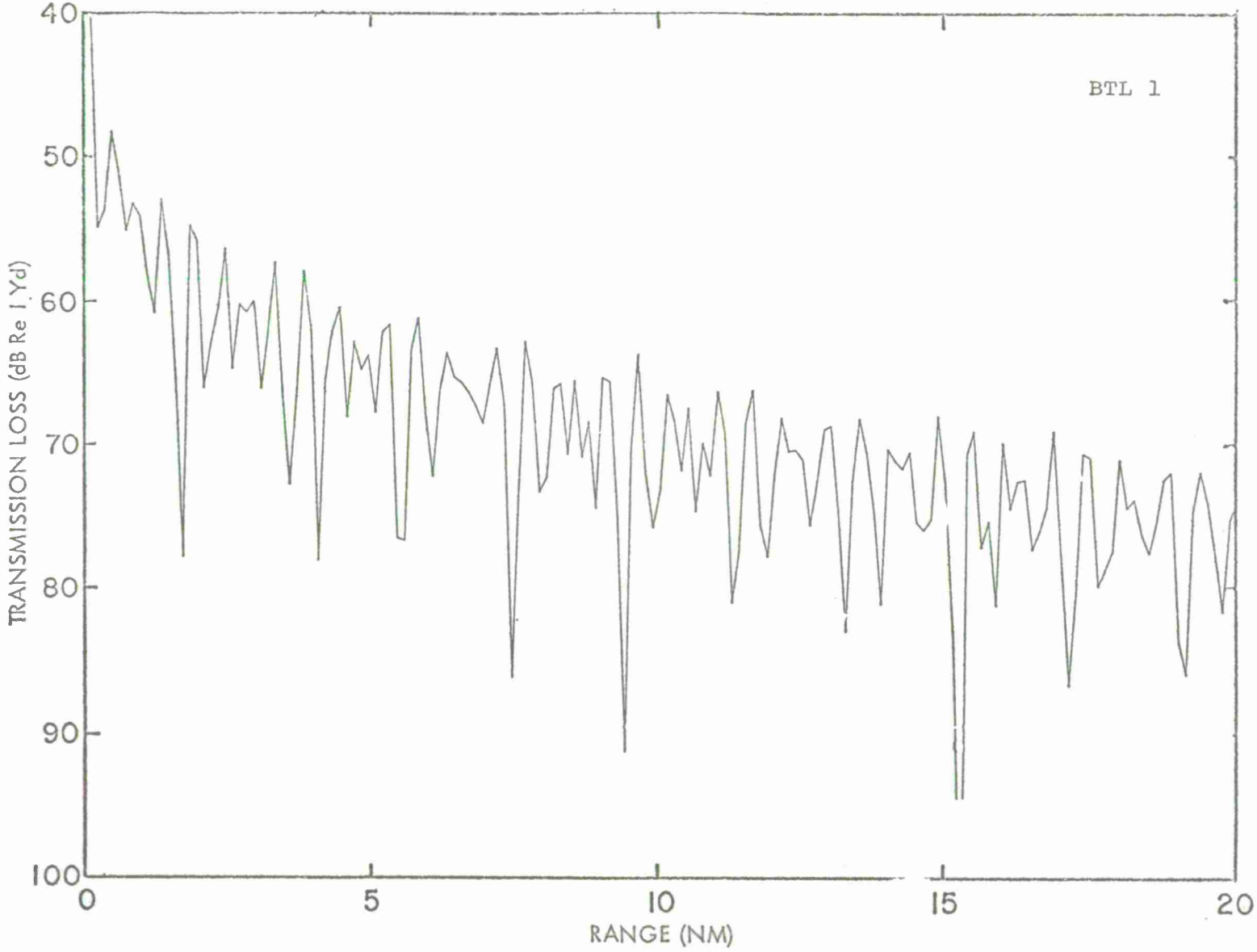

CASE 3α - SHALLOW WATER - Y_s = 20 FT Y_r = 40 FT F = 500 HZ

FIGURE 53

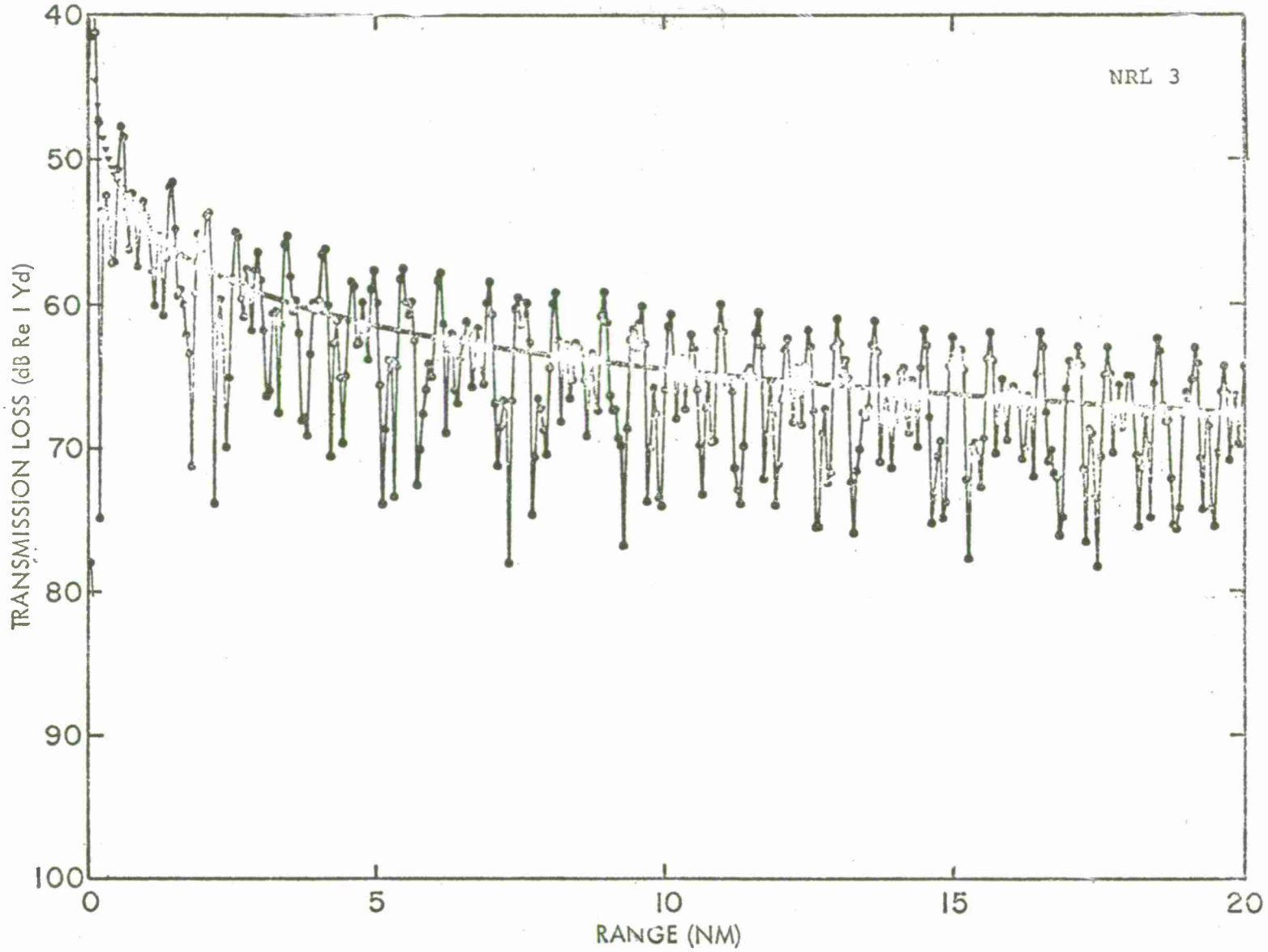

CASE 3a - SHALLOW WATER - $Y_s = 20$ FT $Y_r = 40$ FT F = 500 HZ

FIGURE 54

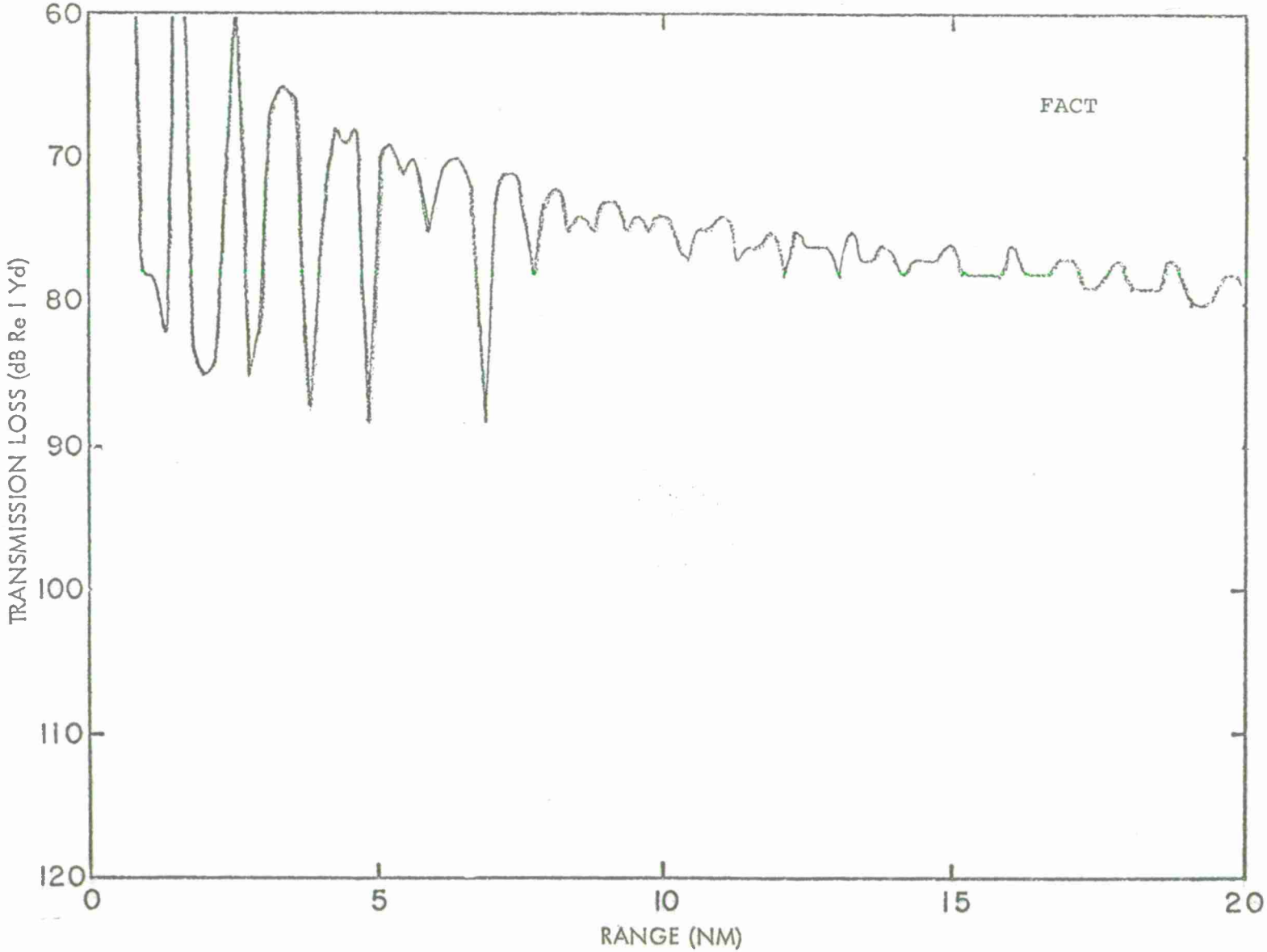

CASE 3b - SHALLOW WATER - $Y_s = 20$ FT $Y_r = 40$ FT F = 50 HZ

FIGURE 55

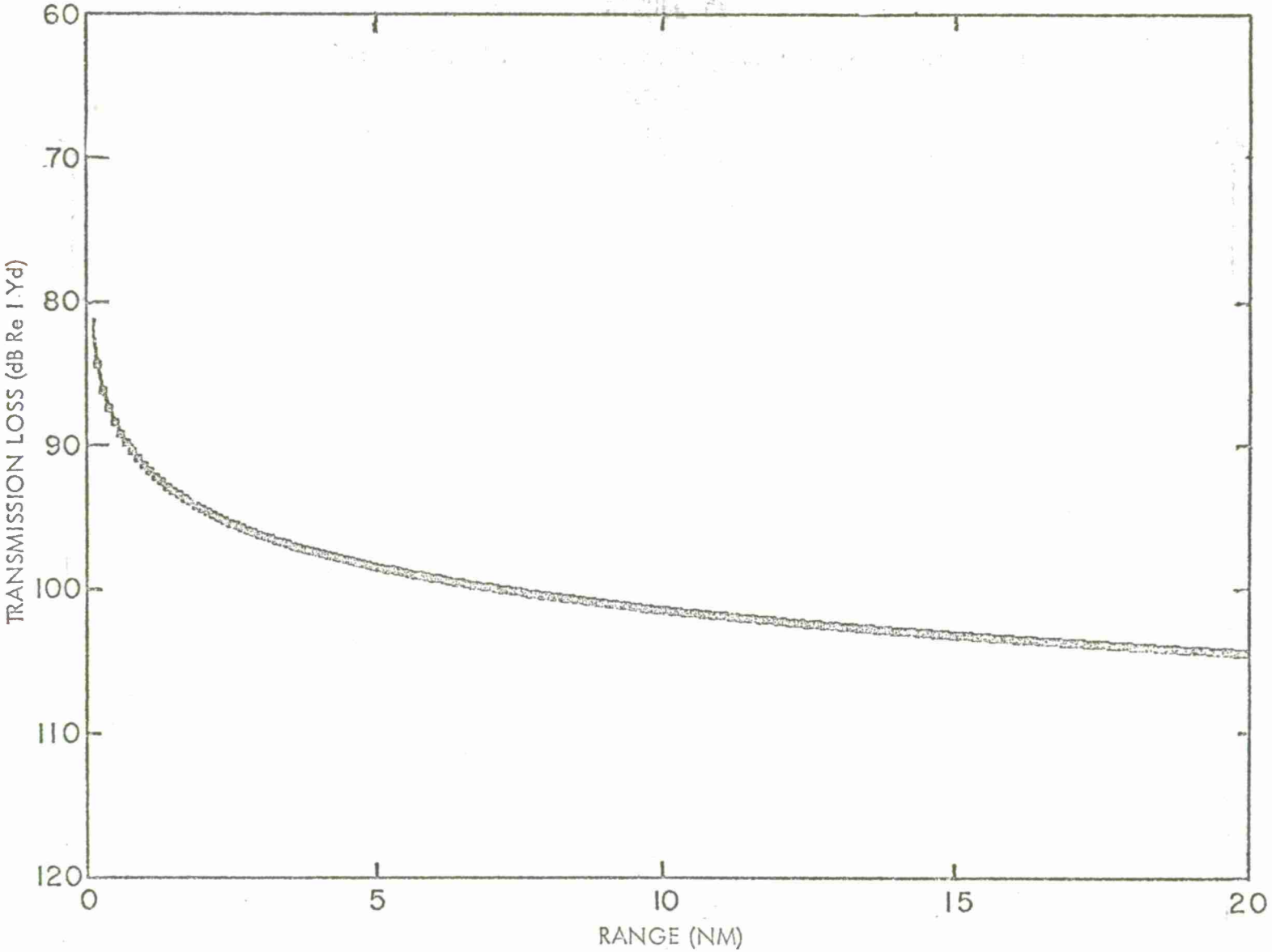

CASE 3b – SHALLOW WATER – Y_s = 20 FT Y_r = 40 FT F = 50 HZ

FIGURE 56

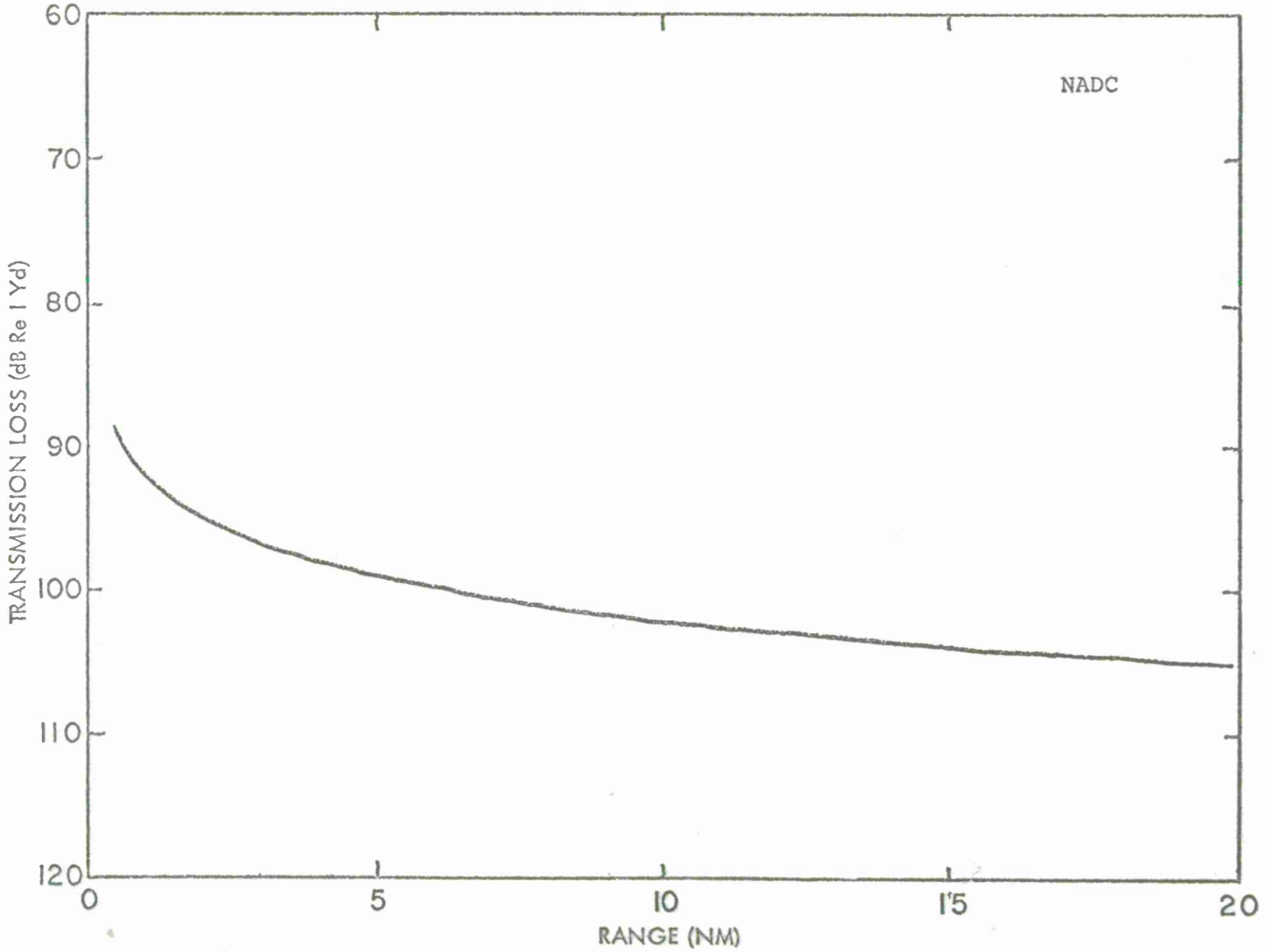

CASE 3b – SHALLOW WATER – $Y_s = 20$ FT $Y_r = 40$ FT T = 50 HZ

FIGURE 57

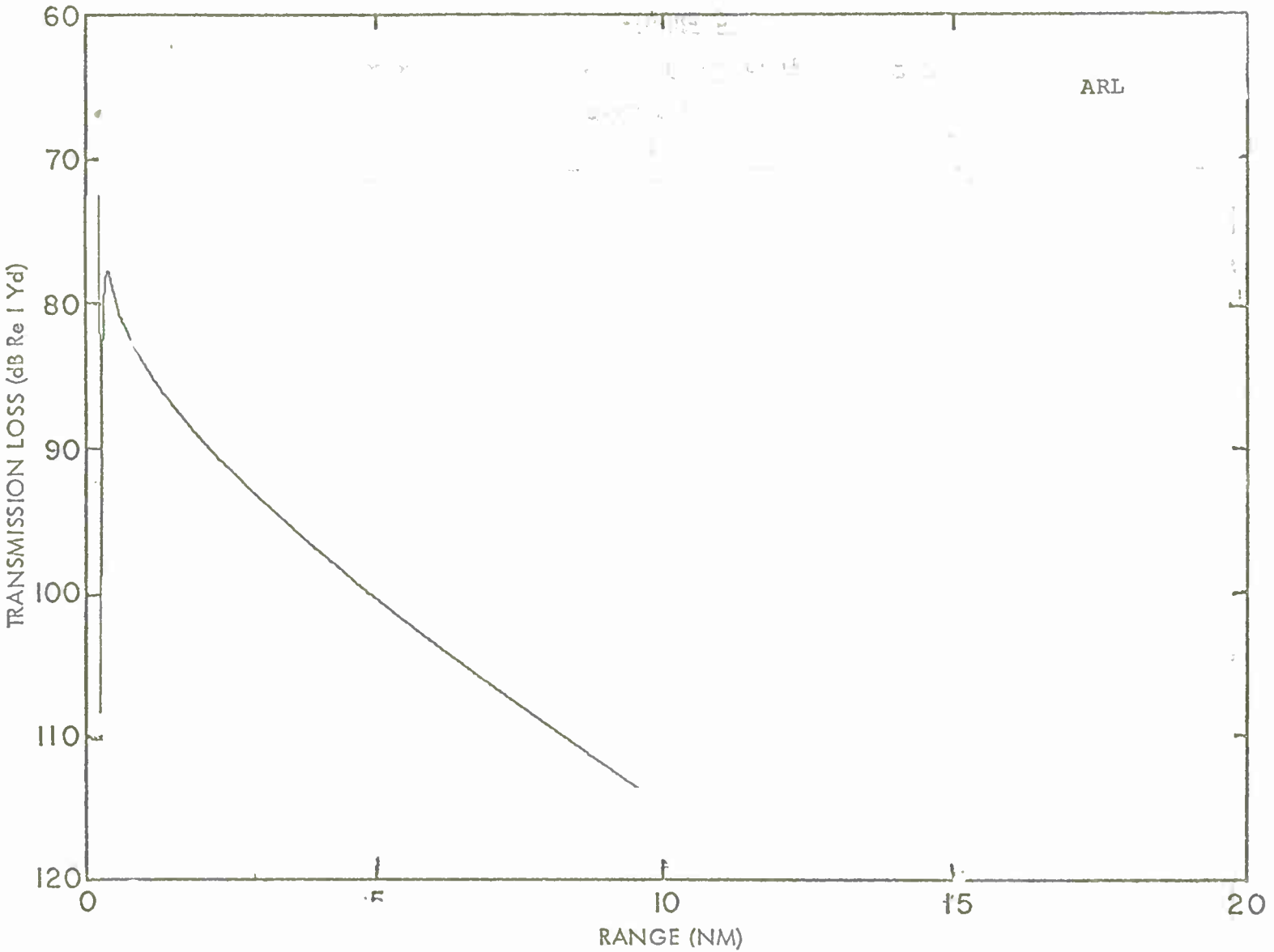

CASE 3b - SHALLOW WATER - Y_s = 20 FT Y_r = 40 FT F = 50 HZ

FIGURE 58

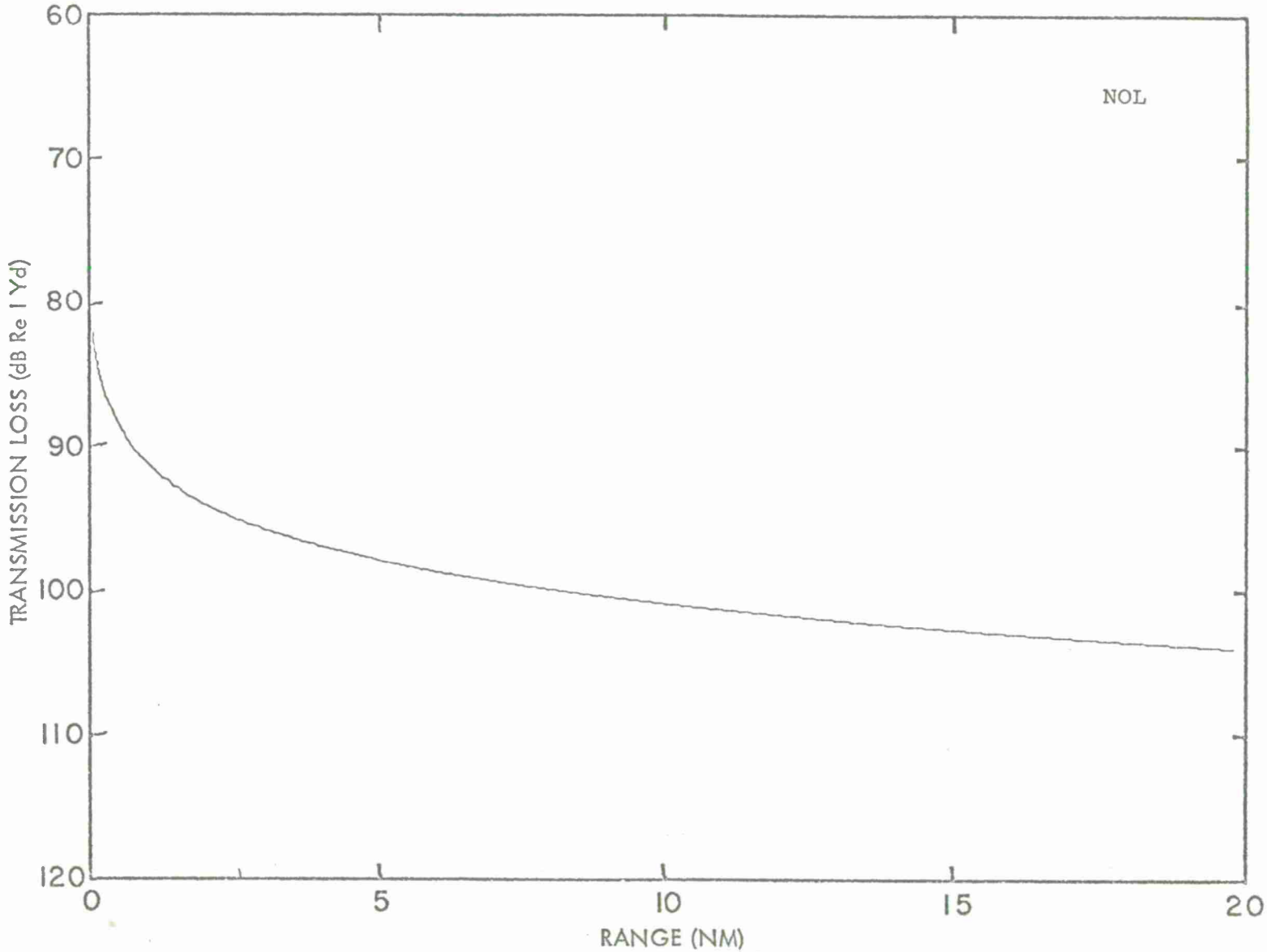

CASE 3b - SHALLOW WATER - $Y_s = 20$ FT $Y_r = 40$ FT F = 50 HZ

FIGURE 59

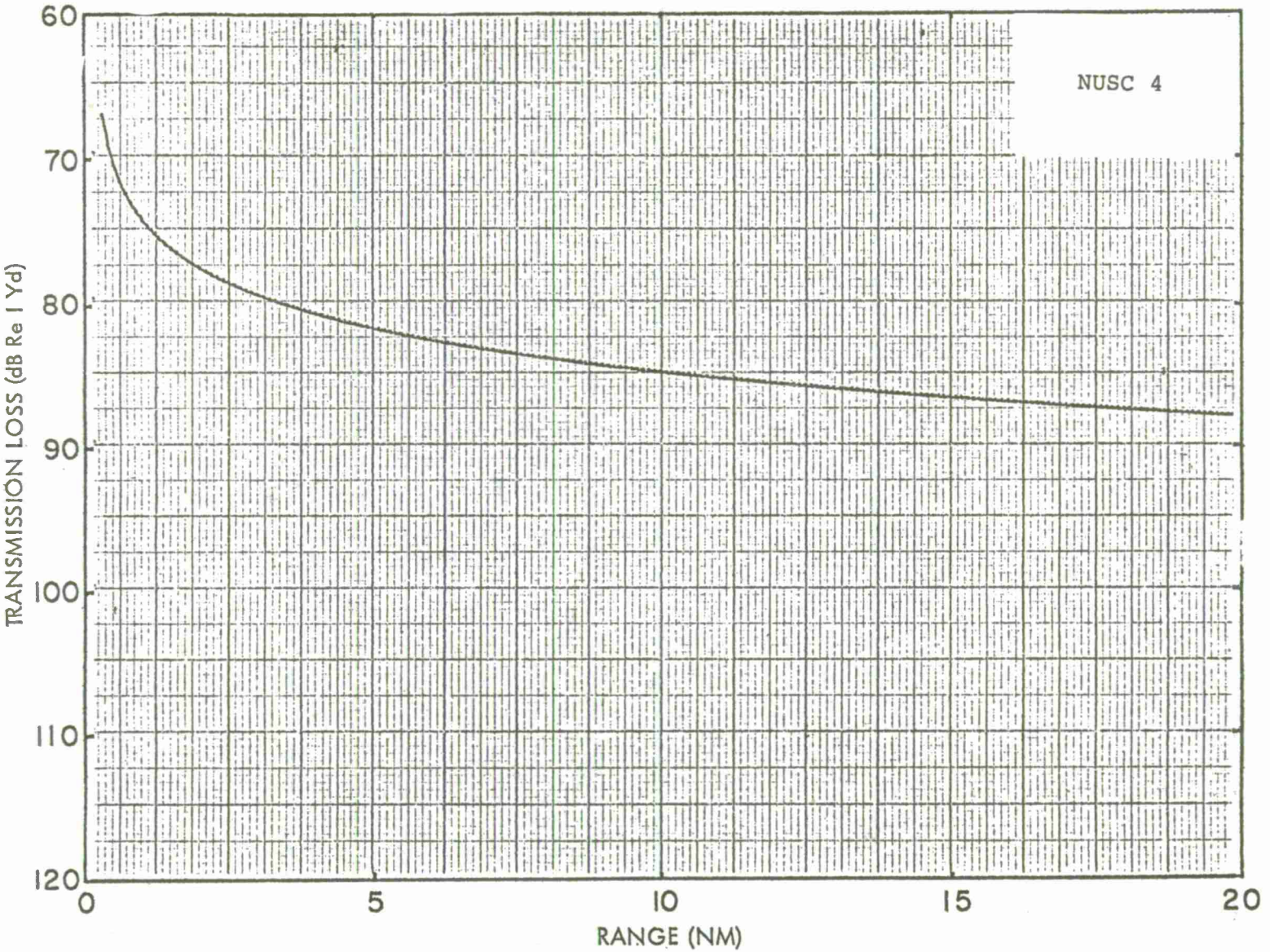

CASE 3b - SHALLOW WATER - Y_s = 20 FT Y_r = 40 FT F = 50 HZ

FIGURE 60

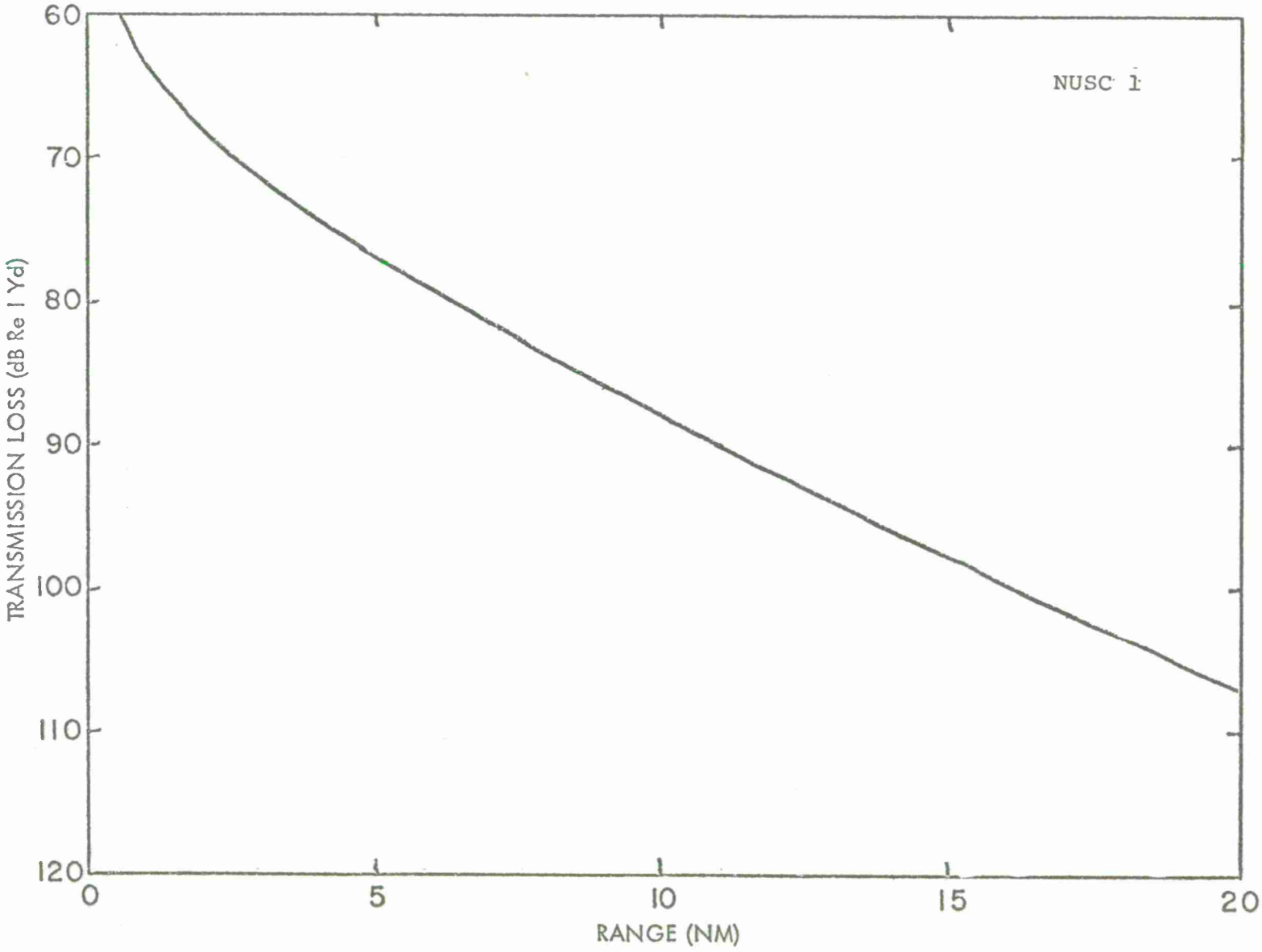

CASE 3b - SHALLOW WATER - $Y_s = 20$ FT $Y_r = 40$ FT F = 50 HZ

FIGURE 61

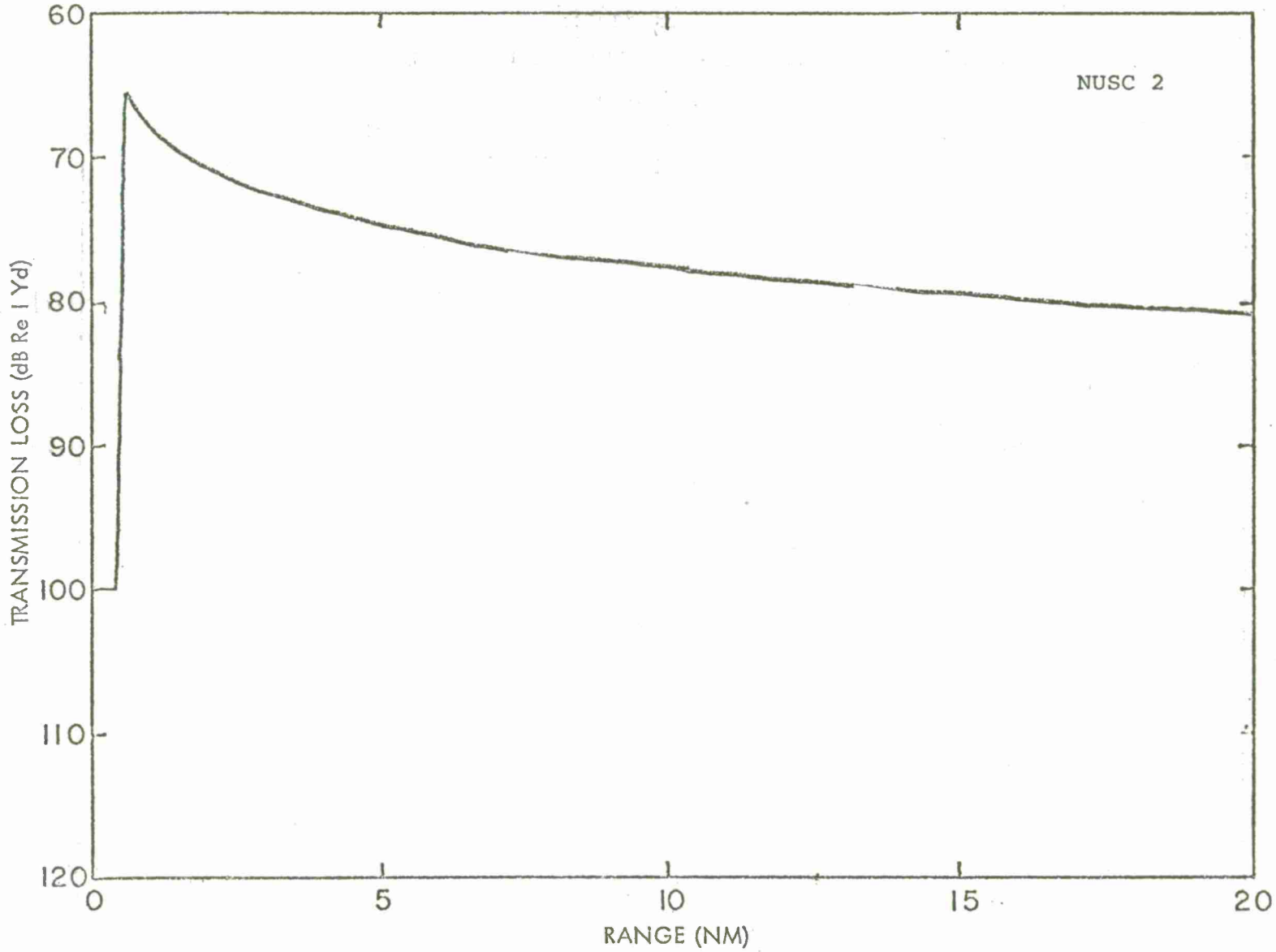

CASE 3b - SHALLOW WATER - $Y_s = 20$ FT $Y_r = 40$ FT F = 50 HZ

FIGURE 62

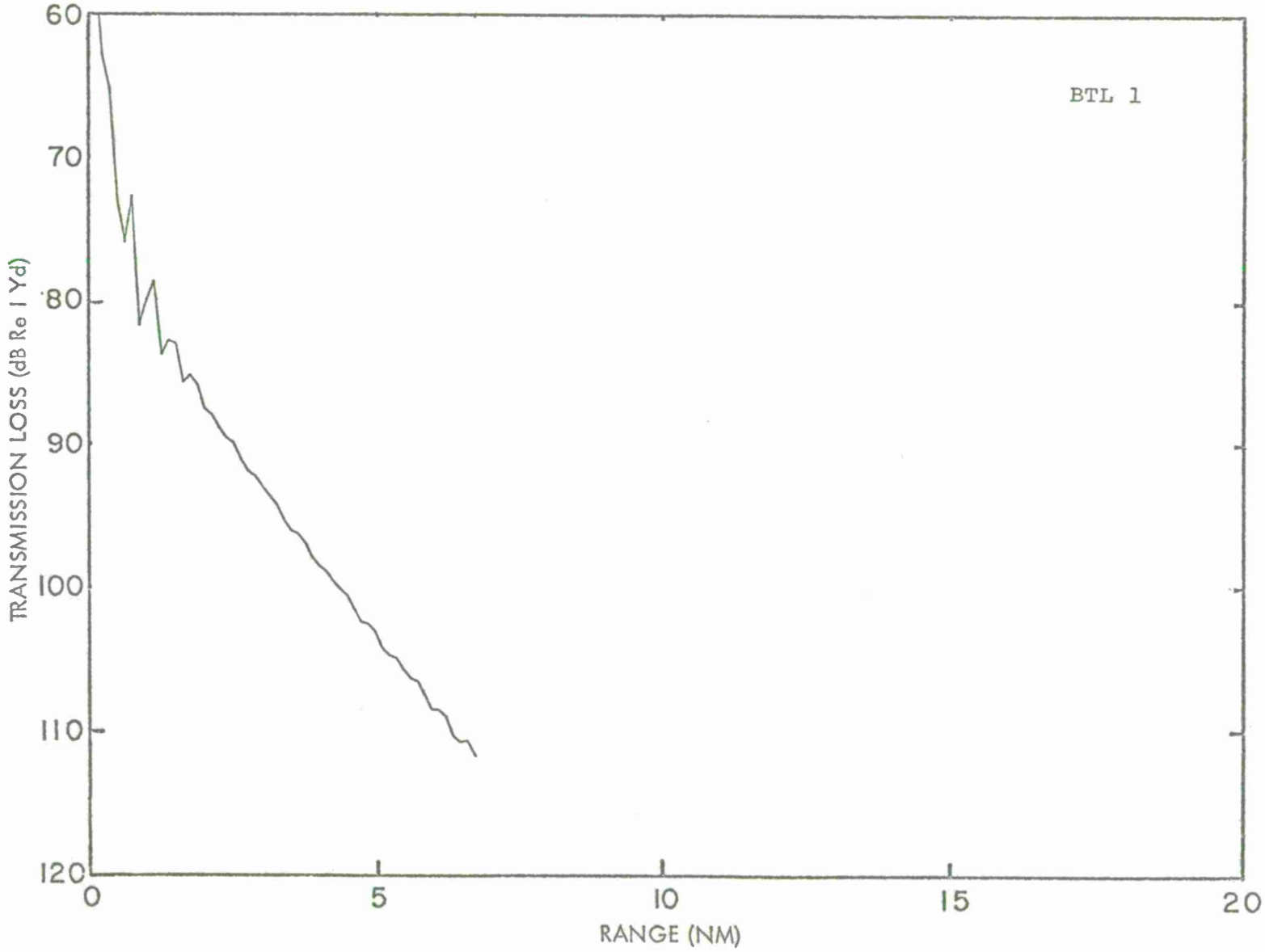

CASE 3b - SHALLOW WATER - Y_s = 20 FT Y_r = 40 FT F = 50 HZ

FIGURE 63

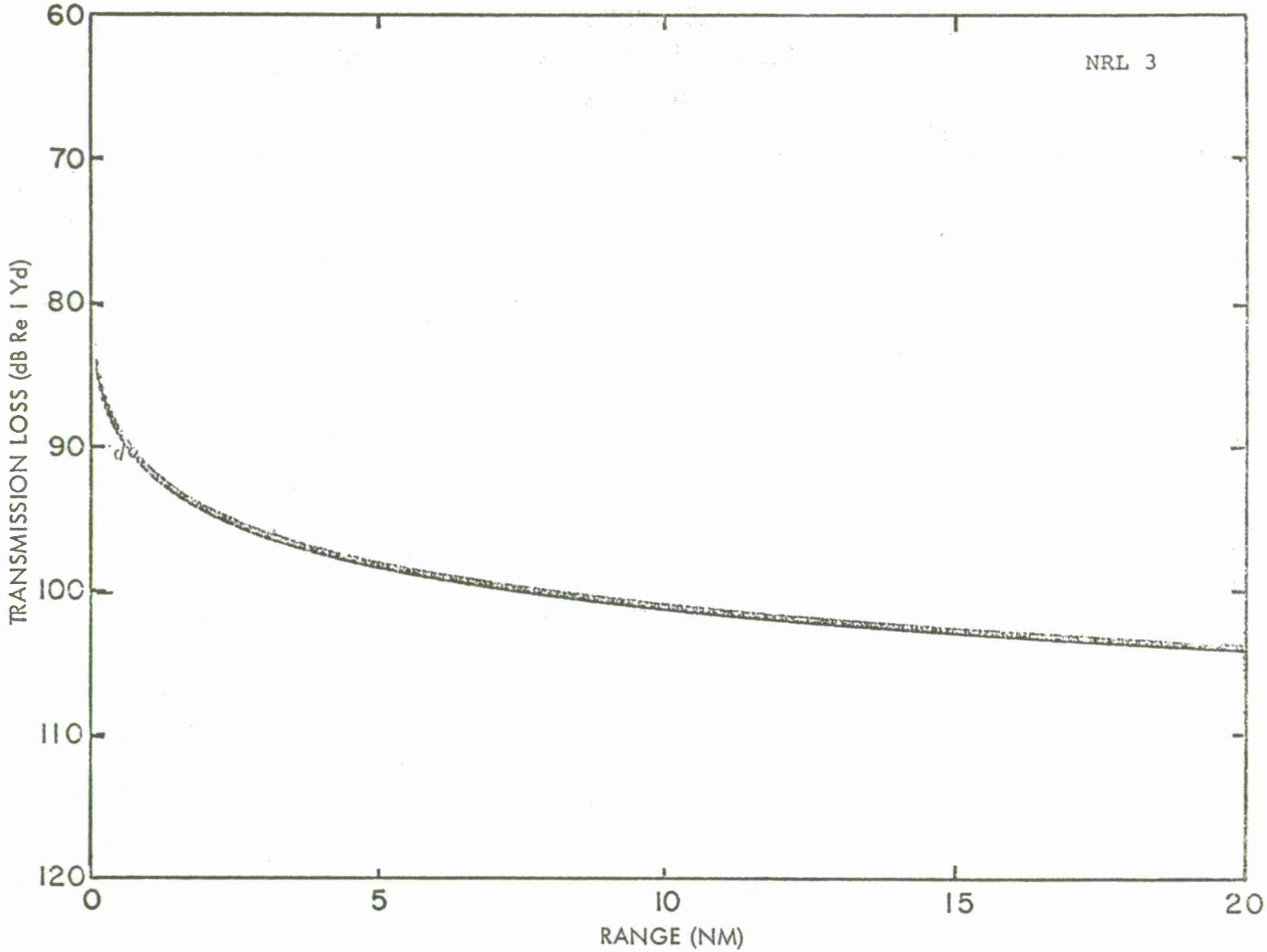

CASE 3b - SHALLOW WATER - Y_s = 20 FT Y_r = 20 FT F = 50 HZ

FIGURE 64

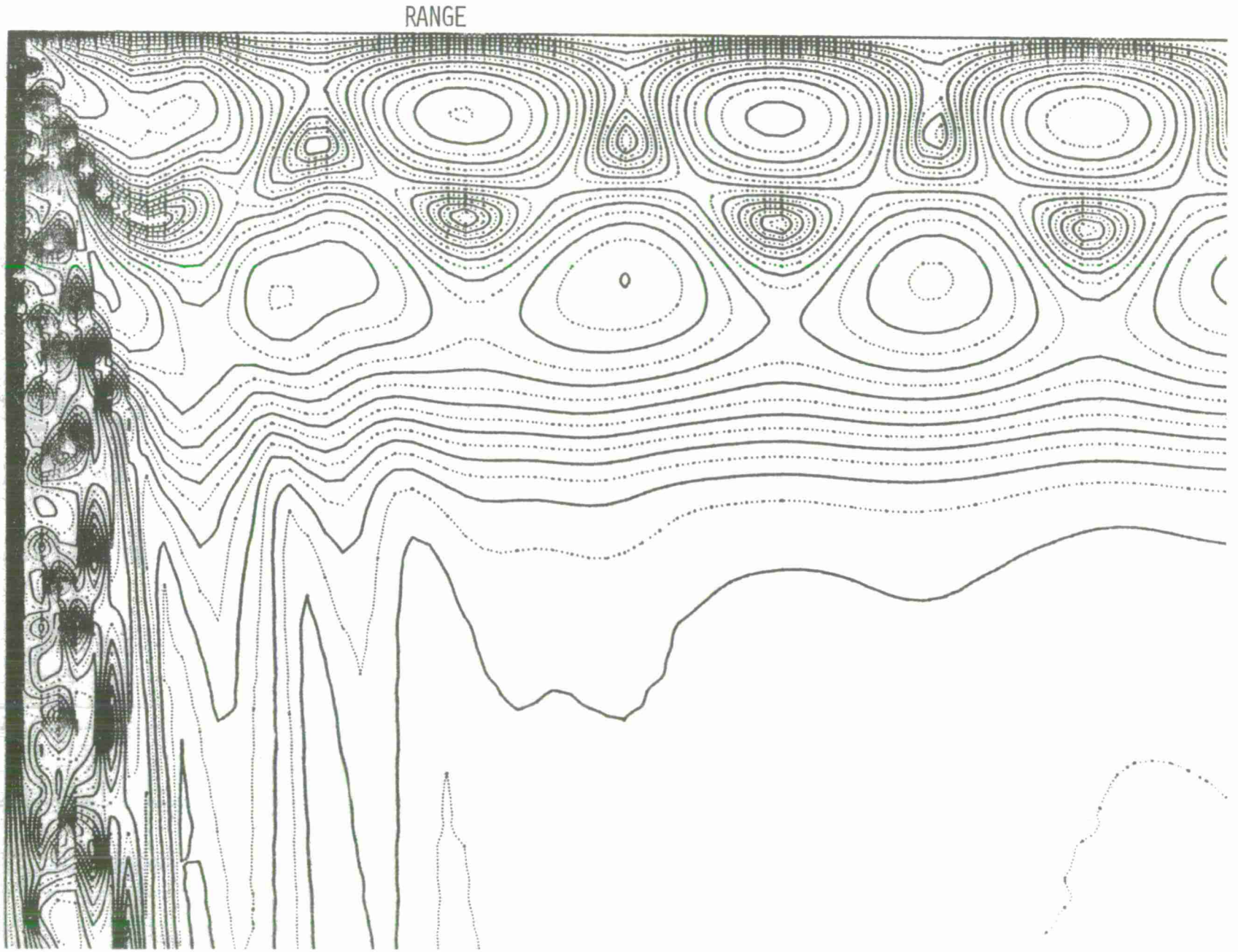

FIGURE 65 - ISOINTENSITY CONTOURS FOR A RANGE INDEPENDENT SURFACE DUCT (BTL-1)

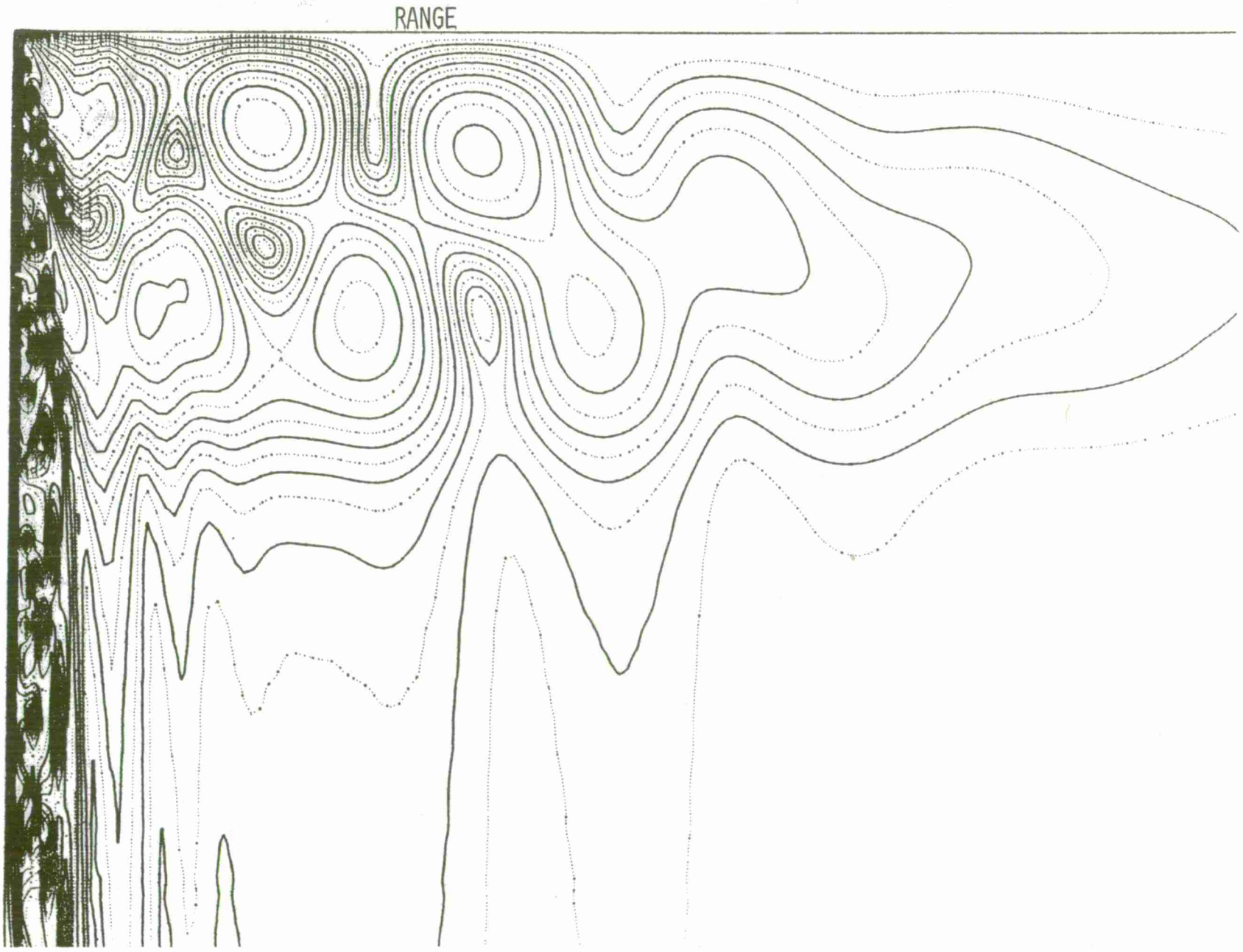

FIGURE 66 - ISOTENSITY CONTOURS FOR A RANGE DECAYING SURFACE DUCT (BTL-1)

DISTRIBUTION LIST

	No. of Copies
Office of Naval Research **Department of the Navy** **Arlington, Virginia 22217**	
Code 101	1
102-OS	1
102-OSC	1
460	1
462	1
466	1
468	1
480	1
484	1
Chief of Naval Operations **Department of the Navy** **Washington, D. C. 20360**	
Code OP-0951F	1
951C	1
951D	1
951E	1
952	1
952E	1
981H	1
987	1
Chief of Naval Material **Department of the Navy** **Washington, D. C. 20360**	
Code NMAT-0341	1
Director **Naval Research Laboratory** **4555 Overlook Avenue, S.W.** **Washington, D. C. 20390**	
Code 1000	1
5715	1
8000	1
8120	2
8160	1
8167	1
8168	1
8170	1
8176	1

DISTRIBUTION LIST (Cont.)

	No. of Copies
Commander Naval Electronics Systems Command Department of the Navy Washington, D. C. 20360	
Code PME-124	1
NELEX-03	1
Commander Naval Ship Systems Command Department of the Navy Washington, D. C. 20360	
Code PMS-302-4	1
Project Manager ASW Systems Project Department of the Navy Washington, D. C. 20360	
Code ASW-14	2
15	1
21	1
22	1
23	1
24	1
Oceanographer of the Navy Hoffman II Building 200 Stovall Street Alexandria, Virginia 22314	
ATTN: Mr. J. Boosman	1
Commander Second Fleet Norfolk, Virginia 23511	1
Commander Third Fleet FPO San Francisco 96610	1

DISTRIBUTION LIST (Cont.)

	No. of Copies
Commander Submarine Development Group 2 Box 70 Naval Submarine Base, New London Groton, Connecticut 06340	1
Commander Destroyer Development Group FPO New York 09501	1
Commander Oceanographic Systems, Atlantic Box 100 Norfolk, Virginia 23511	1
Commander Oceanographic Systems, Pacific Box 1390 FPO San Francisco 96610	1
Commander U. S. Naval Oceanographic Office Washington, D. C. 20390	
Code 01	1
7005	1
3342	1
Officer-in-Charge New London Laboratory Naval Underwater Systems Center New London, Connecticut 06320	
ATTN: Dr. F. DiNapoli	1
Mr. T. Einstein	1
Dr. W. Kanabis	1
Dr. G. Leibiger	1
Mr. M. Pastore	1
Mr. A. Perrone	1
Dr. W. Von Winkle	1
Mr. F. Weigle	1
Mr. H. Weinberg	1
Dr. D. Wood	1

DISTRIBUTION LIST (Cont.)

	No. of Copies
Officer-in-Charge Pasadena Laboratory Naval Undersea Center 3202 East Foothill Blvd. Pasadena, California 91107	1
Officer-in-Charge Environmental Prediction Research Facility Naval Postgraduate School Monterey, California 93940	1
Officer-in-Charge Detachment ADAK Fleet Air Wing Two FPO Seattle 98791	
ATTN: Mr. W. A. Janes, Jr.	1
Commander Naval Undersea Center San Diego, California 92132	
Code 50	1
503	1
0513	1
Dr. H. Bucker	1
Mr. D. Gordon	1
Ms. H. Morris	1
Mr. M. Pedersen	1
Commander Naval Air Development Center Warminister, Pennsylvania 18974	
ATTN: Mr. C. Bartberger	2
Mr. J. Keane	1
Mr. C. Hammond	1
Commander Naval Ordnance Laboratory White Oak Silver Spring, Maryland 20910	
ATTN: Dr. R. Barach	1
Dr. I. Blatstein	1
Mr. B. Urick	1
Dr. W. Wineland	1

DISTRIBUTION LIST (Cont.)

	No. of Copies
Commander Naval Ship Research & Development Center Bethesda, Maryland 20034	
ATTN: Mr. D. Vendittis	1
Commander Naval Facilities Engineering Command Department of the Navy Washington, D. C. 20360	
Code PC-3	1
Chesapeake Division	1
Commander Naval Ordnance Systems Command Department of the Navy Washington, D. C. 20360	
Code NAVORD-5311	1
Commander Naval Weather Service Command Washington Navy Yard Washington, D. C. 20390	1
Commander Naval Weapons Center China Lake, California 93555	1
Commander Naval Weapons Laboratory Dahlgren, Virginia 22448	1
Commanding Officer Fleet Numerical Weather Central Monterey, California 93940	1
Director Defense, Research and Engineering Department of Defense Washington, D. C. 20301	
ATTN: Mr. Gerald Cann	1

DISTRIBUTION LIST (Cont.)

	No. of Copies
Center for Naval Analysis 1401 Wilson Blvd. Arlington, Virginia 22209	1
Defense Documentation Center Cameron Station Alexandria, Virginia 22314	2
Admiralty Research Laboratory Queens Road Teddington, Middlesex, England	
ATTN: Dr. D. Weston	1
Admiralty Underwater Weapons Establishment Portlant, Dorset, England	
ATTN: Dr. M. Daintith	1
Applied Physics Laboratory 8621 Georgia Avenue Silver Spring, Maryland 20910	
SASG	1
Director Applied Physics Laboratory Pennsylvania State University University Park, Pennsylvania 16801	1
Applied Research Laboratory Pennsylvania State University P. O. Box 30 State College, Pennsylvania 16801	
ATTN: Dr. D. Stickler	1
Arthur D. Little, Inc. 26 Acorn Park Cambridge, Massachusetts 02140	
ATTN: Dr. B. Koopman	1
Dr. G. Raisbeck	1

DISTRIBUTION LIST (Cont.)

	No. of Copies
Bell Telephone Laboratory Whippany, New Jersey 07981	
ATTN: Dr. U. Gianola	1
Mr. R. Hardin	1
Dr. E. Harper	1
Dr. R. Holford	1
Dr. F. Labianca	1
Dr. T. Philips	1
Dr. J. Polak	1
Dr. F. Tappert	1
Ms. H. Walkinshaw	1
Dr. G. Zipfel	1
Boeing P. O. Box 3991 Seattle, Washington 98124	1
Bolt Beranek and Newman, Inc. 1701 N. Fort Myer Drive Arlington, Virginia 22209	
ATTN: Mr. C. Burroughs	1
Bolt Beranek and Newman, Inc. 50 Moulton Street Cambridge, Massachusetts 02138	
ATTN: Dr. J. Barger	1
Dr. P. Smith	1
Cambridge Acoustical Associates, Inc. 1033 Massachusetts Avenue Cambridge, Massachusetts 02138	
ATTN: Dr. D. Sachs	1
Catholic University 620 Michigan Avenue, N.E. Washington, D. C. 20017	
ATTN: Prof. F. Andrews	1
Prof. H. Uberall	1

DISTRIBUTION LIST (Cont.)

	No. of Copies
Davidson Laboratory Castle Point Station Hoboken, New Jersey 07030	
ATTN: Dr. E. Arase	1
Dr. T. Arase	1
General Motors Corporation AC Electronics Defense Research Laboratory Santa Barbara, California 93101	
ATTN: Mr. B. Buck	1
Mr. C. Greene	1
Hydrospace-Challenger, Inc. 2150 Fields Road Rockville, Maryland 20850	1
IBM 18100 Frederick Pike Gaithersburg, Maryland 20760	
ATTN: Dr. S. Bjorklund	1
Institute for Defense Analysis 400 Army-Navy Drive Arlington, Virginia 22209	1
John Hopkins University Applied Physical Laboratory 8621 Georgia Avenue Silver Spring, Maryland 20910	
ATTN: Dr. N. Nicholas	1
Lamont Doherty Geological Observatory Palisades, New York 10964	
ATTN: Dr. H. Kutschale	1

DISTRIBUTION LIST (Cont.)

	No. of Copies
Lockheed Missiles and Space Corporation 3251 Hanover Street Palo Alto, California 94304	
ATTN: Director of Research	1
Director Marine Physical Laboratory Scripps Institution of Oceanography San Diego, California 92152	
ATTN: Dr. V. Anderson	1
Marineland Research Laboratory St. Augustine, Florida 32048	
ATTN: Dr. D. Caldwell	1
Ms. M. Caldwell	1
Dr. Verne Nomady 1913 Dulaney Anapolis, Maryland 21401	1
Operations Research, Inc. 1400 Spring Street Silver Spring, Maryland 20910	1
Director North Atlantic Treaty Organization SACLANT ASW Research Centre APO New York, N.Y. 09019	
ATTN: Dr. R. Clarke	1
Dr. E. Murphey	1
Presearch, Inc. 8720 Georgia Avenue Silver Spring, Maryland 20910	1
Raff Associates, Inc. 912 Thayer Avenue Silver Spring, Maryland 20910	
Dr. R. Jennette	1

DISTRIBUTION LIST (Cont.)

	No. of Copies
Rensallaer Polytechnic Inst. 615 Southwest 2nd Avenue Miami, Florida 33103	
ATTN: Dr. M. Jacobson	1
Rosenstiel School University of Miami Miami, Florida 33149	
ATTN: Dr. J. Clark	1
Scientific Research Associates, Inc. 12100 Devilwood Drive Rockville, Maryland 20854	
ATTN: Dr. A. Hudimac	1
Systems Control, Inc. 260 Sheridan Avenue Palo Alto, California 94306	
ATTN: Dr. J. Anton	1
Dr. L. Seidman	1
Tetra Tech, Inc. 1911 N. Fort Myer Drive Arlington, Virginia 22209	
ATTN: Mr. K. Witt	1
Tetra Tech, Inc. 630 N. Rosenead Blvd. Pasadena, California 91107	
ATTN: Dr. D. Milder	1
Tracor, Inc. Ocean Technology Division 50 Evergreen Place East Orange, New Jersey 07018	
ATTN: Dr. W. Murray	1
Mr. E. White	1

DISTRIBUTION LIST (Cont.)

	No. of Copies
TRW Systems, Inc. 7600 Colshire Drive McLean, Virginia 22101	1
Underwater Systems, Inc. 8121 Georgia Avenue Silver Spring, Maryland 20910	
ATTN: Dr. M. Weinstein	1
University of Hawaii Honolulu, Hawaii 99353	
ATTN: Dr. W. Hardy	1
University of Miami School of Marine & Atmospheric Science 10 Rickenbacker Causeway Miami, Florida 33149	
ATTN: Dr. S. Daubin	1
University of Texas Applied Research Laboratory P. O. Box 8029 Austin, Texas 78712	
ATTN: Dr. J. Beard	1
Dr. R. Deavenport	1
University of Washington P. O. Box 999 Richmond, Washington 99353	1
Western Electric Company 2400 Reynolds Road Winston-Salem, North Carolina 27102	
ATTN: Mr. T. Skeen	1

DISTRIBUTION LIST (Cont.)

	No. of Copies
Woods Hole Oceanographic Institution Woods Hole, Massachusetts 02543	
ATTN: Mr. L. Baxter	1
Dr. J. Davis	1
Mr. W. Schevill	1
Mr. W. Watkins	1
Defense Documentation Center Cameron Station Alexandria, Virginia 22314	2